MAMMALIAN CELL-BASED BIOSENSORS FOR FOODBORNE PATHOGEN DETECTION

by

Luping Xu

A Thesis

Submitted to the Faculty of Purdue University

In Partial Fulfillment of the Requirements for the degree of

Master of Science

Department of Food Science

West Lafayette, Indiana

May 2021

THE PURDUE UNIVERSITY GRADUATE SCHOOL

STATEMENT OF COMMITTEE APPROVAL

Dr. Arun Bhunia, Chair

Department of Food Science

Dr. Bruce Applegate

Department of Food Science

Dr. Sophie A. Lelièvre

Department of Basic Medical Sciences

Approved by:

Dr. Arun Bhunia

Dedicated

To my parents, aunt and uncle, and in-laws for their financial backing and spiritual encouragement, to my husband for his intellectual contribution and emotional support, to Mrs. and Mr. Newbold (my non-biological parents) for their faith in my ability to succeed.

ACKNOWLEDGMENTS

I would like to acknowledge my major professor, Dr. Arun Bhunia, for his guidance, support, patience, and trust through 2015-2020, witnessing my growth from an undergrad to now. I would also like to thank Dr. Bruce Applegate and Dr. Sophie Lelièvre, for serving on my committee. A special thank goes to Zhenjing Tang, a former Bhunia lab member, who introduced me to this lab and pointed me out the initial way to Graduate school. Besides, I owe my deepest gratitude to all Bhunia lab members, former and current, for their research work I could refer to, and their assistance throughout the past years. I would also like to extend my sincere thanks to my friends, especially to those I met in Bhunia lab: Wen Lv, Jingyi Ren (and her cat), and Dr. Star Zhu, for companions throughout this journey.

I have greatly benefited from the financial support through the U.S. Department of Agriculture, Agricultural Research Service, under Agreement No. 59-8072-6-001, and the USDA National Institute of Food and Agriculture (Hatch accession no. 1016249) for this research. I would also like to express the appreciation to the Department of Food Science, Purdue University, for my professional growth and educational opportunity.

Lastly, I would like to thank my parents and grandparents, who sacrificed a lot of things, emotionally and financially, sending me abroad since I was 15, which marks a turning point for my life. I would also like to thank my husband, who recognizes my skills and encourages me to do all the things I wouldn't think of in the past, which marks another turning point for my life. And my non-biological parents, Mrs. and Mr. Newbold, for supporting, understanding, and trusting me as if I were their daughter.

TABLE OF CONTENTS

LIST OF TABLES

LIST OF FIGURES

ABSTRACT

Rapid detection of live pathogens is of paramount importance to ensure food safety. At present, nucleic acid-based polymerase chain reaction and antibody-based lateral flow assays are the primary methods of choice for rapid detection, but these are prone to interference from inhibitors, and resident microbes. Moreover, the positive results may neither assure virulence potential nor viability of the analyte. In contrast, the mammalian cell-based assay detects pathogen interaction with the host cells and is responsive to only live pathogens, but the short shelf-life of the mammalian cells is the major impediment for its widespread application. An innovative approach to prolong the shelf-life of mammalian cells by using formalin was undertaken. Formalin (4% formaldehyde)-fixed human ileocecal adenocarcinoma cell line, HCT-8 on 24-well tissue culture plates was used for the capture of viable pathogens while an antibody was used for specific detection. The specificity of the Mammalian Cell-based ImmunoAssay (MaCIA) was validated with *Salmonella enterica* serovar Enteritidis and Typhimurium as model pathogens and further confirmed against a panel of 15 *S.* Enteritidis strains, 8 *S*. Typhimurium,11 other *Salmonella* serovars, and 14 non-*Salmonella* spp. The total detection time (sample-to-result) of MaCIA with artificially inoculated ground chicken, eggs, milk, and cake mix at 1-10 CFU/25 g was 16-21 h using a traditional enrichment set up but the detection time was shortened to 10-12 h using direct on-cell (MaCIA) enrichment. Formalin-fixed stable cell monolayers in MaCIA provide longer shelf-life (at least 14 weeks) for possible point-of-need deployment and multi-sample testing on a single plate.

CHAPTER 1. LITERATURE REVIEW OF BIOSENSOR APPLICATION IN FOODBORNE PATHOGEN DETECTION

1.1 Abstract

Seeking a balance between improving the sensitivity and reducing foodborne pathogen detection time is a perplexing mission for the assay developers and the food industry users. Fast, sensitive, and accurate detection tools are in great demand to resolve the conundrum. Various approaches have been explored in the past few years to find a more effective way to incorporate antibodies, oligonucleotides, phages, and mammalian cells as signal transducers and analyte recognition probes on fiberoptic, surface plasmon resonance, quartz crystal microbalance, and other sensor platforms to achieve high specificity and low detection limits (5-100 bacterial cells or pico-nanogram levels of toxins). Besides, advancement in mammalian cells and bacteriophage-based sensors led to their ability to detect not only low levels of pathogens but also to differentiate live from dead ones. Combining different biotechnology platforms enabled practical utility and application of biosensors in foodborne pathogen detection from complex food matrices. We expect this review to provide future researchers an essential understanding of the current progress and assist prospective studies on novel biosensor development.

1.2 Introduction

The World Health Organization (WHO) reports the global burden of foodborne illness to be about 600 million cases with 420,000 deaths each year caused by 31 foodborne pathogens based on an estimate of 2010 (Kirk et al. 2015). In the United States of America, 48 million foodborne diseases result in 128,000 hospitalizations and 3,000 deaths annually. Among the identified illnesses, only 9.4 million are caused by known 24 pathogens, while most cases (38.6 million) of illnesses are caused by unknown agents or unknown transmission vehicles (Scallan et al. 2011). The economic burden associated with these cases is estimated to be $78 billion per year, including the cost for the loss of work hours, medical bills, product recalls, bankruptcy, and lawsuits (Scharff 2012).

Among all known bacterial foodborne pathogens, *Salmonella* spp., *Clostridium perfringens*, *Campylobacter* spp., *Staphylococcus aureus*, *Shigella* spp. and Shiga toxin-producing *Escherichia*

coli (STEC) are the top six that causes the most cases of illnesses in the US (Scallan et al. 2011). Other commonly found bacterial foodborne pathogens include *Bacillus cereus*, *Brucella* spp. *Clostridium botulinum,* enterotoxigenic *E. coli, Listeria monocytogenes, Vibrio* spp., and *Yersinia enterocolitica* (Scallan et al. 2011; Singh and Bhunia 2018), which are also responsible for millions of infections in the US annually (Scallan et al. 2011). Besides, microbial toxins can cause foodborne intoxication. The potent exotoxins include botulinum toxin from *C. botulinum,* staphylococcal enterotoxin from *S. aureus*, diarrheagenic/emetic enterotoxins from *B. cereus*, mycotoxins by toxigenic molds, and seafood toxins primarily from microalgae. The production of these toxins in nanogram quantities in food could lead to severe consequences.

Controlling foodborne pathogens is vital to protect public health. Various measurements have been implemented to reduce the risk of pathogen exposure through food, including but not limited to the implementation of the new standards and updated testing plans. For example, to verify that the preventative measurements are adequate, the USDA Food Safety and Inspection Service (FSIS) has published a new pathogen reduction performance standard, outlining sampling, testing, and controlling *Salmonella* and *Campylobacter* in poultry products (USDA-FSIS 2019b). The FSIS has identified *Salmonella* as an adulterant in ready-to-eat (RTE) products and adopted the zero-tolerance policy. For an easier implementation of this policy, FSIS has frequently updated the microbial testing plan for *Salmonella* in RTE products (USDA-FSIS 2020b).

In response to government regulations, industries commonly use recall as voluntary corrective actions to remove products containing adulterants (USFDA 2016). However, voluntary recalls usually result in a waste of food, transportation resources, and labor cost. For instance, 118,830 pounds of food were discarded because of three *Salmonella*-related recalls in 2019 (USDA-FSIS 2015; 2019c). Since the FSIS-approved detection method takes 48 h to report the screening result, 120 h to report the presumptive result, and up to 192 h to provide the final result for *Salmonella* (USDA-FSIS 2019a; 2020a), manufacturers are still prompted to ship out the food first and issue a recall later, if tested positive. The lengthy and troublesome recall process puts consumers at great risk of foodborne pathogen exposure. Therefore, rapid pathogen detection is in continued demand for the interest of the food industry and consumers.

The FSIS has employed several rapid pathogen screening methods, such as the 3M™ Molecular Detection System (USDA-FSIS 2020b) and polymerase chain reaction assay (USDA-FSIS 2019a). However, both methods depend on the detection of nucleic acid and may generate

false-positive screening results. Thus, to obtain the final results, the FSIS still requires the completion of its culture-based methods, which include the non-selective and selective enrichment, to be followed by the biochemical or serological confirmatory test and the genotype determination using the whole genome sequencing (WGS) and antimicrobial resistance (AMR) (USDA-FSIS 2020a). The culture-based method is labor-intensive, time-consuming but is still considered the gold-standard for the food industry because it is the only approved test we can rely on to identify viable pathogens in foods (Bhunia 2014).

Researchers continue to develop various alternative detection tools, including biosensor-based methods, recognizing the weaknesses associated with the existing methods. Biosensor-based tools have continued to grasp the attention of researchers due to their sensitivity and potential portability for onsite deployment. The development of a biosensor usually requires incorporating a biological recognition probe on a surface that can transduce an amplified signal upon analytes' binding (Bhunia 2008; 2014). The interaction between the analyte and the recognition molecule can be categorized into four types: immunological interaction, aptamer recognition/DNA hybridization, bacteriophage recognition, and pathogens-eukaryotic cell interaction (**Table 1**) (Bhunia 2014; Cho et al. 2014). Upon binding, the analyte can be detected through either a label-dependent or a label-free method. In a label-dependent biosensor, captured analytes were labeled with a marker (reporter). The signal is usually a colorimetric or fluorescent change mediated by the marker. In a label-free biosensor, the binding of the analyte and the molecule could yield changes in the microsystem, such as an impendence fluctuation. We have included an example of each aforementioned analyte interaction on the biosensor platform in **Figures 1** and **2.** Though each biosensor relies on different binding mechanisms of a recognition molecule and the analyte, they all resemble the basic idea of a biosensor, i.e., to report this interaction as an indicator of the analytes' presence/absence.

Table 1.1 Biosensors with different principles and signal generation mechanisms

Principle	Signal type	Time-to-result	LOD	Targeted organism	Ref
Immunosensor	Surface plasmon resonance	<80 min	< 10 CFU/mL	*Listeria*	(Vaisocherová-Lísalová et al. 2016)
		<30 min + 24 h Enrichment	<10 CFU/25mL	*E. coli*	(Chen et al. 2015a; Morlay et al. 2017a)
	Impedance change	<1 h	< 300 CFU/mL	*Salmonella*	(Liu et al. 2019)
	Colorimetric	~2 h	10 CFU/mL	*Salmonella and Campylobacter*	(Alamer et al. 2018)
	Fluorescence	5 min + 8-10 h Enrichment	1 CFU/mL	*E. coli*	(Song et al. 2016)
	Fiber optic sensors	20 min	247 CFU/mL	*S.* Typhimurium	(Kaushik et al. 2018)
		24 h	10^3 CFU/mL	*L. monocytogenes* *S.* Typhimurium *E. coli* O157:H7	(Ohk and Bhunia 2013)
	Fiber optic + light scattering sensor	24 h	10^3 CFU/mL	*S. enterica*	(Abdelhaseib et al. 2015)
	Fiber optic + Immunomagnetic separation	2 h + 18 h enrichment	3×10^2 CFU/mL	*L. monocytogenes, L. ivanovii*	(Mendonça et al. 2012)
Nucleic acid-based	Chemi luminescence	1 h	4.5×10^3 CFU/mL	*E. coli*	(Khang et al. 2016)
	Fluorescence	135 s	3.7×10^2 CFU/mL	*E. coli*	(Zhang et al. 2019)
	Colorimetric	< 9 h	< 10 CFU/mL	*Salmonella*	(Quintela et al. 2019)
	Differential pulse voltammetry and Impedance change	N/A	2.1 pM and 0.15 pM	*Salmonella*	(Tabrizi and Shamsipur 2015)
	Differential pulse voltammetry	N/A	5.3 pM	*Vibrio*	(Nordin et al. 2016)

Table 1.1 continued

Phage sensor	Chromatography	8 h	1 CFU/mL	*E. coli*	(Martelet et al. 2015)
	Colorimetric	6 h	10 CFU/mL	*E. coli*	(Chen et al. 2015a)
	Chemi luminescence	7 h	5 CFU	*E. coli*	(Zhang et al. 2016b)
		1.5 h	10^4 CFU/mL	*E. coli*	(Franche et al. 2017)
Cell-based sensor	Electrochemical	24 h	3.5 × 10^3 ng/mL	LPS	(Jiang et al. 2020)
	Colorimetric	6 h	10^7 CFU/mL; 32 ng/mL	STEC/STX	(To and Bhunia 2019b)
	Fluorescence	~2 h detection time + 6 h transfection time	0.075 ug/mL	LPS	(Sun et al. 2018)

N/A: not reported; STEC: Shiga toxin producing *E.coli;* STX: Shiga toxin; LPS: lipopolysaccharides

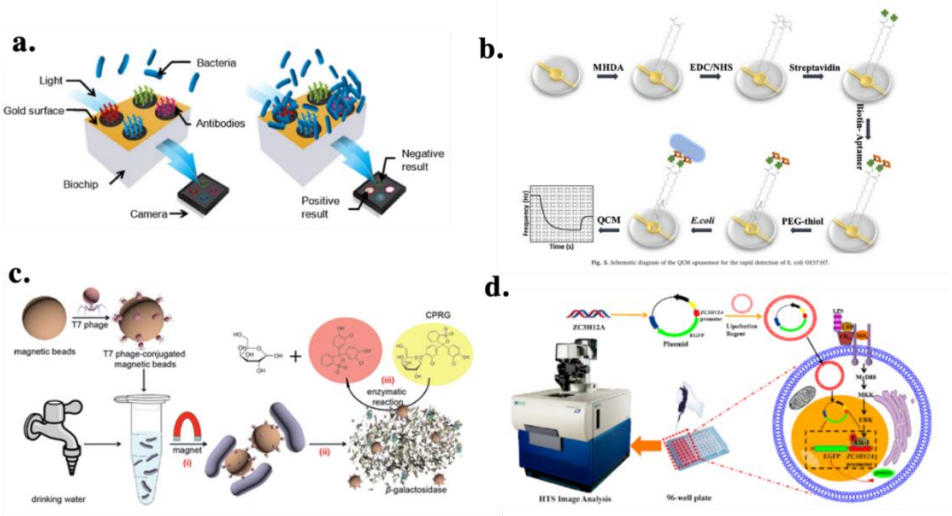

Figure 1.1 Schematic illustration of different working principles of biosensors. (a) On-chip culture of bacteria. Viable cells divide on the microarray and the specific binding of bacteria on dedicated antibodies is monitored in a label-free manner (Morlay et al. 2017a). (b) Schematic diagram of QCM aptasensor for the rapid detection of *E. coli*. MHDA: 16-Mercaptohexadecanoic acid, EDC: N-3-Dimethylaminopropyl-N'-ethylcarbodimide hydrochloride; NHS: N-Hydroxysuccinimide; PEG thiol: poly-ethylene glycol methyl ether thiol. QCM: quartz crystal microbalance (Yu et al. 2018b). (c) Schematic representation of detection of *Escherichia coli* in drinking water using T7 bacteriophage-conjugated magnetic probe. Three steps were involved: (i) Separation of *E. coli* from drinking water using T7 bacteriophage-conjugated magnetic probe to (ii) T7 bacteriophage infection of *Escherichia coli* and the consequent release of β-gal; (iii) β-gal catalyzed CPRG hydrolysis to produce colorimetric readout (Chen et al. 2015a). (d) Schematic Illustration of the Working Principle of a 293/hTLR4A-MD2-CD14 Cell Sensor (Sun et al. 2018).

Another type of label-free biosensors, such as a light-scattering sensor, does not require recognition molecules and is not considered a prototypical biosensor. In light scattering sensor, such as in BARDOT (bacterial rapid detection using optical scattering technology), the specificity of the assay can be improved by using an immunomagnetic bead to capture target bacteria or by using selective agar media to facilitate the growth of the target bacterial colony for interrogation by a laser (Banada et al. 2009). The properties of illuminated scatterers, such as refractive index, size, and shape, decide the light scattered pattern. Since bacterial morphology and composition are expected to be reproducible when growing under similar conditions, the scattered light pattern's characteristics could be used to identify foodborne pathogens at the genus, species, or serovar levels when the bacterial scatter images are compared to a library (Bhunia et al. 2007; Singh et al. 2015b). The detail of this sensor is reviewed below.

Two prevailing characteristics make biosensors an exceptional foodborne pathogen detection tool. First, the limit of detection (LOD) of the most recently developed biosensor is exceptionally low. The LOD can be as low as 5-100 CFU/mL for bacterial pathogens or pico-nanogram levels for toxins (Mendonca et al. 2012; Bhunia 2014; Fulgione et al. 2018; Hice et al. 2018). The low LOD allows the users to cut down the pre-enrichment time, hence reducing the total detection time. Second, the concept of the biosensor can be easily delivered using a microfluidic chip, making it a portable device for point-of-care deployment.

In this review, we will cover the most recent accomplishments on the five types of biosensors aforementioned, especially those based on biorecognition molecules and a label-free light scattering sensor. We will also analyze the feasibility of each method for its near real-time detection capability with a practical perspective. We hope this review is an inspiration to future researchers for the development of advanced rapid foodborne pathogen detection tools to ameliorate the threat of foodborne pathogens to public health.

1.3 Biosensors based on Immunological Interaction

1.3.1 Antibody coated on a surface

The antibody is a critical reagent for establishing the specificity of a biosensor. The biosensor that relies on the antibody is also known as an immunosensor. The final deliverable of immunosensor could involve commonly used immunoassays, such as latex agglutination, lateral

flow assay, and enzyme-linked immunosorbent assay (ELISA) (Banada and Bhunia 2008; Silva et al. 2019). Antibodies can be immobilized on a sensor surface to capture the target analytes. Upon binding, changes in the microenvironment can be measured or visualized. For example, antibody-coated quartz crystal microbalance (QCM) is used as a mass-sensitive biosensor (**Figure 1**). Bacteria bind to antibodies, reducing the oscillation frequency as the crystal mass increases (Senturk et al. 2018). Fulgione et al (Fulgione et al. 2018) employed this method to detect *Salmonella enterica* serovar Typhimurium in chicken meat, and the limit of detection was estimated to be less than 1 CFU/mL using a sample that was enriched for 2-h at 37ºC.

Immunosensors are the major subgroups within the broad category of optical biosensors (Masdor et al. 2017; Widyastuti et al. 2018; Kaushik et al. 2019). Optical sensors measure a parameter of the reaction between a receptor and an analyte as a quantifiable optical signal (Singh and Bhunia 2018). Surface plasmon resonance (SPR) response is one of the commonly measured parameters in the optical sensor (Wang and Park 2020). Upon receptor-analyte interaction, changes in refractive index result in a resonance angle shift (Singh and Bhunia 2018). Morlay et al (Morlay et al. 2017b) employed an immune-chip SPR imaging system to detect *L. monocytogenes* in food samples, where they coated the antibodies on a gold surface of the biochip (**Figure 1**). The SPR signal was monitored in real-time after the addition of the enriched samples. This system detected *L. monocytogenes* in 30 min after a 24-h enrichment of samples.

Antibodies can also be coated on the optical waveguide (fiber-optic). With a laser-diode, an evanescent wave is generated along the optical waveguide to activate the analyte-bound fluorescence-conjugated secondary antibody as an indication of the presence of an analyte. The signal is an electric current proportional to the fluorescence light intensity measured by a photodiode (Valadez et al. 2009). Optical sensors working under this principle are known as fiber-optic sensors. A traditional fiberoptic sensor was developed for *Salmonella enterica* detection (Abdelhaseib et al. 2016). Recent progress of fiber-optic sensors involved the improvement of sensor fabrication. Kaushik et al. (Kaushik et al. 2018) designed a single mode-multimode-single mode (SMS) biosensing device for a simpler and more cost-effective sensor fabrication process. They removed the cladding region of the multimode fiber, which increases the interaction between the propagating modes of guided light and the ambient medium. After immobilizing recognizing antibodies on the sensing platform, the fiber was incubated with bacteria suspended in buffer solution. This fabrication improved assay sensitivity for the *S.* Typhimurium detection. They

achieved a LOD of 247 CFU/mL in the presence of *E. coli* and *S. aureus* (Kaushik et al. 2018). More recently, this group also developed a fiber optic SPR immunosensor interfaced with MoS_2 nanosheet, simplifying and improving the antibody immobilization. The updated version of the fiber-optic sensor has been tested for *E. coli* in spiked-drinking water and orange juice and it achieved a LOD of 94 CFU/mL (Kaushik et al. 2019).

On the other hand, another typical immunosensor, lateral flow strip assay (LFSA), has been evolving for years (Hristov et al. 2019; Silva et al. 2019; Borse et al. 2020; Zhang et al. 2020). It has gained considerable attention due to its disposable, mass-producible, easy-to-fabricate, and point-of-care application (Yetisen et al. 2013; Hristov et al. 2019). In LFSA, chromatic/fluorescent-tagged antibodies are conjugated on a pad. After the sample solution is applied, the analytes labeled with the antibody keeps moving forward by capillary force toward the pad's detection zone and is identified by the colored or fluorescent signal. The recent trend of incorporating LFSA in foodborne pathogen detection focuses on increasing the device's sensitivity (Raeisossadati et al. 2016; Song et al. 2016; Luo et al. 2020), which may require concentrating the analytes in the sample solution before analysis. One of the typical methods is using antibody-conjugated nanoparticles, which are discussed below.

1.3.2 Antibody coated on nanobeads

The incorporation of gold nanoparticles in LFSA is a common practice in more recent approaches (Fei et al. 2016; Wang et al. 2017; Pan et al. 2018; Pissuwan et al. 2020). Gold nanoparticles (AuNPs) were widely used for antibody conjugation ascribed to their high surface to volume ratios, increasing the amount of immobilized antibody. The morphology of AuNPs has a significant effect on the sensitivity of the assay. Zhang et al (Zhang et al. 2015) compared three types of hierarchical flowerlike AuNPs and found out that the tipped flower-like AuNPs exhibit increased detection sensitivity for *E. coli* O157:H7 compared to large-sized flowerlike and popcornlike AuNPs. Due to the hierarchical structure, the tipped flowerlike AuNPs probes can detect as low as 10^3 CFU/mL of *E. coli* O157:H7 as opposed to 10^4 CFU/mL in popcornlike probes and 10^5 CFU/mL in large-sized flowerlike probes. The size of the AuNPs also impacts sensitivity. Cui et al (Cui et al. 2015) found that the AuNPs with a size of 35 nm confer the greatest sensitivity (10^3 CFU/mL) in *E. coli* O157:H7 detection as opposed to the sensitivity (10^3 - 10^6 CFU/mL) for AuNPs of other sizes. Besides, AuNPs-antibody-*E. coli* complex separated from unbound bacteria

showed a LOD of 10^2 CFU/mL, which is much lower than that of a conventional AuNP-based LFSA (Chen et al. 2015b). Modification of AuNPs has also been investigated to seek better performance. Ríos-Corripio et al (Ríos-Corripio et al. 2016) report a stable antibody-AuNPs colloidal solution by decorating AuNPs with protein A. Their study suggests the future application of using protein A-gold nanoparticles bioconjugate colloidal solution as a probe to detect *Salmonella* from contaminated samples.

Another commonly used small particles are magnetic beads. Antibody-coated magnetic (immuno-magnetic) beads are generally used to separate and concentrate bacteria from sample matrices after the enrichment process (Bai et al. 2020), thus avoiding background cross-reaction. Papadakis et al (Papadakis et al. 2018) took advantage of the immuno-magnetic beads to capture S. Typhimurium from milk before the addition of the sample in an acoustic biosensor. The employment of magnetic beads reduced the pre-enrichment process to only three hours. They showed that magnetic nanoparticles of 0.8 μm have the highest capture rate of 73% after 3.5-h incubation over nanoparticles of 1.0 μm and 3 μm (Papadakis et al. 2018). Another group also proved this relationship using chicken rinse and liquid egg white matrices. They found that immuno-magnetic beads of 100 nm have a higher recovery rate of 88% - 96 % for *S.* Enteritidis than beads of 500 nm and 1000 nm after 30-min incubation (Chen and Park 2018).

Antibody conjugated small particles not only have tremendous potential in capturing the analyte but could also be applied in other types of biosensors due to their unique characteristics. For example, the excellence in conductivity of AuNPs enhances signal transduction by allowing enhanced electron transfer (Jiang et al. 2018b). Recent applications of AuNPs-conjugated antibodies in biosensors inclined toward measuring impedance changes upon the antibody-antigen binding. Generally, the binding between recognizing antibodies and antigens can estimate the enzyme activity, such as horse-radish peroxidase (HRP) activity that is conjugated to the antibody. Then, the amount of the enzyme present is further quantified by changes in impedance after adding specific substrates, like redox probe thionine and H_2O_2, that generate electrons (Wang et al. 2014). Biosensors that employ this principle are also known as electrochemical impedance immunosensor. Fei et al (Fei et al. 2015) developed a simple, rapid, and economical immunosensor by coating the antibody conjugated AuNPs on the screen-printed carbon electrode (SPCE) to monitor the impedance change upon binding of two *Salmonella* serovars. To improve the sensitivity and the conductivity of the electrochemical immunosensor using AuNPs, Xiang et al (Xiang et al. 2015)

developed an electrochemical immunosensor for *Salmonella* detection by coating an electrode with chitosan/AuNP composite film. Anti-*Salmonella* capture antibodies are immobilized on the film through anodic oxidation. After incubation with *Salmonella,* a secondary anti-*Salmonella* HRP-conjugated antibody and 2-hydroxy-1,4-naphthoquinone (HNQ) are applied to generate an electronic signal, which is detected by the sensor. The authors claim that the rationale of this ultra-low LOD (5 CFU/mL) of the sensor is that well-dispersed AuNPs enhance the electrochemical signal and the performance of the chitosan film. Liu et al (Liu et al. 2019) coated the antibody on the gold electrode and placed it in microchannels. The impedance change is measured by subtracting the measured impedance after antibody coating from the measured impedance after antigen – antibody binding. This biosensor can detect *Salmonella* from RTE turkey samples in one hour with the LOD of 300 CFU/mL (Liu et al. 2019).

The microfluidics setup was also used in combination with antibody-coated surface-enhanced Raman scattering (SERS)-tagged gold nanostars. The incorporation of antibodies in the SERS platform improves the specificity of the sensor. Rodríguez-Lorenzo et al (Rodríguez-Lorenzo et al. 2019) coated the SERS-tagged gold nanostars with a thin silica mesoporous layer for functionalization with an anti-*Lm* antibody. Due to the higher distribution of mAb C11E9-specific antigens on the cell surface of *L. monocytogenes* than on *L. innocua*, more gold nanostars are distributed on *L. monocytogenes*, therefore, allowing this sensor to differentiate *L. monocytogenes* (pathogenic) from *L. innocua* (non-pathogenic) in real-time (Rodríguez-Lorenzo et al. 2019).

Besides, measuring fluorescence emission in the impedance-based immunosensor is another approach for detection. Quantum dots (QDs) are the commonly used marker for antibody conjugation due to their wide excitation range and narrow emission wavelengths (Chen et al. 2016; Mohamadi et al. 2017; Xue et al. 2020). Hu et al (Hu et al. 2020) incorporated QDs in a lateral flow setup by employing polymer nanobeads as a carrier to assemble QDs layer by layer. The sensor's result could be read by the naked eye after the QDs are excited by using ultraviolet light (Hu et al. 2020). Although generating visible results for naked-eye detection could also be achieved using enzyme-labeled antibodies and certain chromogen, for instance, HRP and DAB (3,3'-Diaminobensidine) as substrate, the merit of QDs is that no substrate is needed, and the results are visible immediately after exposure to UV light. In recent studies, QDs are used with immunomagnetic beads for *Salmonella* detection, using immunomagnetic beads (IMB) to capture bacteria first, then releasing the attached QDs to measure fluorescence intensity. Xue et al (Xue et

al. 2020) fabricated an immunosensor using antibody-conjugated QDs to capture magnetic beads bonded bacteria, forming an IMB-target-QD sandwich complex. This immunosensor can detect *E. coli* and *Salmonella* with a detection limit of 15 CFU/mL and 40 CFU/mL, correspondingly, in 2 h.

Although antibodies grant the specificity for immunosensors, they carry limitations as they only recognize a specific part of the analyte. For commercial applications, antibodies could be costly for the detection of the pathogen. When relying on antibodies alone, immunosensors cannot differentiate live/dead pathogen so that they don't possess advantages over a more economical method, such as PCR. However, one exceptional advantage of immunosensor is its ability to integrate with the lateral flow assay, making it portable for point-of-care deployment for fast results (in less than 20 min). Therefore, for the future development of immunosensor, researchers could focus on the development of the detection platform in a combination of immunosensor with other types of biorecognition molecules to enhance specificity, reliability, and portability.

1.4 Nucleic acid-based biosensors

Nucleic acid-based biosensor utilizes a known sequence of oligonucleotides as the sensing element. This type of biosensor is either based on DNA hybridization of complementary strands or relies on the interaction of DNA molecules and the analytes. Unlike antibodies, nucleic acid strands are easier and cheaper to be synthesized. With the combination of DNA amplification, the nucleic acid-based biosensor can be more sensitive and specific (Fu et al. 2018; Xu et al. 2018; Wang et al. 2020). The basic setup of a nucleic acid-based biosensor is to immobilize a single-stranded DNA on an electrode surface. An electrical signal is generated when the target DNA binds to the immobilized sequence and/or undergo hybridization (Baeumner 2003; Kavita 2017). The newly developed nucleic acid-based sensors also take advantage of nanomaterials to expand the sensors' function for different food materials (Majdinasab et al. 2018; Xu et al. 2018). Here, we discuss the application of sensors based on aptamers and DNA hybridization.

1.4.1 Aptasensors

Aptamers, which are short and single-stranded oligonucleotides with a high binding affinity towards specific proteins and bacteria, are commonly used to capture the target analyte. Nucleic

acid-based biosensors that utilize aptamers are designated aptasensors. Though playing a similar role to antibodies in immunosensors, aptamers can be cost-effectively generated *in vitro* via a process called Systemic Evolution of Ligands by Exponential enrichment (SELEX) (Yu et al. 2018a) (**Figure 1**). This method relies on the exposure of the target protein/bacteria with a DNA/RNA library. The one with the highest binding affinity is selected for further amplification and sequencing (Kruspe and Giangrande 2017).

Comparable to the application of antibodies in immunosensors, aptamers are used in combinations with nanoparticles, such as AuNPs (Zhang et al. 2018), chemiluminescence (Khang et al. 2016), directly on a surface within a microfluidic device (Zhang et al. 2019), or on an optical waveguide (fiber optic) probe (Ohk et al. 2010) to enhance the detection outcome. Researchers also employed different strategies to collect/remove the bacteria-bound aptamer complex or free aptamer. Zhang et al (Zhang et al. 2018) fabricated a dual recognition system using vancomycin, which interacts with the bacterial cell wall, and aptamers to detect *S. aureus* and *E. coli*. Pathogen-specific aptamers are modified on AuNPs as specific surface-enhanced Raman scattering (SERS) tags, while vancomycin is modified with Fe_3O_4@Au magnetic nanoparticles (Fe_3O_4@Au-Van). The bacteria are first captured by the Fe_3O_4@Au-Van and are collected using a magnet. Later, with the addition of the aptamer conjugated AuNP SERs tag, signals are acquired upon laser excitation. This set up allows a LOD of 50 and 20 cells/mL for *E. coli* and *S. aureus*, respectively. The researchers also confirmed the specificity of the assay by demonstrating reduced or low signal from other bacterial pathogens including *Klebsiella pneumoniae*, *Staphylococcus epidermidis, Pseudomonas aeruginosa, Acinetobacter baumannii, L. monocytogenes,* and *Streptococcus pneumonia* (Zhang et al. 2018).

Khang et al (Khang et al. 2016) explored the conjugation of *E. coli* O157:H7-specific aptamer with 6-carboxyfluorescein (6-FAM), which can emit intense light upon the addition of guanine chemiluminescent reagent. The removal of the free aptamer is achieved based on the π–π stacking interaction between the free aptamer and graphene oxide/iron nanocomposites. Data show that the strength of light is proportional to the increase of target concentration, and the LOD of this biosensor is 4.5×10^3 CFU/mL (Khang et al. 2016).

Another group investigated the combination of aptamer and microfluidic devices (Zhang et al. 2019). They successfully developed an aptasensor for *E. coli* detection using bacteria-specific aptamer in conjugation with microchip capillary electrophoresis-coupled laser-induced

fluorescence (MCE-LIF). In this case, the separation of free aptamers and complex peaks by MCE are identified and achieved based on the differences between their electrophoretic mobilities, which is influenced by the charge to mass ratio difference of free aptamer and the complex. The LOD of this device is reported to be 3.7×10^2 CFU/mL (Zhang et al. 2019).

1.4.2 DNA hybridization sensors

Similar to the setup of aptasensors, DNA hybridization sensors also employ single-stranded DNA (ssDNA) as the recognized probe which binds to the complementary ssDNA from targeted bacteria. A common strategy of such a sensor is to immobilize an ssDNA probe on a transducer's surface, which emits a signal upon binding to a complementary DNA target (Rashid and Yusof 2017). So, the critical aspect of this type of sensor is to find a transducer surface that has the optimal characteristic for the detection purpose. In the following section, we describe the hybridization events that can be converted into a quantified signal by the transducer in the electrochemical form.

Carbon is commonly used in the electrochemical biosensor field due to its large surface area, low cost, ease of fabrication, and good conductivity. Its biocompatibility and robust mechanical strength also contribute to its wide application (Hu et al. 2011; Zhang et al. 2013; Rashid and Yusof 2017). Tabrizi et al (Tabrizi and Shamsipur 2015) developed an electrochemical DNA biosensor using a nanoporous glassy carbon electrode. They covalently linked the amino-modified *Salmonell*a ssDNA probe sequence with the carboxylic group on the carbon electrode's surface. Differential pulse voltammetry (DPV) and electrochemical impedance spectroscopy (EIS) are used to monitor the hybridization events. Moreover, the LOD is reported to be 2.1 pM and 0.15 pM for DPV and EIS, respectively (Tabrizi and Shamsipur 2015). Similar strategies are implemented in the biosensor for the detection of *Vibrio parahaemolyticus*. Nordin et al. (Nordin et al. 2016) used a screen-printed carbon electrode modified with polylactide-stabilized gold nanoparticles (PLA-AuNPs) as the surface to bind and immobilize with ssDNA. DPV is also used to assess hybridization events. The LOD of this sensor is reported to be 5.3 pM (Nordin et al. 2016).

Another DNA hybridization-based biosensor strategy includes the use of ssDNA with a fluorescence tag as the probe for flow cytometry (FCM). Generally, the bacteria are first permeabilized and then incubated with a complementary fluorescence-labeled ssDNA probe, and analyzed by FCM. Because of the abundance of ribosomal RNA (rRNA) in bacteria, 16S and 23S

rRNA are usually used as the common target for the ssDNA probe (Rohde et al. 2015) For instance, Bisha et al (Bisha and Brehm-Stecher 2009) developed a flow-through imaging cytometry for the characterization of *Salmonella* subpopulations in alfalfa sprouts, using a cocktail of two 23 rRNA-targeted ssDNA probes.

To be employed as a recognition probe on a biosensor, aptamers are also found to be very effective when compared with antibodies. First, aptamers are smaller, easier to be made, and more stable for storage than antibodies. Second, antibodies could compromise the signal by interfering with the nanomaterial by forming large insulating layers on electrochemical sensors (Kaur and Shorie 2019). On the other hand, antibodies offer a higher affinity to their target than aptamers (Piro et al. 2016); thus future studies on the aptamer sensor could focus on improving aptamer-analyte interaction.

Another exciting and emerging technology that has recently been applied in foodborne pathogen detection is DNA sequencing using a handheld device. Yang et al (Yang et al. 2020) applied direct metatranscriptome RNA-seq and multiplex RT-PCR amplicon sequencing using Oxford Nanopore MinION sequencer to detect three pathogens (*Listeria, E. coli,* and *Salmonella*) in lettuce juice extract (LJE) or brain heart infusion (BHI) medium simultaneously. After extracting RNA from a bacteria cocktail incubated in LJE or BHI, whole metatranscriptome or mRNA of bacteria-specific genes are converted to DNA libraries and sequenced using Nanopore MinION. Results showed that both metatranscriptome RNA-seq and RT-PCR amplicon sequencing could detect all three pathogens; however, the samples tested by sequencing RT-PCR amplicon needs shorter incubation time (4 h) than their counterparts (24 h). Besides, metatranscriptome RNA-seq miss-identified some reads to be *Bacillus*, *Lactobacillus*, or *Staphylococcus*, which is probably due to their genetic similarity with *Listeria*. This work shows that the excellent portability and efficiency of Nanopore MinION make the technology promising to be applied in foodborne pathogen detection.

1.5 Phage-based biosensors

Phage-based biosensors employ bacteriophage as the recognition element (Goodridge et al. 2018; Aliakbar Ahovan et al. 2020; Paczesny et al. 2020; Singh et al. 2020). The advantage of this approach owes to the unique characteristics of phages. Usually, they are easily produced and less sensitive to the effect of pH and temperature (Jończyk et al. 2011). Due to the diversity of bacteriophage and selection through phage-display, phage-based recognition also demonstrates high specificity and accuracy. Similar to the immunosensor and aptasensor mentioned above, the binding of the target to the immobilized phages can generate signals that can be detected via quartz crystal microbalance, magnetoelastic platform, surface plasmon resonance, and electrochemical methods (Farooq et al. 2018; Singh et al. 2020). Horikawa et al (Horikawa et al. 2016) combined wireless phage-coated magnetoelastic (ME) biosensors and a surface-scanning detector, allowing real-time monitoring of bacterial growth.

Phage-display technology has been applied as an effective method to develop probe phages that can bind to various bacteria of interest. In 1985 (Smith 1985), it was discovered that a foreign peptide can be inserted into the viral chromosome and expressed on the surface of the recombinant filamentous phages without affecting their general fitness. The finding became the foundation of phage-display technology, which generally uses numerous recombinant phages expressing a library of peptides to select the ones with strong and specific binding to the target (Tan et al. 2016). For instance, De Plano et al (De Plano et al. 2019) constructed a library of M13 phage expressing recombinant major coat protein (pVIII) containing random 9-mer peptides from which viral clones that specifically bind to *S. aureus, P. aeruginosa* or *E. coli* are selected. The specificity of the phages is also confirmed using ELISA. Furthermore, the selected clones are covalently conjugated to magnetic beads as recognizing probes. After incubating the beads with a blood sample containing certain pathogens, the targeted pathogens incubating the beads with blood containing certain pathogens, the targets are captured and detected using micro-Raman spectroscopy. The method can detect 10 CFU in 7 mL of blood. Generally, phage-display technology provides a powerful tool to develop probes similar to antibodies rapidly, and it can be incorporated into various biosensors.

The second strategy of phage-based biosensor takes advantage of the infection mechanism of host-specific phages, allowing various forms of signals generating from either the increasing

number of progeny phages and cell lysis content or the transferred signaling-gene harboring plasmid (Paczesny et al. 2020).

To detect the increasing number of progeny phages, Martelet et al (Martelet et al. 2015) employed specific immunomagnetic separation beads to capture the progeny phages and detected them by liquid chromatography coupled with targeted mass spectrometry. In their platform, phage T4 is used for *E. coli* infection. This method allows them to detect viable *E. coli* in food matrices (Martelet et al. 2015). To detect the cell lysis content, Chen et al (Chen et al. 2015a) fabricated a bacteriophage-based sensor for *E. coli* (**Figure 2**). The bacteriophage-conjugated magnetic beads are used to capture *E. coli*. Once the phage-mediated lysis happened, the endogenous β-galactosidase is detected using chlorophenol red-β-d-galactopyranoside (CRPG) (Chen et al. 2015a). Zhang et al (Zhang et al. 2016a) developed a phage-based sensor relying on the last principle: detecting signals from the phage-infected bacteria plasmid. They modified the *E. coli* -specific bacteriophage ΦV10 to allow the expression of NanoLuc luciferase. Once the phage infects the *E. coli*, it harbors the plasmid containing luciferase coding gene and produces a robust bioluminescent signal upon the addition of luciferin (Zhang et al. 2016a). Likewise, Franche et al (Franche et al. 2017) developed a substrate-independent phage-based sensor by integrating the full *luxCDABE* operon and tested it under different bacterial promoters. They found that P*rplU* bacterial promoter is the most efficient in terms of signal emission for *E. coli* detection. This tool has a LOD of 10^4 CFU/mL, and the detection time is 1.5 h without employing an enrichment or a sample concentration step (Franche et al. 2017).

The leading advantage of phage-based sensors is their capability of differentiating live or dead bacteria because bacteriophages can only proliferate in live bacterial cells. Besides, as opposed to antibodies, phages can be produced in bulk, making phage-based sensors a more economical choice (Farooq et al. 2018). An obvious challenge is to isolate a bacteriophage that has a broad host range so that false-negative results can be avoided. Besides, bacteriophages usually recognize a particular receptor on the bacterial surface; therefore, it is critical to test a phage-based sensor with a relatively large group of isolates of the target and non-target bacteria to reduce the possibility of false-negative detection.

1.6 Mammalian cell-based sensor

The limitation of previously mentioned sensors is that none of these tests can confirm the functionality of the targeted toxin and pathogen, as antibody only picks up a specific region on the surface, and aptamers only recognize a partial sequence of the analyte. Phage-based sensors may detect live bacteria but still cannot confirm their pathogenetic attributes. Cell-based sensor (CBS) overcomes this problem by employing live cells as recognition elements (To et al. 2020). The targeted analytes can interact with the cells, just like how they interact with human intestines or other tissues. Signals can be generated through various types of cellular responses upon the addition of the analytes. On the other hand, the cell-based sensor can generate similar electrochemical (Ge et al. 2018; Jiang et al. 2020), colorimetric (To and Bhunia 2019a), or fluorescent (Sun et al. 2018) signals as other types of biosensors mentioned above. The three-dimensional (3D) cell-based sensor is in high demand because cells grow in a 3D matrix that mimics the actual tissue configuration of the mammalian host, therefore, have great potential in the development of a highly sensitive and accurate sensor (Banerjee et al. 2008; Banerjee and Bhunia 2010; To and Bhunia 2019a; Jiang et al. 2020).

The commonly used approach to monitoring cellular responses is to measure cytotoxicity (Banerjee et al. 2008; Banerjee and Bhunia 2009; 2010). To and Bhunia (To and Bhunia 2019a) recently proposed a three-dimensional Vero cell-based sensor to detect Shiga-toxin producing *E. coli* cells or Shiga toxin (Stx). When exposed to STEC/Stx, the cytotoxicity values are increased, which are then used as an indicator of the STEC presence in the food sample (To and Bhunia 2019a). The sensor's detection limit is estimated to be 10^7 CFU/mL for bacteria and about 32 ng/mL for Stx in 6 h. Other cellular activities, such as cell viability, apoptosis, and intracellular calcium could also be monitored as alternative approaches for pathogen/toxin detection because the exposure to different triggers influences those activities. Jiang et al (Jiang et al. 2017) recently reported a mast cell-based electrochemical sensor for detecting N-acyl-homoserine-lactones (AHL), a pathogenic bacterial quorum signaling molecule. They utilized rat basophilic leukemia (RBL-2H3) mast cell line to detect AHL and effectively convert the biological recognition into a quantified signal using β-hexosaminidase assay, flow cytometry, and calcium measurement (Jiang et al. 2017).

To have the signal produced simultaneously as these cells respond to the analytes, one could transfect a reporter gene carried plasmid into the cell or insert a reporter gene after a gene that is

inducible upon analyte exposure. The reporter gene system application could be used to predict the toxicity level by measuring the chemical-induced response. Alternatively, it could be used to predict the presence of pathogens by detecting the bacterial component-induced signaling pathway. Abu-Baker et al. (Abu-Bakar et al. 2018) employed a luciferase reporter plasmid to reflect *in vivo* response from toxin insult. Under chemical-induced stress, transcription factors, such as aryl hydrocarbon receptor (Ahr) and nuclear factor (erythroid-derived 2) - like wild-type (Nrf2) are activated, resulting in elevated murine cytochrome P450 2a5 (Cyp2a5) gene transcription. By constructing the regulatory regions of Cyp2a5 in a luciferase reporter plasmid, they could predict the toxicity level in a sample (Abu-Bakar et al. 2018). Sun et al (Sun et al. 2018) took advantage of the recognition ability of TLR4 to lipopolysaccharides (LPS), an outer membrane component of Gram-negative bacteria. They developed a cell-based sensor to detect LPS in the food product as a biomarker for Gram-negative bacterial contamination (**Figure 2**). They transfected the cell with a recombinant plasmid that contains the key target gene MCPIP1 promoter of the LPS toxicity pathway and a green fluorescent protein. Upon exposure to LPS, the intensity of fluorescence was analyzed to reflect the LPS concentrations (Sun et al. 2018).

One problem that hinders CBS from being used commercially is that they are expensive due to the high maintenance cost and short shelf-life. Extending the shelf-life and reducing the maintenance effort of CBS are essential for realizing its practical utility. In general, there are three approaches to do so: utilizing lyophilization or encapsulation, using cells that can naturally survive well or incorporating an automated machine to maintain a constant pool of actively growing cells (Roggo and van der Meer 2017). Lyophilization and encapsulation methods still require a specific storage condition, such as -20°C or -80°C, to maintain viability (Hicks et al. 2020). For the second approach, Widder et al (Widder et al. 2015) have explored the possibility of seeding the rainbow trout gill epithelial cells on a microfluidic biochip to monitor drinking water toxicity by measuring the impedance. This sensor could be stored at 6°C to maintain the cell line's biological property (Widder et al. 2015). As for the latter approach, an automated system could keep the cells alive or active for a longer time, but it is not portable, thus limiting its point-of-care deployment.

Most recently, Xu et al (Xu et al. 2020) reported another method to extend the shelf life of CBS to 14 weeks. They used the formalin fixation method to preserve the biological activity of the cells. Live enteric pathogens can adhere to the cell surface and be detected using specific antibodies. Such a sensor takes advantage of the target pathogen's adhesion capacity to the host

cells (mammalian cells) and specific detection of the captured pathogen by antibodies hence designated mammalian cell-based immunoassay or MaCIA. MaCIA can detect *Salmonella* Enteritidis from inoculated ground chicken, cake mix, milk, and egg samples at 10 CFU/25 g within 16-21 h employing the traditional enrichment method, but the detection time could be shortened to 10-12 h when employing "on-cell enrichment" method. MaCIA also can differentiate live from dead *Salmonella* based on the principle that live *Salmonella* has a much higher adhesion efficiency than the dead ones. Admittedly, MaCIA still needs further optimization and rigorous testing with various food matrices before routine use is recommended. Besides, the utility of MaCIA could be broadened for the detection of other foodborne pathogens by using pathogen-specific antibodies. Combining the principle of different biosensors, in this case, immunosensor and cell-based sensors, are worth to be explored, because such an approach could enhance the accuracy of testing results by utilizing the positive attributes of each platform.

1.7 Light scattering sensor

Light scattering sensors have been evolved for years, from detecting bacterial cells in suspension to direct-on-plate colony detection (Banada et al. 2009). It is a phenotypic screening tool to identify the bacteria at the genus, species, or even at the serovar level when comparing the light scattered pattern to the scatter signature classification library. Unlike the previously described biosensors, light scattering sensors do not need a biorecognition molecule, making it easier to fabricate. It is not a prototypical biosensor where biorecognition molecules are essential, however, biorecognition systems such as IMB can improve assay specificity by isolating target bacteria from the food matrix before subjecting them to a light scattering sensor. After selective enrichment and plating on a selective agar plate, the unique light scattered pattern of each colony is projected using the laser diode of 635 nm (Singh et al. 2014). This unique scatter pattern is then compared with the classification library for identification. During this operation, the colony integrity and viability of the bacteria are maintained thus viable cells are available for further molecular, biochemical, or pathogenesis-based confirmatory tests. Therefore, light scattering sensors can serve as an alternative real-time, non-destructive detection and identification method, as opposed to the traditional identification methods, such as biochemical tests or PCR.

The recent research progress of light scattering sensors focuses on establishing a comprehensive signature library. BARDOT is the leading technology for light scattering sensors

in the past decades and was developed at Purdue University, and its application has been investigated by expanding the library. BARDOT has been used for rapid screening of *Bacillus* (Singh et al. 2015b), *Salmonella* (Singh et al. 2014; Abdelhaseib et al. 2016), *Listeria* (Banada et al. 2007; Abdelhaseib et al. 2019), *Vibrio* (Huff et al. 2012), Shiga-toxin producing *E. coli* (Tang et al. 2014; Abdelhaseib et al. 2019), and *Staphylococcus* spp. (Alsulami et al. 2018; Kitaoka et al. 2020). Moreover, the accuracy rate is often greater than 90%. BARDOT has been also used for the identification and differentiation of the *Enterobacteriaceae* family (Singh and Bhunia 2016). It is also a valuable tool to study bacterial phenotypes resulting from mutation (Singh et al. 2016) or antibiotics exposure (Singh et al. 2015a; Zhu et al. 2018).

What sets BARDOT apart from other biosensors is its ability to identify bacteria in real-time with little effort. However, unlike other biosensors, which incorporate a recognition molecule to target virulence properties, such as a pathogenic gene (nucleic acid-based sensors), a pathogenic factor (immunosensors), or a pathogenic interaction (cell-based sensors), BARDOT relies solely on the scatter signature, which makes it difficult to distinguish pathogenic and non-pathogenic strains that display a similar pattern. Besides, bacterial culturing conditions, such as incubation time and growth media, may also affect the pattern, limiting the application of this tool within a specific time range and enrichment condition. The commercial success of BARDOT depends on the availability of a reliable library for each pathogenic strain, which may take a considerable amount of time for optimization. BARDOT may find its broad utility as a screening tool before confirmatory tests (PCR, WGS, mass-spec), which are often expensive and lengthy, could be performed.

1.8 Conclusions and future perspectives

To reduce the numbers of foodborne illness cases, and at the same time reduce the amount of food waste due to false-positive result, researchers have always been seeking ways to develop new detection tool that is faster and more accurate. The progress of biosensors in the last five years, as this review covered, has been growing tremendously. Even though these studies have used various approaches to build the sensors, their ultimate goals of enhancing the sensitivity, reducing the detection time, and improving the portability remain coherent.

The traditional immunoassays for foodborne pathogen detection include enzyme-linked immunosorbent assay and lateral flow. Current immunosensors have leveraged the basic principles

of the traditional methods while boosting the assay's sensitivity. The recent trend is to utilize nanoparticles, such as gold nanoparticles for antibody coating, to increase the amount of coated antibody needed and the conductivity for excellent electrochemical signal transduction. Other trends of improving the sensitivity include incorporating QCM and SPR into the detection process to construct a faster and more sensitive tool. The limitation of these sensors is that the sampling amount is relatively small compared to the FSIS or the FDA methods, where 25 g of food sample homogenized in 225 ml of enrichment broth is suggested. Better sample concentration technologies that collect bacteria from food samples of 25 g into small volumes will be necessary for the further practical application of those ultrasensitive immunosensors.

Similar to the immunosensors, nucleic acid-based biosensors are also attractive. Instead of using an antibody as the recognition molecule, researchers employ ssDNA to capture the analytes, but the assay requires an extra step to release nucleic acid from cells. One advantage of this type of sensor is that oligonucleotide is cheaper to produce than the antibody, which makes it a more economical option. Though both immunosensors and nucleic acid-based biosensors have shown promising results in producing accurate identification in a shorter time, they can't differentiate functional from nonfunctional analytes (dead cells), thus has greater potential to generate a false-positive result.

Phage-based and mammalian cell-based biosensors can overcome certain limitations. Researchers take advantage of the phages' biological properties or the cells to design a biosensor that could serve as a functionality test. A serious concern of these biosensors also arises due to the dependence of their biological activity. These sensors usually require critical maintenance and storage conditions to preserve their biological activities. Therefore, discovering new approaches for extending these biosensors' shelf-life will become the essential goal for futures investigations.

Light scattering sensor interrogates bacterial phenotypes with a laser diode and computer interface and can identify bacteria at genus, species, and serovar levels. The actual detection time is much faster than any of the biosensors above but has limitations. Since the accuracy is dependent on the scattered patterns, growing time and condition for these colonies are extremely critical. Finding the proper combination of enrichment media, incubation time, and developing an exhaustive library for each pathogenic strain, could be time-consuming but is worthwhile to investigate due to its highly accurate real-time detection capabilities.

In general, biosensors have received extreme attention over the past five years. Researchers have tried numerous approaches to close gaps in the biosensor design and assay performance. However, more studies should be focused on advancing each sensor's practical utility as a screening tool or as a final decision-making tool to ascertain the safety of the food products. These faster and more sensitive sensors could be used commercially to improve food safety and security while reducing unnecessary food waste.

CHAPTER 2. MAMMALIAN CELL-BASED IMMUNOASSAY FOR DETECTION OF VIABLE BACTERIAL PATHOGENS

*This chapter has been recently published in the peer-reviewed journal, Frontiers in Microbiology (Xu, L., Bai, X., Tenguria, S., Liu, Y., Drolia, R., and Bhunia, A.K. 2020. Mammalian cell-based immunoassay for detection of viable bacterial pathogens. Front. Microbiol. 11:575615; doi: 10.3389/fmicb.2020.575615.)

2.1 Introduction

Pathogen interaction with the host cells is the crucial first step for initiating infection (Finlay and Falkow 1997; Kline et al. 2009), and harnessing such interaction may yield a robust detection platform not only to assess pathogenic potential but also its viability. Mammalian cell-based biosensors (CBBs) exploit host-pathogen interactions including pathogen adhesion, activation of host cell signaling events, cell-cycle arrest, apoptosis, and/or cytotoxicity (Banerjee and Bhunia 2009). The ability to detect host-pathogen interaction makes CBB a functionality test, thus sets it apart from other conventional methods (Banerjee and Bhunia 2009). A common approach to monitoring such interaction is to measure the cytotoxic effects of the analytes on mammalian cells. Gray et al. (Gray et al. 2005) used lymphocyte (Ped-2E9)-based cytotoxicity assay to detect toxin produced by *Bacillus cereus*. Later, this cell line was used in a collagen-encapsulated 3-D platform to detect *Listeria monocytogenes* cells and its toxins (Banerjee et al. 2008) and several other toxin-secreting foodborne pathogens (Banerjee and Bhunia 2010). Most recently, a 3-D Vero cell-platform was made to screen Shiga-toxin producing *Escherichia coli* (STEC) by measuring lactate dehydrogenase (LDH) release.(To and Bhunia 2019b) Although these studies demonstrate the versatility of CBBs in detecting foodborne pathogens and toxins, the specificity of CBBs cannot be guaranteed when the detection solely relies on cytotoxicity measurement because cytosolic proteins/enzymes could be released from cells in response to more than one type of triggers. Furthermore, researchers have pointed out the short-comings of the practical applicability of CBBs due to the short shelf-life and the requirement for stringent growth conditions of mammalian cells outside a controlled laboratory environment (Bhunia et al. 1995; Banerjee et al. 2007; Banerjee and Bhunia 2009; Ye et al. 2019). Thus, novel approaches for developing CBBs with higher specificity and longer shelf-life are in continued demand.

Pathogen detection is categorized into three basic types: culture-based, immunological, and nucleic acid-based (Bhunia 2014; Lee et al. 2015; Bell et al. 2016; Schlaberg et al. 2017; Ricke et

al. 2018; Rajapaksha et al. 2019). The detection time for the culture-based method is usually 4-7 days. Immunological and nucleic acid-based PCR methods are faster, but the inherent inability to assess the viability or the pathogenic potential of the target microorganisms is of concern (Bhunia 2014; Kasturi and Drgon 2017; Ricke et al. 2018). Moreover, these methods are often prone to interferences from sample inhibitors and resident microflora. Alternative detection methods that are faster, user-friendly, and accurate are in high demand (Bhunia 2014). Therefore, CBBs have been proposed to serve as a reliable tool for the rapid screening of viable pathogens or active toxins in foods (Ngamwongsatit et al. 2008; Banerjee and Bhunia 2009; Bhunia 2011; Ye et al. 2019; To et al. 2020). However, maintaining the viability of mammalian cells outside the laboratory environment is a major challenge thus limits CBB's utility in routine foodborne pathogen testing (Bhunia et al. 1995; Banerjee et al. 2007; Banerjee and Bhunia 2009; Ye et al. 2019).

In this study, we took an innovative approach and developed a shelf-stable Mammalian Cell-based ImmunoAssay (MaCIA) platform for the detection of live pathogenic bacteria. Shelf-life of MaCIA was prolonged by fixing the mammalian cells in formalin (4% formaldehyde) which is a common practice in histology and tissue imaging to preserve the cells by preventing protein degradation (Eltoum et al. 2001). Furthermore, instead of measuring cytotoxicity, we took advantage of the adhesion ability of enteric pathogens to the intestinal cells followed by antibody-based assay for specific detection of the adhered target pathogens. Adhesion to the epithelial cells is the crucial first step for enteric pathogens (Kline et al. 2009; dos Reis and Horn 2010). For example, *L. monocytogenes* binds to Hsp60 and E-cadherin on the epithelial cell surface through *Listeria* adhesion protein (LAP) and Internalin A (InlA), respectively to initiate adhesion, invasion, translocation, and systemic spread during the intestinal phase of infection (Drolia et al. 2018; Drolia and Bhunia 2019). Enterohaemorrhagic *E. coli* employs intimin, fimbrial proteins, flagella, and autotransporter proteins to attach to the host cells at different stages of its life cycle during infection (McWilliams and Torres 2014). Likewise, *Salmonella enterica* utilizes multiple fimbrial adhesins, such as type 1 fimbriae (T1F) and long polar fimbriae (Lpf), and several autotransporter adhesins, such as ShdA and MisL, to promote adhesion to D-mannose receptors on M cells in Peyer's Patches and assist colonization in the intestine (Bäumler et al. 1996; Wagner and Hensel 2011; Bhunia 2018; Kolenda et al. 2019). Therefore, detecting only adhered pathogens using antibodies is a rational approach. We chose human ileocecal adenocarcinoma cell line, HCT-8, as the target cells for building MaCIA platform on 24-well tissue culture plates. HCT-8 is one of the

commonly used model cell lines to study the adhesion of enteric pathogens (McKee and O'Brien 1995; Dibao-Dina et al. 2015; Hu and Wai 2017). Unlike other cell lines used, HCT-8 cells can form a fully confluent monolayer in only five days.

The objective of this study was to develop a shelf-stable MaCIA platform for the rapid detection of viable bacterial pathogens and to validate its performance using *Salmonella enterica* serovar Enteritidis as a model foodborne pathogen.

Salmonella enterica is a major foodborne pathogen of global public health concern. Meat, poultry, eggs, nuts, fruits, and vegetables are common vehicles for *Salmonella* transmission. Each year, *Salmonella* infections contribute to 1.3 billion cases of gastroenteritis and 3 million deaths worldwide (Kirk et al. 2015) and 1.35 million cases, 26,500 hospitalizations, and 420 deaths in the United States of America (CDC 2020). Among *Salmonella* serovars, *Salmonella enterica* serovar Enteritidis is one of the most prevalent serovars in the US. The Centers for Disease Control and Prevention (CDC) has reported eight major outbreaks between 2006 and 2018 resulting in about 4,000 cases (CDC 2018). In a survey of salmonellosis outbreaks (total 2447) in the USA between 1998 and 2015, *S*. Enteritidis (29.1%) was reported to be the most common serovar followed by *S*. Typhimurium (12.6%), *S*. Newport (7.6%), and others (Snyder et al. 2019). The frequent occurrence of food-associated *S*. Enteritidis outbreaks with the high number of infections was the motivation for developing a mammalian cell-based functional bioassay for the detection of *S*. Enteritidis.

The initial study involved screening of MaCIA with a panel of food-associated bacterial cultures (**Table 1**) in confirming the specificity and the limit of detection (LOD) from artificially inoculated food samples. Next, the performance of MaCIA was validated using the US Department of Agriculture (USDA-FSIS 2013) and the Food and Drug Administration (FDA 2001) reference methods. “On-cell enrichment” and “one-step antibody probing methods” of MaCIA were also explored to reduce the assay steps and total detection time. Overall, the data showed that MaCIA could detect viable *S*. Enteritidis (1-10 CFU/25g) in ground chicken, shelled eggs, whole milk, and cake mix using a traditional enrichment set up, but the detection time was shortened to 10-12 h using direct on-cell (MaCIA) enrichment. We also demonstrated the versatility of MaCIA by using a commercial anti-*Salmonella* reporter antibody for the detection of *S*. Typhimurium. Formalin-fixed cells in the MaCIA platform permits a longer shelf life (at least 14-week at 4°C), minimum on-site maintenance care, and a stable cell monolayer for point-of-need deployment.

2.2 Materials and Methods

2.2.1 Mammalian cell culture

HCT-8 cell line (ATCC, Manassas, VA) was maintained in Dulbecco's modified Eagles medium (DMEM) (Thermo Fisher Scientific) with 10% fetal bovine serum (FBS) (Bio-Techne Sales Corp, Minneapolis, MN) at 37°C with 5% CO_2 in cell culture flasks (T25). For all experiments, HCT-8 cells were seeded in 24-well tissue culture plates (Fisher Scientific) at a density of 5×10^4 cell/mL/well. Media were replaced on day 4 and a final cell density of 2×10^5 cell/mL (monolayer) was achieved on day 5. Cell monolayers were washed twice with PBS (0.1 M, pH 7.0) and used immediately (Live HCT-8 cell assay) or exposed to 4% formaldehyde (Polysciences Inc., Warrington, PA) of 500 µL/well and incubated at room temperature for 10 min (Formalin-fixed HCT-8). Formaldehyde solution was removed and the cell monolayers were washed three times with PBS. Formalin-fixed cells were stored in 1 mL PBS/well for 14 weeks at 4°C or until use.

2.2.2 Bacterial Culture and Growth Media

Bacterial strains (**Table 2.3**) were stored as 10% glycerol stocks at -80°C. To revive frozen cultures, each strain was streaked onto tryptic soy agar (TSA) (Thermo Fisher Scientific, Rochester, NY) plate and incubated at 37°C for 18 h to obtain pure colonies. A single colony of each strain was inoculated and propagated in tryptic soy broth containing 0.5% yeast extract (TSBYE) (Thermo Fisher Scientific) at 37°C for 18 h with shaking at 120 rpm.

2.2.3 Development of Specificity of MaCIA

HCT-8 cell monolayers were prepared and maintained as described above in 24-well plates. Overnight grown bacterial cultures (**Table 2.3**) were diluted in PBS to achieve a cell concentration of 1×10^7 CFU/ml. To obtain dead cells, cell suspensions were treated with heat (80°C for 10 min) or formaldehyde (4% for 10 min) and plated on TSA to ensure bacterial inactivation. One milliliter of bacterial cell suspensions was added into each well containing HCT-8 cells and incubated for 30 min at 37°C (Jaradat and Bhunia 2003; Barrila et al. 2017). Cell monolayers (live or formalin-fixed) were washed 2-3 times with PBS gently and sequentially probed with either mAb-2F11 (3.06 µg/mL) (Jaradat et al. 2004) or mAb-F68C (0.2 µg/mL) (Catalog # MA1-7443; Thermo

Fisher Scientific) as primary antibodies, and anti-mouse HRP-conjugated IgG (0.1 μg/mL) (Cell-Signaling, Danvers, MA) as secondary antibodies for 1.5 h each at room temperature. Both antibodies were suspended in PBS containing 3% bovine serum albumin (BSA) (Sigma-Aldrich). For one-step antibody probing, both mAb-2F11 and anti-mouse HRP conjugated secondary antibodies were mixed in PBS containing 3% BSA and incubated for 1.5 h. Cell monolayers were washed 3 times with PBS and the color was developed by adding 500 μl/well substrate solution (o-phenyl diamine, OPD) containing hydrogen-peroxide) (Sigma-Aldrich). The oxidative coupling of OPD to 2,3-diaminophenazine, an orange-brown substance, was catalyzed by HRP at room temperature in the dark for 10 min. The intensity of the colored product was measured using a microplate reader (BioTek, Winooski, VT) at a wavelength of 450 nm.

2.2.4 Sandwich ELISA

High-affinity (4HBX) ELISA plates (Thermo Fisher Scientific) were coated with mAb-2F11 for 2 h at 37°C, followed by 3 times wash with PBS-T (PBS containing 0.01% Tween-20). Freshly prepared BSA-PBS solution (1 mg/mL) was used for blocking at 4°C overnight, followed by 2× PBS-T wash. Freshly prepared viable or formalin-inactivated cells of *S.* Enteritidis (1×10^8 cells/100 μl) were added to each well and incubated at 37°C for 30 min or 2 h. Anti- *Salmonella* pAb-3288 (2.86 μg/mL) used as a reporter (Abdelhaseib et al. 2016) and an HRP-conjugated anti-rabbit antibody (0.25 μg/mL) as the secondary antibody. After 3 washes with PBS-T, the OPD substrate was added and the absorbance (450 nm) was measured.

2.2.5 Western blot

The whole-cell lysate of *L. monocytogenes* F4244, *Pseudomonas aeruginosa* PRI99, *E. coli* EDL933, and *S.* Enteritidis PT21 overnight cultures (5 mL each) was prepared by sonication (Branson, Danbury, CT). Bacterial samples were sonicated in an ice bucket (three 10 seconds cycles at 30-sec intervals) and centrifuged for 10 min at 14,000 rpm (Eppendorf) at 4°C to separate the soluble fraction (supernatant) from the bacterial debris (pellet). The protein concentration was determined by the BCA method (Thermo Fisher Scientific). Equal amounts of proteins were separated on SDS-PAGE gel (10% polyacrylamide) and electro-transferred to polyvinylidene difluoride (PVDF) membrane (Fisher Scientific) (Singh et al. 2016; Drolia et al. 2018). Primary

and secondary antibodies were diluted as above. Membranes were first probed with mAb-2F11 at 4°C overnight, and then with anti-mouse HRP conjugated antibody at room temperature for 1.5 h. LumiGLO reagent (Cell-Signaling Technology) was used to visualize the bands using the Chemi-Doc XRS system (Bio-Rad).

2.2.6 Immunofluorescence and Giemsa Staining

After exposure of formalin-fixed HCT-8 cell monolayers to viable or dead *S.* Enteritidis (1×10^8 cells/ml) for 30-min, the wells of the chambered slides (Fisher Scientific) were washed with PBS to remove unattached bacterial cells (as above). After immunoprobing with mAb-2F11, the monolayers were washed and probed with Alexa Fluor 488 conjugated anti-mouse antibody for 1.5 h at room temperature in the dark, followed by three PBS wash. Note, antibody concentrations used were the same as above. The monolayers were counterstained with DAPI (500 ng/mL) (Cell-Signaling) for nuclear staining and the slides were mounted using an antifade reagent (Cell-Signaling). Images were acquired using the Nikon A1R confocal microscope with a Plano AP VC oil immersion objective (Drolia et al. 2018) and were processed with the Nikon Elements software at the Purdue Bindley Bioscience Imaging Facility.

For Giemsa staining, the formalin-fixed HCT-8 cell monolayers were exposed to viable or dead *S.* Enteritidis cells as above, air-dried, and immersed in Giemsa staining solution for 20 min. Giemsa staining solution was prepared using a 20-fold dilution of the KaryoMAX Giemsa staining solution (Thermo-Fisher) in deionized water. The slides were examined under a Leica DAS Microscope at the magnification of 1000×.

2.2.7 Sensitivity of MaCIA

HCT-8 cell monolayers were prepared and maintained as described above in 24-well tissue culture plates. Overnight grown fresh *S.* Enteritidis PT21 culture was serially diluted to obtain 1×10^8 CFU/mL to 1×10^4 CFU/mL using PBS or homogenized 25 g food samples (**Table 2.1**) in 225 mL BPW (Becton Dickinson, Sparks, MD). One milliliter of each diluted sample was added onto HCT-8 cell monolayer and was incubated at 37°C for 30 mins. The remaining steps were the same as above.

Table 2.1: Total detection time required for each method

Test sample	Assay completion time (hour)			
	MaCIA (Out-cell enrichment)	MaCIA (On-cell Enrichment)	USDA-FSIS	FDA-BAM
Ground Chicken	16	10	72	NA
Shelled egg	21	10	NA	168
Whole milk	18	12	NA	72
Cake mix	18	12	NA	72

NA, not applicable

2.2.8 Detection of stressed cells using MaCIA

Freshly prepared *S.* Enteritidis cells (2.17×10^8 CFU/ml) suspended in TSB were exposed to cold (4ºC), heat (45ºC), acidified TSB (pH, 4.5) and 5.5% NaCl for 3 h, as reported before (Hahm and Bhunia 2006). Bacterial cells were washed with PBS and added onto the fixed HCT-8 monolayer for 30-min and probed with mAb-2F11 as above.

2.2.9 *Salmonella* Growth Kinetics Assessment

Overnight-grown *S.* Enteritidis PT21 cultures were serially diluted in PBS to achieve a concentration of 1×10^2 CFU/mL. One hundred microliters of the diluted culture were added into 25 g of each ground chicken, whole fat milk, liquid eggs, and cake mix with 225 mL BPW and were incubated at 4°C for 24 h. The samples were then incubated at 37°C for 20 h with shaking at 120 rpm and enumerated on XLD (xylose lysine deoxycholate) agar plates (Remel, San Diego, CA) at every hour. *S.* Enteritidis counts in artificially inoculated samples at earlier stages of growth was determined by directly plating 1 mL, 0.5 mL, 0.1 mL of the sample on XLD plates with four repeats (1 h, 2 h, and 3 h); and *S.* Enteritidis counts from the later stages of growth (3 h and after) was obtained after serially diluting the samples in PBS. The growth of *S.* Enteritidis in food samples enriched using BPW was modeled using the Gompertz equation (Silk et al. 2002; Kim and Bhunia 2008) through Prism software version 8.0. Lag-phase duration (LPD) and exponential growth rate (EGR) were calculated from the Gompertz model and were used to determine an enrichment time required for each food product to reach an optimum *S.* Enteritidis concentration required for detection by MaCIA, assuming the initial concentration was 1 CFU/25 g of sample.

2.2.10 Food Sample Testing with MaCIA and Validation with the FDA and USDA Methods

Food samples (ground poultry, milk, egg, or cake mix) were inoculated with variable concentrations of *S.* Enteritidis PT21. To simulate cold storage, inoculated foods were stored at 4°C for 24 h. Samples (25 g in 225 mL BPW) were then homogenized or pummeled using hands and incubated at 37°C for 14-19 h (**Table 2.4**) with shaking at 120 rpm. One milliliter of enriched food sample was added into each well of MaCIA for 30 min, followed by immunoprobing as above.

For direct on-cell enrichment, the homogenized food suspensions (1 ml of each food sample) were dispensed into wells containing formalin-fixed HCT-8 cells (MaCIA) and incubated for 7-9 h. After the removal of food samples, wells were washed 3 times with PBS before immunoprobing and color development. *Salmonella* counts in enriched food samples (inoculated or uninoculated) were enumerated on XLD plates. The presence of background bacteria in uninoculated food samples was assessed on TSA plates after incubation at 37°C for 24 h. For the blind test, the inoculation of the samples was performed by XB, while the MaCIA test was done by LX in a blinded fashion without prior knowledge of samples that were inoculated with *Salmonella*.

Inoculated food samples were also analyzed by the FDA-BAM (FDA 2001) or USDA-FSIS (USDA-FSIS 2013) method as before. The ground chicken was processed according to the USDA-FSIS method, while shelled egg, whole milk, and cake mix were prepared based on the FDA-BAM. Twenty-five gram of each prepared sample was then enriched in 225 mL of BPW (ground chicken), trypticase soy broth (shelled egg), and lactose broth (whole milk and cake mix) at 37°C for 24 h followed by sequential enrichment in RV (Rappaport-Vassiliadis) broth and TT (tetrathionate) broth at 42°C for 24 h. Samples were then plated on selective BGS (Brilliant Green Agar with Sulfadiazine) or XLD agar plates to isolate colonies, which were further confirmed by PCR assay.

For PCR assay, DNA was extracted from the isolated colonies by the boiling method (Kim and Bhunia 2008; Kim et al. 2015). The primer sequences and the putative product sizes for each amplicon are listed in **Table 2.2** (Wang and Yeh 2002; Paião et al. 2013). PCR reaction mixture (25 μL) contained 1 μL of DNA template, 0.2 μM of each primer, 2.5 mM $MgCl_2$, 200 μM of dNTP, 1 x GoTaq Flexi buffer of buffer and 1 U of GoTaq Flexi DNA polymerase (Promega) (Singh et al. 2014). The PCR amplification was performed in the Proflex PCR system with an initial denaturation at 94°C for 3 min, 35 amplification cycles consisting of 1 min of denaturation at 94°C, 1.5 min of annealing at 50°C, and 1.5 min of elongation at 72°C. DNA amplicons were

analyzed using agarose gel (1.5%, wt/vol) electrophoresis containing ethidium bromide (0.5 μg of /mL).

Table 2.2: PCR primer sequences used

Pathogen	Target gene	Primer	Sequence (5'-3')	Product Size (bp)	References
Salmonella enterica serovar Enteritidis	Insertion element (IE-1)	F	AGT GCC ATA CTT TTA ATG AC	316	(Fratamico and Strobaugh 1998; Wang and Yeh 2002)
		R	ACT ATG TCG ATA CGG TGG G		
	Insertion element (IE-2)	F	GGA TAA GGG ATC GAT AAT TGC	559	(Wang and Yeh 2002)
		R	GGA CTT CCA GTT ATA GTA GG		
Salmonella enterica serovar Enteritidis and Typhimurium	Invasion protein A (Inv-A)	F	CGG TGG TTT TAA GCG TAC TCT T	796	(Fratamico and Strobaugh 1998; Paião et al. 2013)
		R	CGA ATA TGC TCC ACA AGG TTA		

2.2.11 Swab Sample Testing

Chicken thigh cuts (procured from a local grocery store) were inoculated with overnight grown *S.* Enteritidis PT21 at 1.35×10^3 to 1.35×10^5 CFU per 50 cm^2 evenly on the skin of chicken thighs. Inoculated samples were stored at 4°C for 24 h. BPW-soaked sterile rayon tipped swab applicators (Puritan, ME) were used to swab the chicken skin and were vortexed in 1.1 mL of BPW. One milliliter of the sample was added into each well of MaCIA and incubated at 37°C for 7 h for on-cell enrichment, followed by immunoprobing as above. The rest of the swabbed sample (0.1 mL) was used to enumerate *Salmonella* on XLD plates.

2.2.12 Statistical Analysis

All data were analyzed using GraphPad Prism software (San Diego, CA). The unpaired *t*-test was used when comparing two datasets. Tukey's multiple comparison test was also used when comparing more than two datasets. All data were presented with mean ± standard error of the mean (SEM).

2.3 Results

2.3.1 Development of MaCIA (Mammalian Cell-based ImmunoAssay) Platform

The MaCIA platform was built on a 24-well tissue culture plate, and it consisted of two steps: fixation of mammalian cells and immunoassay for specific detection of adherent target pathogens. We used the formalin-fixed HCT-8 cell line for *Salmonella* adhesion/capture (30 min) and anti-*S.* Enteritidis monoclonal antibody, mAb-2F11 (Masi and Zawistowski 1995), or anti-*Salmonella* mAb-F68C (Thermo Fisher Scientific) (1.5 h), horseradish peroxidase (HRP)-conjugated second antibody and a substrate for color development (1.5 h). The mAb-2F11 is highly specific for *S.* Enteritidis (Masi and Zawistowski 1995; Jaradat et al. 2004), and the Western blot analysis confirmed its specificity without showing any reaction with bands from whole-cell preparations of *L. monocytogenes*, *E. coli* O157:H7 or *Pseudomonas aeruginosa* (**Fig. 2.1A**).

To fix mammalian cells on the MaCIA platform, HCT-8 cell monolayers in 24 well-plates were treated with a 4% formaldehyde solution for 10 min, followed by three sequential wash using phosphate-buffered saline (PBS, 0.1 M, pH 7). Initially, the performance of formalin-fixed MaCIA was compared with a live cell-based MaCIA platform to detect *S.* Enteritidis PT21 that was incubated for 30 min at 37°C. Remarkably, both assay configurations showed strong positive signals towards viable *S.* Enteritidis, which was significantly ($P < 0.0001$) higher than the equivalent amounts of dead *S.* Enteritidis cells (verified by plating) and the negative control (PBS) (**Fig. 2.1B**).

The performance of MaCIA was also compared with traditional sandwich ELISA where mAb-2F11 was used as capture and anti-*Salmonella* pAb-3238 (Abdelhaseib et al. 2016) was used as the reporter. MaCIA gave positive results when tested with viable *S.* Enteritidis cells (1×10^8 CFU/mL), which is significantly higher ($P < 0.0001$) than that of the equivalent numbers of dead cells or the PBS control. On the other hand, both viable and dead *S.* Enteritidis cells showed positive signals with sandwich ELISA, though the signals for viable cells were slightly higher than those of the dead cells (**Fig. 2.1C**). Furthermore, the total detection time (after addition of bacteria to the wells of assay plates) required for sandwich ELISA was 5.5 h, while 4 h for MaCIA (**Fig. 2.1C**).

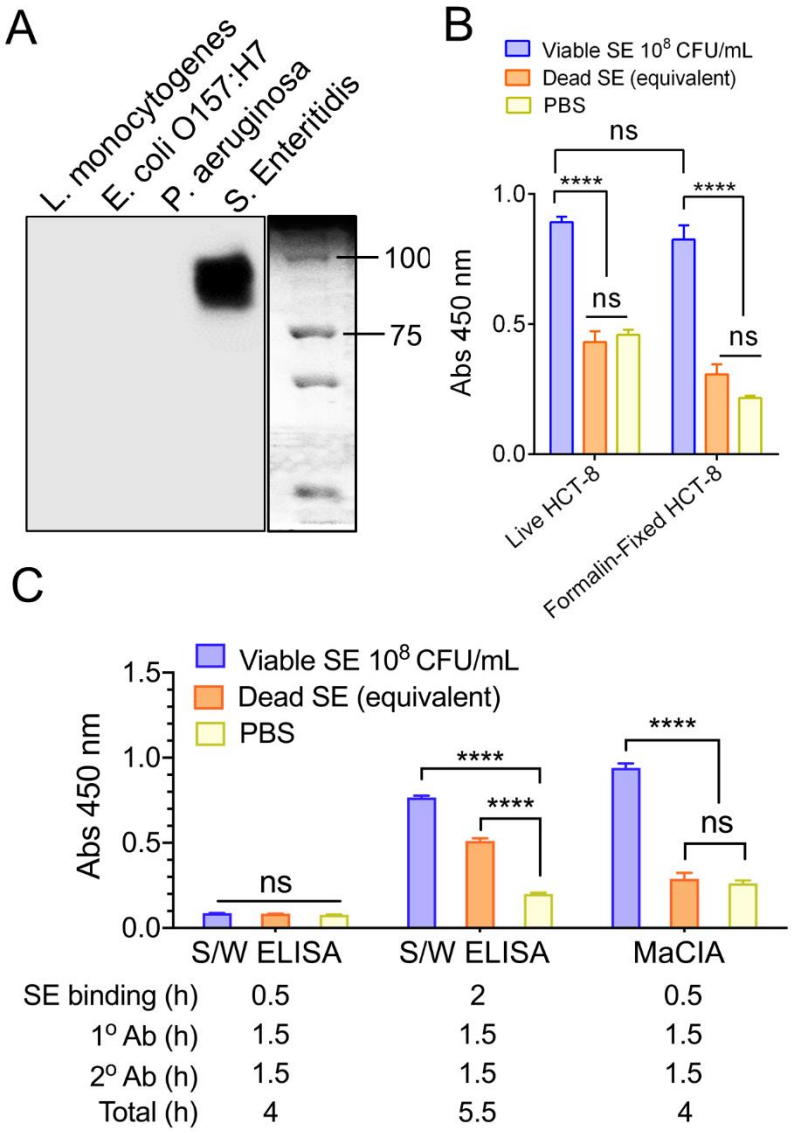

Figure 2.1. Mammalian cell-based immunoassay (MaCIA) development. (A) Western blot showing the reaction of 2F11 to Salmonella enterica serovar Enteritidis PT21 but not to L. monocytogenes F4244, E. coli O157:H7 EDL933 and Pseudomonas aeruginosa PRI99. (B) MaCIA analysis with live (Live HCT-8) and formalin-fixed (Formalin-fixed HCT-8) HCT-8 cell. (C) Comparison of MaCIA with sandwich ELISA (S/W ELISA). Error bars represent the standard error of the mean (SEM). ****P < 0.0001; ns, no significance. Cut-off for positive: P < 0.001. SE, S. Enteritidis; Ab, Antibody

2.3.2 Specificity of the MaCIA Platform

Next, the specificity of the MaCIA was determined by testing a panel of 15 *S*. Enteritidis strains, eight *S*. Typhimurium strains, 11 other *Salmonella* serovars, and 14 non-*Salmonella* spp. at ~ 1×10^6 to 1×10^7 CFU/mL each. The data showed that MaCIA was highly specific towards all tested viable strains of *S*. Enteritidis or *S*. Typhimurium serovars depending on the reporter antibody used and the signals were significantly ($P < 0.001$) higher than the signals obtained for other *Salmonella* serovars or non-*Salmonella* species (**Table 2.1, Figs. 2.2A, 2.2B**). Thus, any sample showing a significantly higher signal ($P < 0.001$) than the negative control was considered positive. Furthermore, samples containing live *S*. Enteritidis cells gave significantly ($P < 0.0001$) higher absorbance values (signals) than that of the values obtained for dead cells or the PBS control (**Fig. 2.2B**). The specificity of MaCIA towards viable cells was not affected when tested against a mixture containing equal amounts of viable and dead *S*. Enteritidis cells (**Fig. 2.2C**), and non-*S*. Enteritidis bacteria (**Fig. 2.2D**). Immuno-stained confocal images, the Z-stacking (three-dimensional image), and Giemsa stain images confirmed increased adhesion of viable *S*. Enteritidis cells to HCT-8 cells than that of the dead *S*. Enteritidis cells (**Fig. 2.2E, F, G**). Confocal imaging further revealed the absence of non-specific binding of mAb-2F11 to the HCT-8 cell monolayer (**Fig. 2.2E, F**). Furthermore, MaCIA successfully detected *S*. Enteritidis cells when exposed to various stressors for 3 h (Hahm and Bhunia 2006) including cold (4ºC), heat (45ºC), acidic pH (4.5), and 5.5% NaCl (**Fig. 2.3**).

Table 2.3 : Specificity of mammalian cell-based immunoassay (MaCIA) platform tested against Salmonella and non-Salmonella spp.

		MaCIA Result*			
Bacteria	**CFU/Well**	**mAb-2F11**		**mAb-F68C**	
		Abs_{450nm} ±SD	Result	Abs_{450nm} ±SD	Result
***Salmonella enterica* serovars**					
Enteritidis PT21	$2.0\text{-}13 \times 10^7$	0.95±0.08	+	0.10±0.01	-
Enteritidis 13ENT1344	2.9×10^7	1.13±0.16	+	NT	NT
Enteritidis 13ENT1374	$2.8\text{-}3.3 \times 10^7$	0.91±0.15	+	0.09±0.00	-
Enteritidis 13ENT1376	2.0×10^7	1.06±0.03	+	NT	NT
Enteritidis 13ENT1375	3.1×10^7	1.07±0.15	+	NT	NT
Enteritidis 13ENT1032	2.2×10^7	1.08±0.25	+	NT	NT
Enteritidis PT1	2.8×10^7	1.19±0.04	+	NT	NT
Enteritidis PT4	2.0×10^7	1.17±0.06	+	NT	NT
Enteritidis PT6	1.8×10^7	1.41±0.04	+	NT	NT
Enteritidis PT7	7.5×10^6	0.70±0.06	+	NT	NT
Enteritidis PT8	1.4×10^7	1.42±0.06	+	NT	NT
Enteritidis PT13a	1.5×10^7	0.74±0.02	+	NT	NT
Enteritidis PT13	1.1×10^7	0.90±0.06	+	NT	NT
Enteritidis PT14b	1.3×10^7	1.05±0.04	+	NT	NT
Enteritidis PT28	1.1×10^7	0.53±0.05	+	NT	NT
Typhimurium 13ENT906	$6.7\text{-}8.8 \times 10^7$	0.33±0.03	-	1.14±0.06	+
Typhimurium NOS12	4.0×10^7	0.33±0.03	-	0.98±0.04	+
Typhimurium NOS3	3.3×10^8	NT	NT	0.80±0.04	+
Typhimurium NOS10	1.3×10^8	NT	NT	0.90±0.12	+
Typhimurium NOS2	6.7×10^8	NT	NT	0.73±0.08	+
Typhimurium NOS4	6.7×10^8	NT	NT	0.89±0.04	+
Typhimurium NOS1	3.3×10^7	NT	NT	0.84±0.06	+
Typhimurium ST1	3.8×10^6	0.13±0.02	-	NT	NT
Newport 13ENT1060	$2.3\text{-}23 \times 10^7$	0.32±0.04	-	0.13±0.01	-
Braenderup 12ENT1138	6.3×10^7	0.33±0.03	-	NT	NT
Agona 12ENT1356	$2.7\text{-}13 \times 10^8$	0.32±0.02	-	0.09±0.01	-

Table 2.3 continue

Hadar 13ENT979	4.3×10^7	0.27±0.02	-	NT	NT
Paratyphi 11J85	2.4×10^7	0.27±0.05	-	NT	NT
Heidelberg 18ENT1418	4.0×10^7	0.29±0.04	-	NT	NT
Saintpaul 13ENT1045	5.0×10^7	0.30±0.04	-	NT	NT
Javiana 13ENT86F	$0.4\text{-}2.7 \times 10^8$	0.38±0.10	-	0.14±0.07	-
Infantis 13ENT866	2.0×10^7	0.32±0.02	-	NT	NT
Bareilly 12ENT1164	$0.1\text{-}4.0 \times 10^8$	0.32±0.09	-	NT	NT
Pullorum DUP-PVUII 1006	1.9×10^7	0.34±0.04	-	NT	NT
Miscellaneous					
Listeria monocytogenes F4244	$0.5\text{-}1.6 \times 10^8$	0.27±0.03	-	0.13±0.01	-
L. innocua F4248	5.0×10^7	0.27±0.03	-	NT	NT
Escherichia coli O157:H7 EDL933	$0.4\text{-}1.3 \times 10^8$	0.26±0.03	-	0.08±0.04	-
Hafnia alvei 18066	$3.3\text{-}6.3 \times 10^7$	0.28±0.03	-	0.15±0.02	-
Citrobacter freundii ATCC8090	$0.3\text{-}1.0 \times 10^8$	0.29±0.02	-	0.13±0.01	-
Citrobacter freundii ATCC43864	$0.4\text{-}3.3 \times 10^7$	0.11±0.00	-	0.11±0.01	-
Citrobacter freundii ATCC3624	$0.3\text{-}1.3 \times 10^8$	0.13±0.01	-	0.12±0.02	-
Serratia marcescens ATCC8100	$0.6\text{-}5.3 \times 10^7$	0.33±0.02	-	0.12±0.01	-
Serratia marcescens ATCC43862	$0.1\text{-}1.0 \times 10^8$	0.11±0.01	-	0.13±0.01	-
Serratia marcescens B-2544	$0.6\text{-}3.3 \times 10^7$	0.13±0.01	-	0.11±0.02	-
Pseudomonas aeruginosa PRI99	2.25×10^7	0.24±0.02	-	NT	NT
Proteus mirabilis B-3402	$0.7\text{-}6.7\times 10^8$	0.11±0.01	-	0.11+0.01	-
Proteus vulgaris DUP-10086	$0.4\text{-}4.0 \times 10^8$	0.11±0.01	-	0.10±0.02	-
Klebsiella pneumoniae B-41958	6.7×10^6	0.10±0.01	-	0.13±0.01	-

*Values are from four independent replicates; Results (+/-) are decided by comparing to the negative control in each experiment. Values that are significantly different ($P < 0.001$) from the negative control in each experiment are regarded as +; NT: not tested.

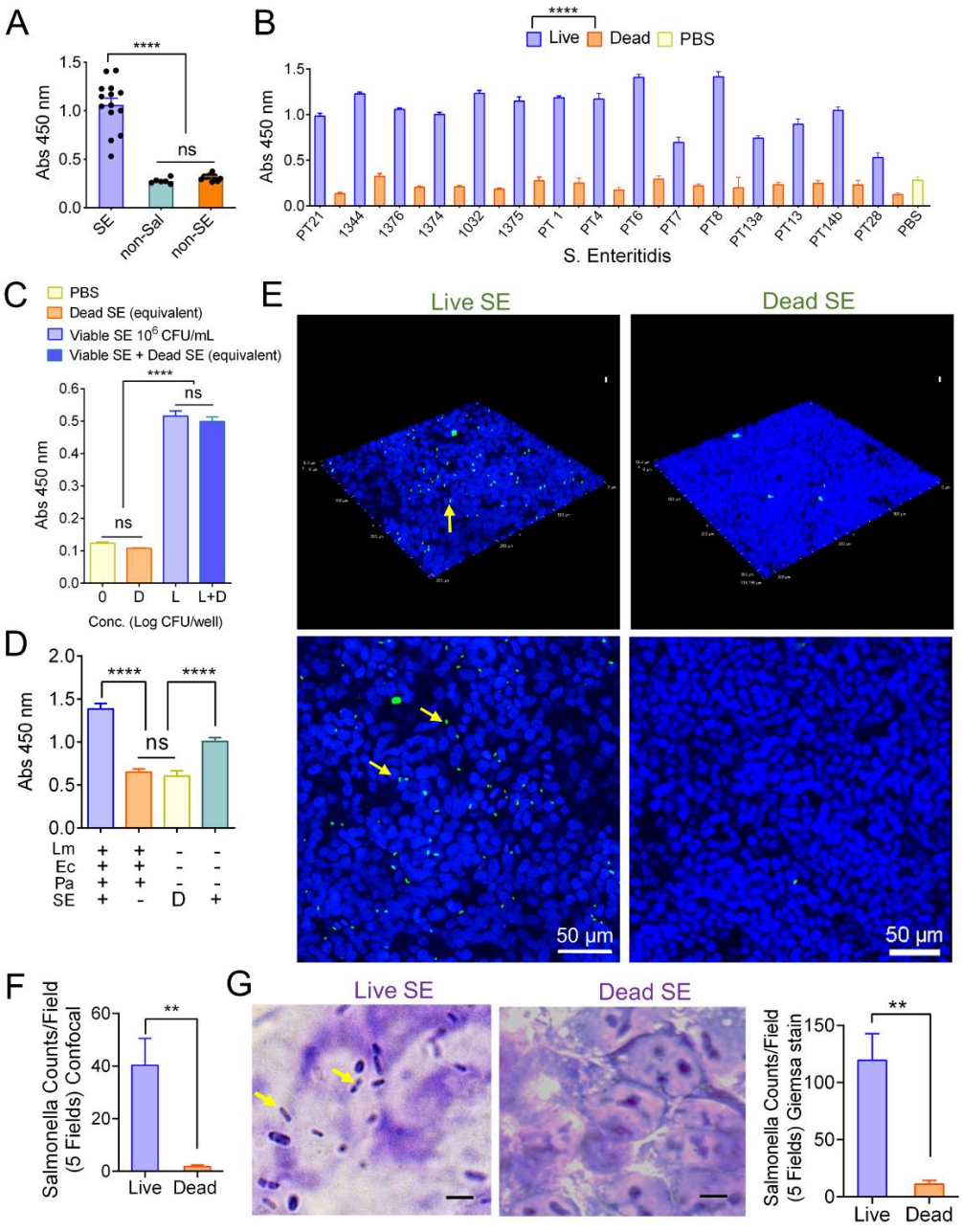

Figure 2.2. Mammalian cell-based immunoassay (MaCIA) specificity. MaCIA reaction with 15 *Salmonella* Enteritidis strains (SE), 12 non-SE and 7 non-*Salmonella* bacteria (A), with viable and dead *S*. Enteritidis serovars (B), to viable *S.* Enteritidis in the presence of the equivalent amount of dead *S.* Enteritidis (C), and *S*. Enteritidis PT21 in the presence of other bacteria (Lm, *L. monocytogenes* F4244; Ec, *E. coli* EDL933 and Pa, *Pseudomonas aeruginosa* PRI99). L: live SE; D: Dead SE (D). Confocal image and Giemsa staining analyses of adhesion of live (Live SE) and dead (Dead SE) *S*. Enteritidis PT21 to formalin-fixed HCT-8 cells; (E) Z-stack of the scanned images, (F) total bacterial counts per five fields for confocal images. Blue: nucleus, green: *S*. Enteritidis, (G) Giemsa stained images showing adhesion of live (Live SE) but not dead (Dead SE) *S*. Enteritidis PT21 to formalin-fixed HCT-8 cells. Rod-shaped dark blue, *S.* Enteritidis (arrows); purple, nucleus; Bar graph showing bacterial counts per field from five fields. Error bars represent SEM. ****$P < 0.0001$; **$P<0.01$; ns, no significance. Cut-off for positive: $P < 0.001$.

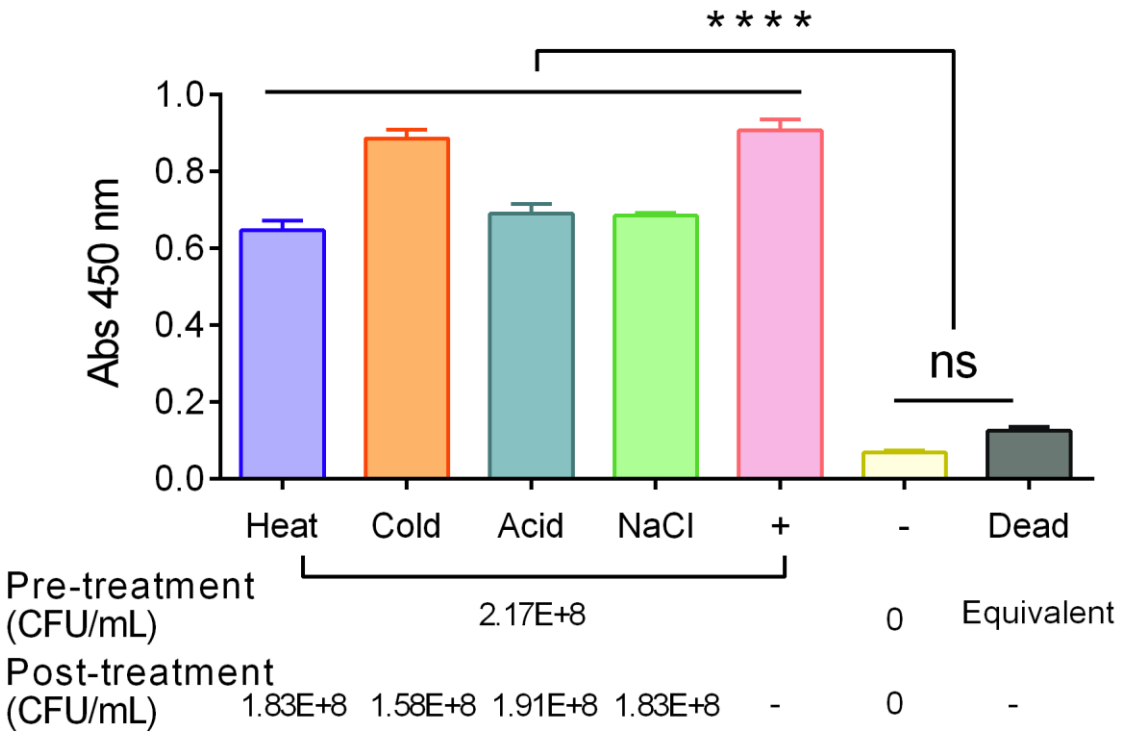

Figure 2.3. Detection of stress-exposed *S*. Enteritidis PT21 using MaCIA. Bacteria were exposed to heat (45ºC), cold (4ºC), acidic pH (4.5) and NaCl (5.5%) for 3 h before analysis. +, Positive control (bacteria without any stress exposure); -, No bacteria; dead, heat-killed *S*. Enteritidis cells. Error bars represent SEM. ****$P < 0.0001$; ns, no significance.

2.3.3 Detection Sensitivity of MaCIA

To determine assay sensitivity, *S*. Enteritidis cells were serially diluted using either PBS or ground chicken suspended in buffered peptone water (BPW) and added to the wells containing formalin-fixed HCT-8 cell monolayers (30-min post-fixation). After a 30-min incubation at 37°C with test samples, the monolayers were washed, probed with mAb-2F11, and the color was developed. An initial bacterial concentration of 1×10^6 to 1×10^8 CFU/mL showed significantly ($P < 0.001$) higher signal than the wells containing 1×10^5 CFU/mL or dead cells (1×10^6 cells) suspended in PBS (**Fig. 2.4A**) or ground chicken slurry (**Fig. 2.5**) and the absorbance values showed strong correlation ($R^2 = 0.9344$) with *S.* Enteritidis cell numbers (1×10^6 CFU/mL to 1×10^8 CFU/mL) (**Fig. 2.4B**). Furthermore, MaCIA also showed a similar concentration-dependent rise in signals when bacteria were suspended in ground chicken, liquid egg, milk, and cake mix slurry (**Fig. 2.4C**). However, the detection sensitivity varied depending on the food matrix tested. In milk, the detection limit was determined to be 1×10^5 CFU/mL while in ground chicken, 1×10^6 CFU/mL, in cake mix, 1×10^7 CFU/mL, and in egg, 1×10^8 CFU/mL (**Fig. 2.4C**). These results indicate that assay sensitivity for MaCIA for the detection of *S*. Enteritidis varies from 1×10^5 CFU/mL to 1×10^8 CFU/mL depending on the food matrix tested.

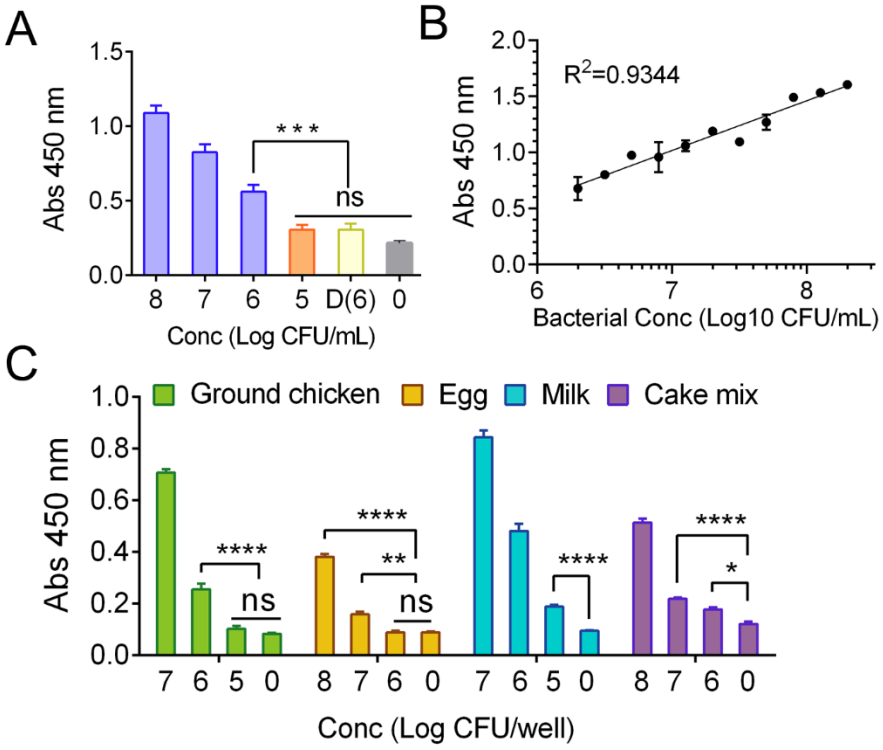

Figure 2.4. Assay sensitivity for MaCIA. (A) Analysis of limit of detection (LOD) of MaCIA against *S.* Enteritidis PT21 at 1×10^5 CFU/mL to 1×10^8 CFU/ml suspended in PBS; and (B) corresponding correlation coefficient of absorbance and bacterial concentration. (C) Analyses of LOD of MaCIA when *S.* Enteritidis PT21 was suspended in different food matrices. 0, no bacteria; D(6), dead *S.* Enteritidis PT21 at 1×10^6 cells/ml. In all figures, samples with higher concentrations were also significantly ($P < 0.001$) different than the dead samples and negative control. Error bars represent SEM. ****$P < 0.0001$; ***$P < 0.001$; **$P<0.01$; *$P < 0.05$; ns, no significance. Cut-off for positive: $P < 0.001$.

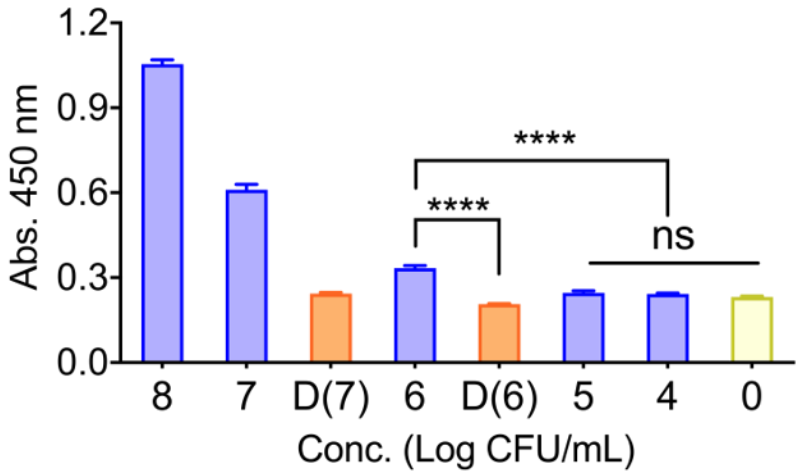

Figure 2.5. Detection sensitivity of MaCIA tested against the different concentrations of *S. enterica* serovar Enteritidis cells suspended in ground chicken slurry (in buffered peptone water). D, dead cells.

2.3.4 Further Optimization of MaCIA

(i) One-step antibody probing method

To shorten the detection time, we explored if a one-step antibody probing approach is feasible. Ground chicken was inoculated with *S.* Enteritidis at 6×10^2 CFU/25 g in a stomacher bag. After 10-h enrichment at 37°C, the enriched chicken samples (1 mL) were added to the fixed HCT-8 cell monolayer for 30 min, followed by PBS wash (3 times). The cell monolayers were probed with an antibody cocktail that contained both primary (mAb-2F11) and secondary (anti-mouse HRP-conjugated IgG) antibodies, followed by the colorimetric substrate. Data showed that the signal obtained from the one-step antibody probing was comparable to the results when the sequential antibody probing method was used (**Fig. 2.6A**). This experiment indicates that one-step antibody probing is equally effective as the sequential antibody probing method, thus shortening the assay time by 2.5 h.

(ii) On-cell food sample enrichment

Direct on-cell (MaCIA platform) enrichment of test samples was pursued to simplify the assay procedure and to reduce the sample handling steps. *S.* Enteritidis inoculated food suspensions (with an initial inoculation of 10 CFU/mL) were directly added to the wells (1 mL/well) containing formalin-fixed HCT-8 cell monolayers and incubated at 37°C. The assay was performed after 6,

7, 8, and 9-h on-cell sample enrichment followed by sequential antibody probing (3 h). After 7-h on-cell enrichment, both ground chicken and egg samples gave positive results while the whole milk and cake mix needed 9-h enrichment to give positive results when compared with uninoculated food samples (**Fig. 2.6B**). A similar result was obtained when the food samples were tested in a blinded fashion (**Fig. 2.7**). Total assay time (sample-to-result) for on-cell enrichment was estimated to be 10-12 h. Remarkably, the HCT-8 cell monolayers remained intact without any visible damage during on-cell enrichment (**Fig. 2.6C**). Due to the limitation in the amount of sample volume (1 mL/well), that can be tested, the "on-cell enrichment" option is suitable only when the starting *S.* Enteritidis concentration is above 10 CFU/mL (2.5×10^3 CFU/25 g); hence it may not be suitable for routine testing of bulk-food samples that may contain <100 CFU/g.

We then examined if the on-cell enrichment set up is suitable for testing surface swab samples. Skin swabs from inoculated chicken thigh parts (1.35×10^3 to 1.35×10^5 CFU/50 cm^2 at 4°C for 24 h) were resuspended in 1.1 mL of BPW, and 1 ml of each suspension was added to the wells of MaCIA. After 7-h enrichment followed by sequential immunoprobing (3 h), MaCIA generated significantly ($P < 0.0001$) higher signals than that of the values obtained from the negative control (swabbed suspension of the uninoculated sample) (**Fig. 2.6D**). These data indicate that MaCIA is suitable for testing surface swab samples, and results can be obtained in less than 12 h.

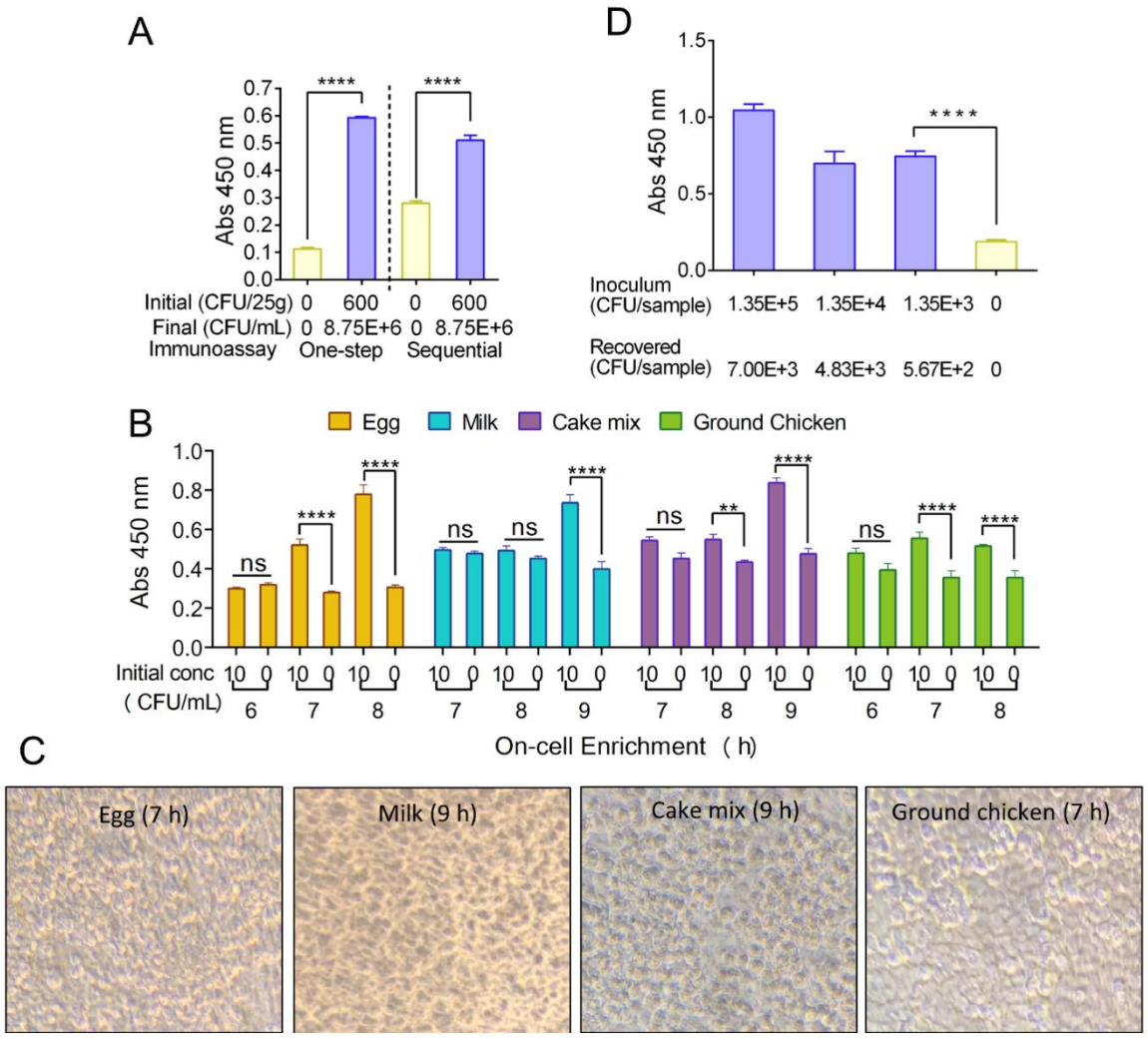

Figure 2.6. MaCIA assay optimization. (A) One-step antibody probing vs sequential antibody probing against a bacterial cell concentration of 8.75 × 106 CFU/ml of S. Enteritidis. (B) Analysis of time (h) required for positive MaCIA result during on-cell enrichment of S. Enteritidis PT21 (~10 CFU/mL) inoculated into different food products. (C) Light microscopic images of formalin-fixed HCT-8 cell monolayers after on-cell enrichment for 7-9 h. Magnification (400×). (D) MaCIA analysis of skin swab samples after on-cell enrichment (7 h). Samples with higher concentrations were also significantly ($P < 0.001$) different than the negative control. Error bars represent SEM. ****$P < 0.0001$; ***$P < 0.001$; **$P < 0.01$; *$P < 0.05$; ns, no significance. Cut-off for positive: $P < 0.001$.

A

Sample			Negative control
Chicken	0	25	0
Egg	25	0	0
Milk	25	0	0
Cake mix	0	25	0

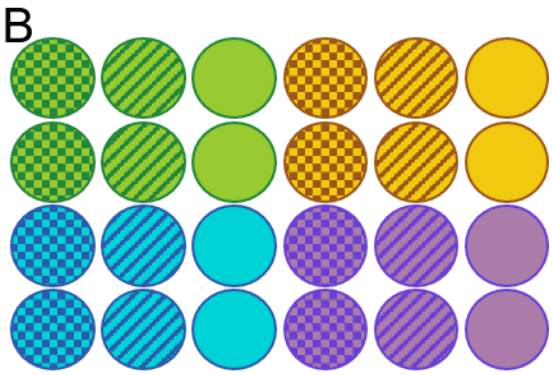

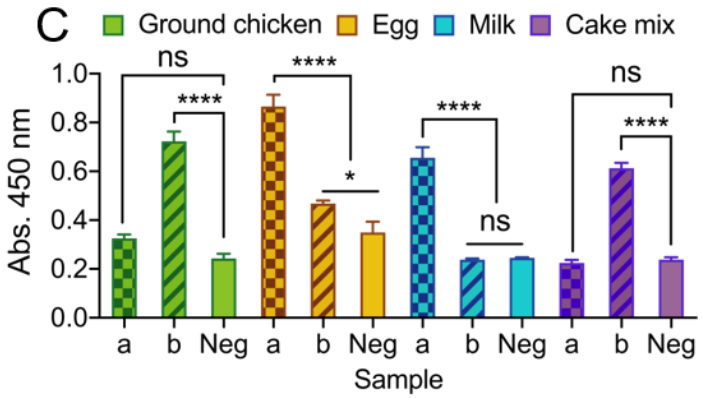

Figure 2.7. Experimental set-up of the blind test using an on-cell (MaCIA) enrichment method. (A&B) The checkerboard filled areas correspond with sample a; the diagonal stripes filled areas correspond with sample b; No pattern-filled area corresponds with negative control for each food product. The numbers in the table represent the concentration (CFU/mL) of the inoculant, *S.* Enteritidis PT21. (C) Blinded test using on-cell enrichment. Positive samples were inoculated with 25 CFU/mL cold-stored *S.* Enteritidis PT21. Neg: negative control. a, b: blind tested samples.

2.3.5 Comparison of MaCIA with the USDA/FDA Detection Methods

To compare the performance of MaCIA with USDA/FDA detection methods, *S.* Enteritidis inoculated food samples (ground chicken, egg, milk and cake mix held at 4°C for 24 h) were also tested in parallel using the US Department of Agriculture (USDA-FSIS 2013) or Food and Drug Administration (FDA 2001) reference method.

(i) Growth kinetics of S. Enteritidis in different foods

Freshly grown (37°C, 18 h) *S.* Enteritidis PT21 culture was inoculated (<10 CFU/ml) into 25 g of each ground chicken, egg, whole milk, or cake mix in 225 mL BPW in a stomacher bag (Seward Inc., Bohemia, NY) and held at 4°C for 24 h. Inoculated food samples were then incubated at 37°C and bacterial counts were determined every 2-h intervals until 18 h. The growth data of *S.* Enteritidis in all tested food samples were fitted with the Gompertz model to generate a growth curve (**Fig. 2.9A**). The R^2 values of Gompertz fitted growth curves of *S.* Enteritidis PT21 in ground chicken, egg, whole milk, and cake mix were 0.99, 0.99, 0.96, and 0.99, respectively. Based on the Gompertz modeled growth curve equations, the lag phase duration (LPD) and exponential growth rate (EGR) were estimated to be 2.204 - 2.427 h and 0.767 - 0.934 log (CFU/mL)/h, respectively (**Table 2.4**). Utilizing LPD, EGR, and the MaCIA detection limit data, we were able to estimate the required enrichment time for each food product, assuming the starting *S.* Enteritidis concentration is 1 CFU/25 g (**Table 2.4**). The required enrichment time for ground chicken, egg, milk, and cake mix was estimated to be 14, 19, 16, and 16 h, respectively (**Table 2.4**).

Table 2.4: Proposed enrichment time for different food products before testing with MaCIA

Food sample	Lag phase duration (LPD) (h)	Exponential growth rate (EGR) (Log (CFU/mL)/h)	Proposed enrichment time (h)	MaCIA detection time using on-cell enrichment (h)
Ground chicken	2.204±0.130	0.896±0.019	14	7
Shelled eggs	2.319±0.100	0.934±0.016	19	7
Whole milk	2.427±0.110	0.767±0.013	16	9
Cake mix	2.260±0.710	0.983±0.133	16	9

(ii) Sample-to-result time

To confirm the sample-to-result time, we inoculated the selected food samples with *S*. Enteritidis at 0, 9, or 45 CFU/25 g (**Fig. 2.9B**) and 0, 2 or 45 CFU/mL (**Fig. 2.9C**). After a specified enrichment period, we analyzed the samples using MaCIA. All *S*. Enteritidis-inoculated samples produced significantly higher signals ($P < 0.001$) than the uninoculated food samples (**Fig. 2.9B, C**) even in the presence of background microflora (**Fig. 2.8**). The sample-to-result time was estimated to be 16-21 h. Analysis of food samples by the USDA-FSIS or FDA-BAM method followed by polymerase chain reaction (PCR) assay using three sets of primers targeting *invA*, IE-1, and IE-2 genes (**Fig. 2.9D**) confirmed the presence of *S*. Enteritidis in these food samples. Note, the USDA method needed 72 h, while the FDA method needed 72-168 h to confirm the presence of *Salmonella* in the inoculated food samples.

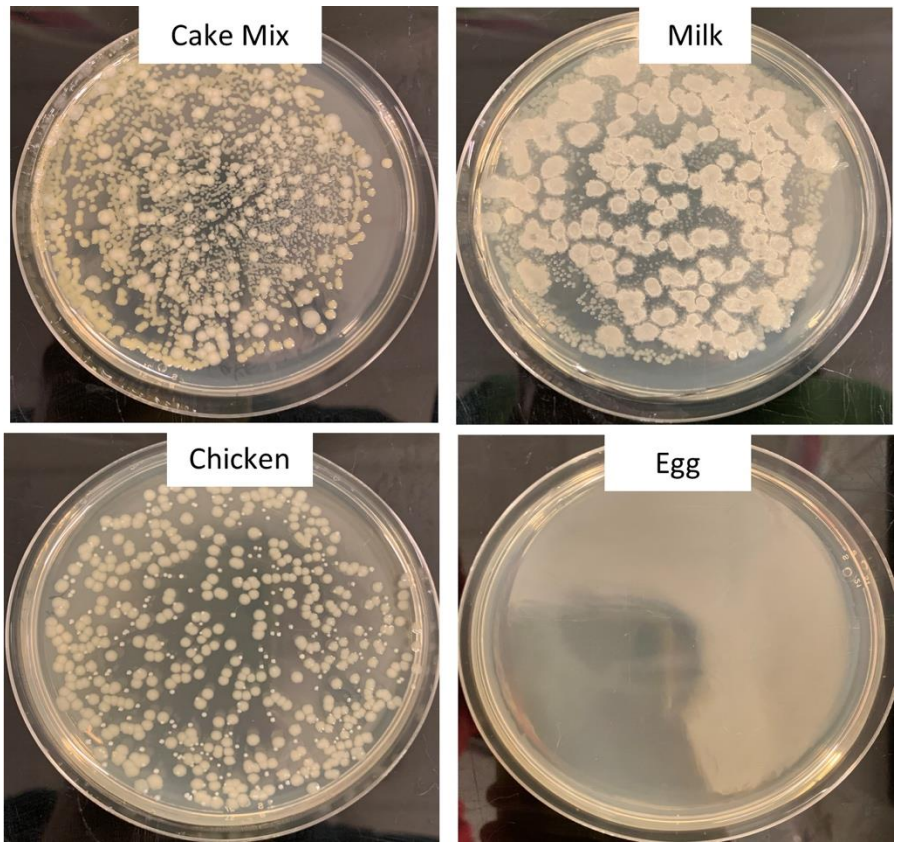

Figure 2.8. Tryptic soy agar (TSA) plates showing the presence of background bacterial populations from different food samples except for the eggs.

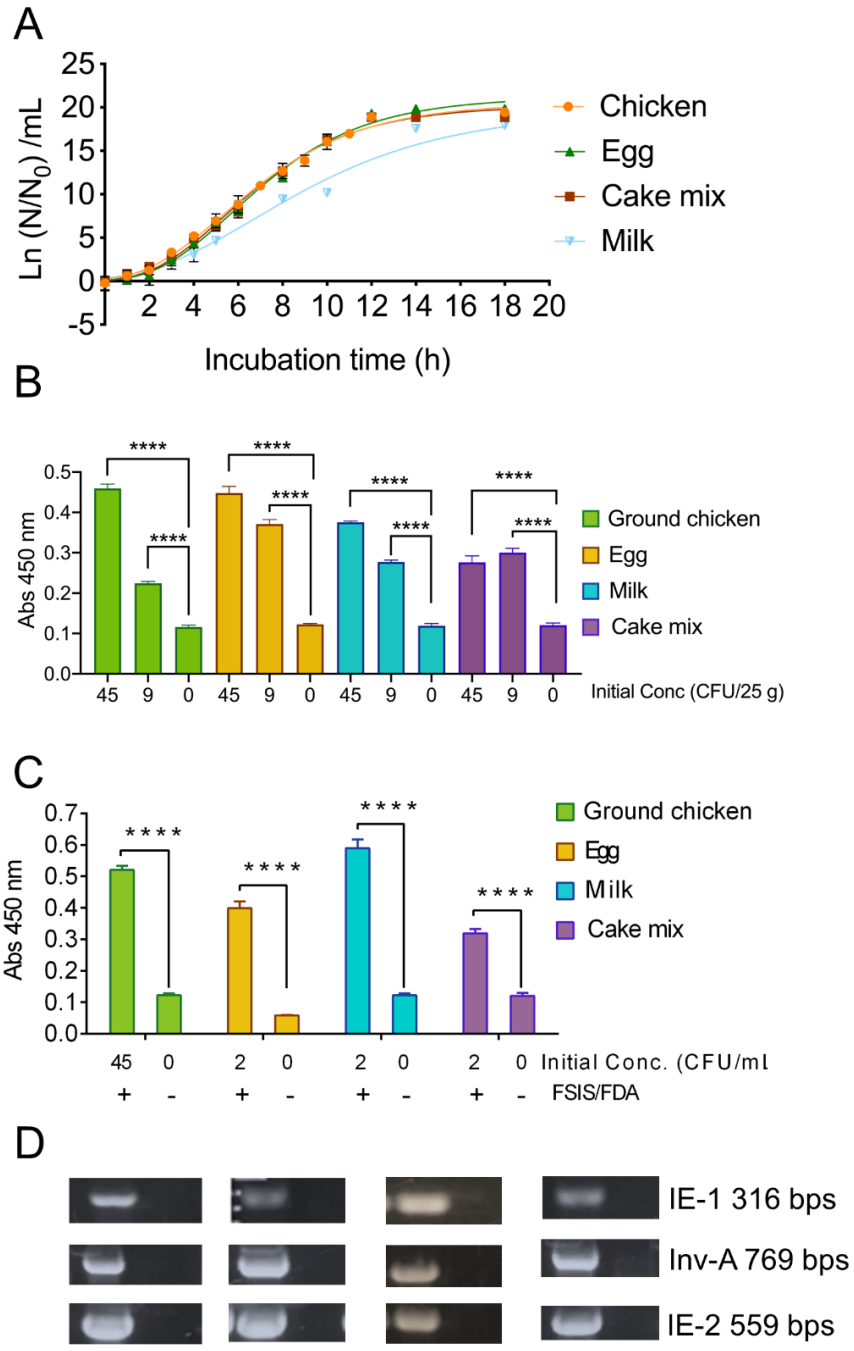

Figure 2.9. MaCIA validation with inoculated food samples. (A) Growth curve of *S.* Enteritidis PT21 in various food products suspended in buffered-peptone water (BPW) at 37°C. Before growth analysis, inoculated food samples were held at 4°C for 24 h. The best-fit curves for *Salmonella* growth in different foods were generated by using the Gompertz model. R^2 values of each fitted Gompertz curve are 0.99 (Chicken), 0.99 (Egg), 0.99 (cake mix) and 0.96 (Milk). N_0, initial *S.* Enteritidis concentration; N, *S.* Enteritidis concentration at the corresponding time point. MaCIA results of *S.* Enteritidis inoculated (at 0, 9, 45 CFU/25 g) (B) and at 0, 2, 45 CFU/mL (C) food samples after 14-19 h enrichment. (D) PCR confirmation of *S.* Enteritidis targeting *Salmonella* specific genes. Error bars represent SEM. ****$P <$ 0.0001.

2.3.6 Formalin-fixation Prolongs the Shelf-life of MaCIA

The bottleneck for widespread use of cell-based sensors is its limited shelf-life. As we have demonstrated earlier (**Fig. 2.1B**), the performance of MaCIA prepared with live HCT-8 cells is equally sensitive to the formalin-fixed HCT-8 cells (30 min after fixation). In this experiment, we investigated if the prolonged storage (4, 8, and 14 weeks at 4ºC or 4 weeks at room temperature) of formalin-fixed HCT-8 cell would uphold MaCIA's performance. Data showed that formalin-fixed HCT-8 cells stored for 4–12 weeks at 4ºC generated comparable results to that of live HCT-8 cells when tested with viable *S*. Enteritidis PT21 at a concentration of 1×10^7 CFU/ml and signals were significantly higher ($P < 0.0001$) than the signals generated by an equivalent amount of dead *S*. Enteritidis cells or the PBS control (no bacteria) (**Fig. 2.10A**). The light microscopic photomicrographs further confirmed that the cell monolayer and the cellular morphology in formalin-fixed HCT-8 cells were unaffected after 14 weeks of storage at 4ºC or even after bacterial exposure and the subsequent three PBS wash (**Fig. 2.10B**). These results indicate that formalin fixation was able to prolong the shelf-life of HCT-8 cells up to 14 weeks without affecting their performance, thus showing a promising application of the MaCIA for point-of-need deployment.

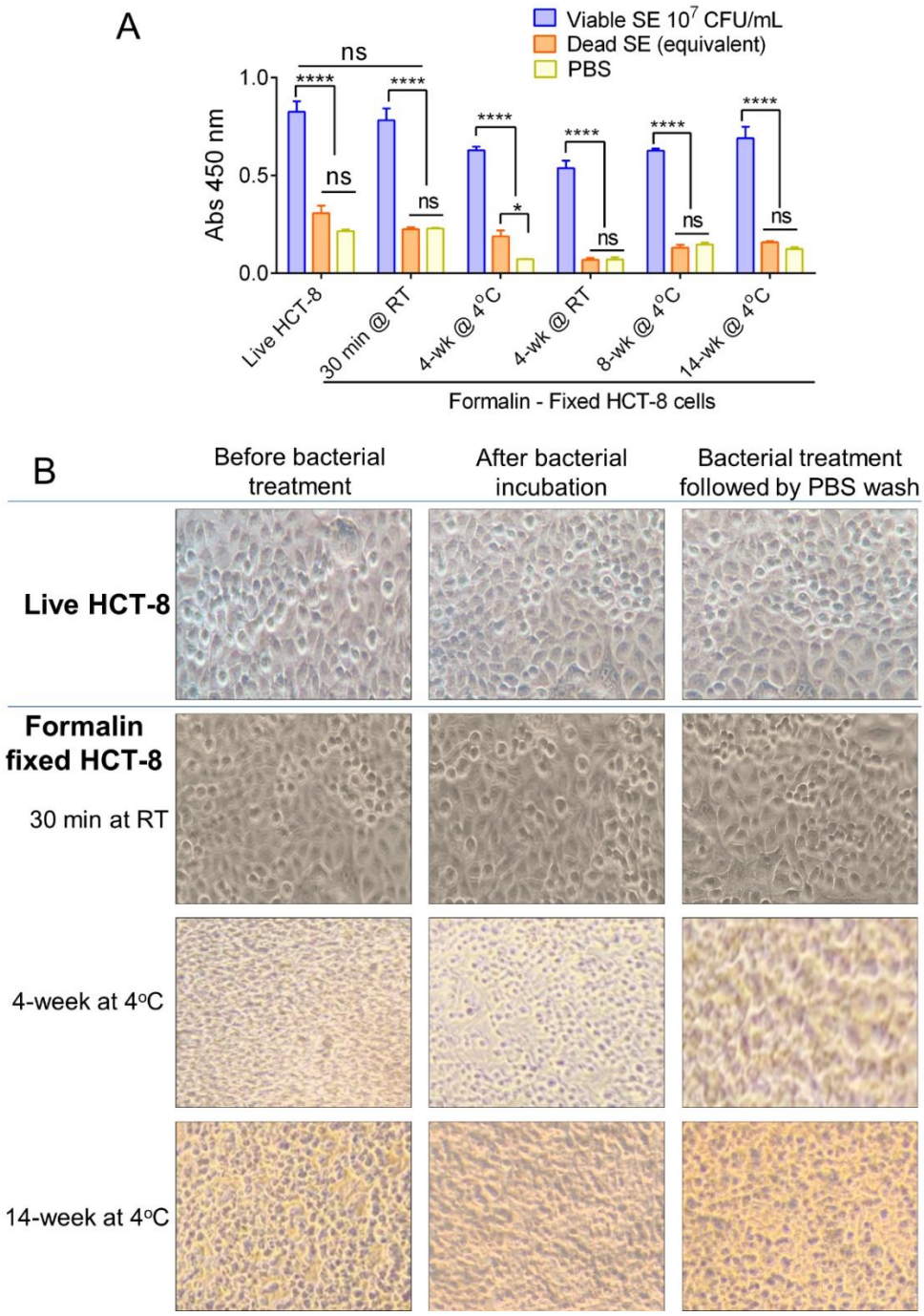

Figure 2.10. Performance of MaCIA after prolonged storage. (A) Comparison of MaCIA signals (absorbance reading) of *S.* Enteritidis cells (1×10^7 cells/ml) originating from live HCT-8 and formalin-fixed HCT-8 cells stored at 4°C for 30 min to 14 weeks. (B) Light microscopic analysis of cell morphology of formalin-fixed HCT-8 cells stored up to 14 weeks. Panels showing intact cell morphology before bacterial treatment, after treatment, and after PBS wash. Magnification, 400×. Error bars represent SEM. ****$P < 0.0001$; ns, no significance.

2.4 Discussion

The conventional culture-based detection methods (sample-to-result) take 4-7 days to obtain the results (FDA 2001; USDA-FSIS 2013; Bell et al. 2016), and the so-called rapid methods take at least 24-48 h (Bhunia 2014; Lee et al. 2015; Ricke et al. 2018; Rajapaksha et al. 2019). This is a major inconvenience for the food industries since some foods have a limited shelf-life. Furthermore, holding of products until the microbiological safety assessment can also increase the cost of storage. Therefore, products are released into the supply chain even before obtaining test results. Such practice is very costly, resulting in more than hundreds of recalls each year and the loss of millions of pounds of food (Buzby et al. 2014; Elkhishin et al. 2017). Therefore, rapid, accurate, and user-friendly viable pathogen detection tools are in high demand to lower recalls, reduce food waste and financial loss, and prevent foodborne outbreaks.

Mammalian cell-based assays are highly attractive functional screening tools to assess the presence of viable pathogens or active toxins in near-real-time (Bhunia 2011; Bhunia 2014; To et al. 2020). CBB monitors host-hazard interaction (Banerjee and Bhunia 2009); therefore, nonpathogenic, non-hazardous, dead, or nontoxic agents do not yield false results. However, the major drawback is its short self-life i.e., the mammalian cells may not survive on the sensor platform for a prolonged period without the proper growth conditions. Mammalian cells have stringent requirements for specialized growth media and growth conditions for survival, such as temperature and CO_2-controlled humidified environment. Limited self-life of cells is a monumental deterrent for CBB's widespread application affecting its deployment for point-of-need use. To overcome the limitation, we employed formalin (4% formaldehyde) to preserve the functionality of the mammalian cells. We used the human ileocecal cell line, HCT-8, as our model cell line, which maintained its functionality after formalin-fixation, at least for 14 weeks at 4°C. The fixed HCT-8 cells showed selective interaction with viable or even stress-exposed *Salmonella*, while dead cells had negligible or no interaction at all (**Figs. 2.1 - 2.3**). Further specificity of the assay was accomplished by immunoprobing the adhered bacterial cells using a specific antibody. The MaCIA was found to be highly specific for the detection of *S*. Enteritidis or *S*. Typhimurium without showing any cross-reaction with other *Salmonella* serovars or non-*Salmonella* species tested. The assay was further validated for its ability to detect *S*. Enteritidis in inoculated ground chicken, egg, whole milk, and cake mix in the presence of background natural microflora. A brief

sample enrichment step also allows the resuscitation of stressed or injured cells before detection (Wu 2008).

In the MaCIA platform, HCT-8 cells were used as a capture element instead of an antibody, which is traditionally used in a sandwich ELISA. In this study, HCT-8 cells out-performed the antibody (**Fig. 2.1C**), and 30 min incubation was sufficient for optimal capture of viable bacteria by HCT-8 cells (Jaradat and Bhunia 2003; Barrila et al. 2017) while 2 h was needed for sandwich ELISA. Improved bacterial capture by HCT-8 is attributed to the formation of a three-dimensional structure by mammalian cell monolayer (**Fig. 2.2E**), creating a larger surface area for bacteria to bind. Furthermore, HCT-8 cell possesses surface receptor molecules for specific interaction with *Salmonella* adhesion factors. *S.* Enteritidis utilize type 1 fimbria to recognize and bind to high-mannose oligosaccharides, which are carried by various glycoproteins on the host cell surface (Kolenda et al. 2019). Long polar fimbriae also mediate adhesion of *Salmonella* to Peyer's patches on the host cell (Bäumler et al. 1996). Besides, MaCIA was able to differentiate viable cells from dead *Salmonella* cells while sandwich immunoassay was unable. Lack of adhesion of dead *Salmonella* to HCT-8 may be due to the loss or denaturation of bacterial adhesins (**Fig. 2.2G**). While in sandwich ELISA, bacterial surface antigens from dead cells were still able to bind the capture-antibody. MaCIA also showed strong signals when tested with stress-exposed *S.* Enteritidis cells suggesting a brief stress exposure (3 h) does not affect bacterial ability to interact with the HCT-8 cells (**Fig. 2.3**) while such exposure caused a 20-48% reduction in ELISA signal for *Salmonella* in a previous study (Hahm and Bhunia 2006).

The sensitivity of MaCIA was found to be about 1×10^6 CFU/mL to 1×10^7 CFU/mL, which is in agreement with a typical ELISA where antibodies serve as the capture molecule (Mansfield and Forsythe 2000; Eriksson and Aspan 2007) or ELISA with bacteriophage as a recognition molecule (Galikowska et al. 2011). However, MaCIA has the potential to outperform ELISA in some aspects, due to its ability to differentiate viable from dead bacteria. Viable pathogens that can adhere and invade into intestinal cells are of food safety concerns. MaCIA is a better choice over ELISA for the food industry when viable pathogens in food are the target. False-positive results generated by either ELISA or PCR due to the presence of nonviable pathogens could lead to unnecessary recalls, food waste, and economic loss. On the other hand, assays with higher sensitivity may be useful for detecting samples with low bacterial concentration, but enrichment is considered a necessary step to ensure accuracy (Bhunia 2014). Assuming a 25 g sample contains

1 CFU of bacteria unless one performs a test on the entire 25 g sample, there is a high possibility that one would not be able to accurately detect the bacteria even with a sensor that has the sensitivity to detect 1 CFU. So, the sensitivity of an assay not only depends on the limit of detection but also on the sample size. Therefore, we proposed to perform MaCIA in concert with the traditional enrichment step, to offer a more reliable and accurate testing result.

The assay sensitivity was also affected by the food matrices tested. Ground chicken, raw eggs, whole milk, and cake mix were chosen since these products were implicated in *Salmonella* outbreaks, and they also represent foods with high protein, fat, or carbohydrate contents. In milk, the detection limit for *S*. Enteritidis was 1×10^5 CFU/mL while in ground chicken, 1×10^6 CFU/mL, in cake mix, 1×10^7 CFU/mL, and in egg, 1×10^8 CFU/mL (**Fig. 2.4C**). Among the foods tested, eggs exhibited the highest interference while milk had the least. Egg contains about 13 g protein and 11 g fat per 100 g while whole milk contains only 3.15 g of protein and 3.25 g of fat per 100 g (Kuang et al. 2018).

MaCIA is highly specific for *S*. Enteritidis and did not show any non-specific reaction with other *Salmonella* serovars, non-*Salmonella* organisms, or natural microflora present in uninoculated food samples. The specificity of MaCIA is attributed to the specificity of the reporter antibody, mAb-2F11 used, that binds the O-antigen (LPS) on the surface of *S*. Enteritidis (Masi and Zawistowski 1995; Jaradat et al. 2004). The advantage of the MaCIA platform is that the specificity depends on the primary reporter antibody used. We have demonstrated that using a commercial anti-*Salmonella* mAb-F68C (Thermo-Fisher) as a reporter antibody, *Salmonella* enterica serovar Typhimurium can be detected on the MaCIA platform (**Table 2.3**). These results indicate that the MaCIA platform is versatile and can be adapted for a different target pathogen using an appropriate antibody.

The accuracy of MaCIA for *S*. Enteritidis was also confirmed by comparing the results with the reference methods, such as the FDA-BAM, USDA-FSIS, and PCR (**Fig. 2.9D**). The three primer sets that were used in PCR (**Table 2.2**) target *IE-1*, *IE-2* in *S*. Enteritidis, and *InvA* in *S*. Enteritidis and *S*. Typhimurium (Fratamico and Strobaugh 1998; Wang and Yeh 2002; Paião et al. 2013), which again confirm the accuracy of MaCIA for its ability to detect *S*. Enteritidis from spiked food samples.

The major advancement of the MaCIA is its extended shelf-life, at least for 14 weeks, that was achieved through formalin-fixation of HCT-8 cells. Formalin is routinely used to preserve

tissues and cells and it protects protein from denaturation (Eltoum et al. 2001). Therefore, receptor molecules on formalin-fixed HCT-8 cells, remained active and enabled viable *Salmonella* binding without diminishing MaCIA's performance. Previously, many attempts have been made to extend the shelf-life (functionality) of cells in CBB; however, none were satisfactory. Bhunia et al. (Bhunia et al. 1995) used ultra-low temperature (freezing at -80°C and -196°C) to extend the shelf-life of cells (up to 8 weeks) before performing the cytotoxicity assay for *L. monocytogenes*. However, the major drawback was the generation of high background signal originating from freeze-injured or dead mammalian cells. Banerjee et al. (Banerjee et al. 2007) used modified growth conditions that included 5% fetal calf serum without any exogenous CO_2 and was able to extend the viability of the lymphocyte cell line for 6-7 days at room temperature. Curtis et al. (Curtis et al. 2009) used an automated media delivery system integrated with a thermoelectric controller to keep endothelial cells healthy up to 16 weeks. More recently, Jiang et al. (Jiang et al. 2018a) used a screen-printed hydrogel-encapsulated rat basophilic leukemia mast cell-based electrochemical sensor for the detection of quorum sensing molecules for fish spoilage and the sensor-generated stable signal for 10 days. However, these attempts required incorporating mammalian cells in a specially designed external device to ensure the success of detection.

In conclusion, the present study demonstrates that MaCIA is a highly specific functional cell-based assay coupled with an immunoassay for the rapid and specific detection of the viable target pathogen. *S.* Enteritidis was used as a model pathogen which was successfully detected from food samples (ground chicken, shelled egg, whole milk, and cake mix) in 16-21 h using a conventional sample enrichment set up. The assay time (sample-to-result) was shortened to 10-12 h when an on-cell (on the MaCIA platform) sample enrichment was used. Thus, MaCIA could serve as a universal platform for other pathogens provided an appropriate cell line and a pathogen-specific antibody is used. The extended shelf-life of mammalian cells made MaCIA an attractive screening tool for point-of-need deployment. Furthermore, the MaCIA platform (24-well tissue culture plate) is suitable for testing at least 10 samples (plus positive and negative controls) in duplicate on a single plate thus reducing overall cost per sample testing.

CHAPTER 3. CONCLUSION AND FUTURE SUGGESTION

In cell-based biosensor (CBB), pathogen/toxin interaction with specific mammalian cells (via cell receptor) results in cell death or loss of cellular metabolic activity, which is interrogated via optical or electrical means. As mentioned earlier, maintaining the viability of mammalian cells on sensor platforms for an extended period is a major hindrance to its point-of-care deployment. This is the reason that we used a formalin-fixed mammalian cell line coupled with antibody-based immunoassay (MaCIA) for specific detection of target pathogens to extend the shelf life to 14 weeks and to reduce the maintenance effort.

Binding of viable pathogens or active toxins to host cells is the critical first step for initiation of infection (dos Reis and Horn 2010); therefore, monitoring their interaction via immunoassay provides a viable means for pathogen detection in CBB. Briefly, in MaCIA, a mammalian cell monolayer in a well is exposed to test samples (food slurry or enriched samples) for 30 min. After a brief wash, primary antibody (specific for target pathogen) and enzyme-conjugated secondary antibody cocktail is added for 1.5 h, followed by the addition of a substrate mixture. Color change (15 min) in the wells signifies positive results and which can be quantified after absorbance reading in a plate reader. In the project described in Chapter 2, we have demonstrated that low levels (<10 CFU/25 g) of viable *Salmonella enterica* serovar Enteritidis (SE) can be detected on human ileocecal adenocarcinoma cell line (HCT-8) followed by an enzyme-linked immunoassay using SE-specific mAb-2F11 in 16 h-20 h. We have also demonstrated that both live HCT or formalin-fixed HCT cells in MaCIA efficiently detected viable SE cells from various food matrices (liquid egg, whole chicken carcass rinse, ready-to-eat meat) without any interference. The use of formalin-fixed HCT cells improved the shelf-life of CBB over a month when stored at 4°C. Furthermore, direct enrichment of pathogens in the food matrix on the MaCIA platform did not interfere with the assay.

The application of MaCIA can be expanded for the detection of other foodborne pathogens, including the top 10 *Salmonella enterica* serovars, *Campylobacter*, STEC, and *Listeria monocytogenes*. Besides HCT-8, several other intestinal or non-intestinal cell lines from our collection (Int-407, HT-29, Caco-2, Hep-G2, Vero, CHO, HEK293) could also be tested depending on the target pathogens to be interrogated. Pathogen-specific antibodies from our collection could be used. However, procuring antibodies from commercial sources would be more

practical for implementing this method in the food industry. Fluorophore such as Alexa-flour 488-conjugated secondary antibody could be used instead of the enzyme-conjugated second antibody to provide a one-step assay platform without any requirement for a substrate. SEL broth (Kim and Bhunia 2008; Gehring et al. 2012) could be used as a multi pathogen selective enrichment broth prior to testing on MaCIA. Lastly, as this study indicated, MaCIA is an antibody-based assay. This means that the sensitivity of the assay might be interfered with different macronutrients in food products. Therefore, MaCIA should always be validated with various cooked or raw food matrices to propose a proper enrichment time and detection procedure for an accurate application.

REFERENCE

Abdelhaseib, M.U., Singh, A.K., Bailey, M., Singh, M., El-Khateib, T. and Bhunia, A.K. (2016) Fiber optic and light scattering sensors: Complimentary approaches to rapid detection of *Salmonella enterica* in food samples. *Food Control* **61**, 135-145.

Abdelhaseib, M.U., Singh, A.K. and Bhunia, A.K. (2019) Simultaneous detection of *Salmonella enterica*, *Escherichia coli* and *Listeria monocytogenes* in food using a light scattering sensor. *Journal of applied microbiology* **126**, 1496-1507.

Abu-Bakar, A., Hu, H. and Lang, M.A. (2018) Cyp2a5 promoter-based gene reporter assay: A novel design of cell-based bioassay for toxicity prediction. *Basic and Clinical Pharmacology and Toxicology* **123**, 72-80.

Alamer, S., Eissa, S., Chinnappan, R., Herron, P. and Zourob, M. (2018) Rapid colorimetric lactoferrin-based sandwich immunoassay on cotton swabs for the detection of foodborne pathogenic bacteria. *Talanta* **185**, 275-280.

Aliakbar Ahovan, Z., Hashemi, A., De Plano, L.M., Gholipourmalekabadi, M. and Seifalian, A. (2020) Bacteriophage Based Biosensors: Trends, outcomes and challenges. *Nanomaterials* **10**, 501.

Alsulami, T.S., Zhu, X., Abdelhaseib, M.U., Singh, A.K. and Bhunia, A.K. (2018) Rapid detection and differentiation of *Staphylococcus* colonies using an optical scattering technology. *Anal Bioanal Chem* **410**, 5445-5454.

Baeumner, A.J. (2003) Biosensors for environmental pollutants and food contaminants. *Anal Bioanal Chem* **377**, 434-445.

Bai, X., Shen, A. and Hu, J. (2020) A sensitive SERS-based sandwich immunoassay platform for simultaneous multiple detection of foodborne pathogens without interference. *Analytical Methods* **12**, 4885-4891.

Banada, P.P. and Bhunia, A.K. (2008) Antibodies and immunoassays for detection of bacterial pathogens. In *Principles of Bacterial Detection: Biosensors, Recognition Receptors and Microsystems* eds. Zourob, M., Elwary, S. and Turner, A. pp.567-602. Manchester: Cambridge University.

Banada, P.P., Guo, S., Bayraktar, B., Bae, E., Rajwa, B., Robinson, J.P., Hirleman, E.D. and Bhunia, A.K. (2007) Optical forward-scattering for detection of *Listeria monocytogenes* and other *Listeria* species. *Biosensors and Bioelectronics* **22**, 1664-1671.

Banada, P.P., Huff, K., Bae, E., Rajwa, B., Aroonnual, A., Bayraktar, B., Adil, A., Robinson, J.P., Hirleman, E.D. and Bhunia, A.K. (2009) Label-free detection of multiple bacterial pathogens using light-scattering sensor. *Biosensors and Bioelectronics* **24**, 1685-1692.

Banerjee, P. and Bhunia, A.K. (2009) Mammalian cell-based biosensors for pathogens and toxins. *Trends in Biotechnology* **27**, 179-188.

Banerjee, P. and Bhunia, A.K. (2010) Cell-based biosensor for rapid screening of pathogens and toxins. *Biosensors and Bioelectronics* **26**, 99-106.

Banerjee, P., Lenz, D., Robinson, J.P., Rickus, J.L. and Bhunia, A.K. (2008) A novel and simple cell-based detection system with a collagen-encapsulated B-lymphocyte cell line as a biosensor for rapid detection of pathogens and toxins. *Lab Invest* **88**, 196-206.

Banerjee, P., Morgan, M.T., Rickus, J.L., Ragheb, K., Corvalan, C., Robinson, J.P. and Bhunia, A.K. (2007) Hybridoma Ped-2E9 cells cultured under modified conditions can sensitively detect *Listeria monocytogenes* and *Bacillus cereus*. *Applied Microbiology and Biotechnology* **73**, 1423-1434.

Barrila, J., Yang, J., Crabbé, A., Sarker, S.F., Liu, Y., Ott, C.M., Nelman-Gonzalez, M.A., Clemett, S.J., Nydam, S.D., Forsyth, R.J., Davis, R.R., Crucian, B.E., Quiriarte, H., Roland, K.L., Brenneman, K., Sams, C., Loscher, C. and Nickerson, C.A. (2017) Three-dimensional organotypic co-culture model of intestinal epithelial cells and macrophages to study *Salmonella enterica* colonization patterns. *npj Microgravity* **3**, 10.

Bäumler, A.J., Tsolis, R.M. and Heffron, F. (1996) The lpf fimbrial operon mediates adhesion of *Salmonella typhimurium* to murine Peyer's patches. *Proceedings of the National Academy of Sciences* **93**, 279-283.

Bell, R.L., Jarvis, K.G., Ottesen, A.R., McFarland, M.A. and Brown, E.W. (2016) Recent and emerging innovations in *Salmonella* detection: a food and environmental perspective. *Microb Biotechnol* **9**, 279-292.

Bhunia, A.K. (2008) Biosensors and bio-based methods for the separation and detection of foodborne pathogens. *Advances in Food and Nutrition Research* **54**, 1-44.

Bhunia, A.K. (2011) Rapid pathogen screening tools for food safety. *Food Technol* **65**, 38-43.

Bhunia, A.K. (2014) One day to one hour: how quickly can foodborne pathogens be detected? *Future Microbiology* **9**, 935-946.

Bhunia, A.K. (2018) *Salmonella enterica*. In *Foodborne Microbial Pathogens: Mechanisms and Pathogenesis* ed. Bhunia, A.K. pp.271-287. New York, NY: Springer New York.

Bhunia, A.K., Banada, P.P., Banerjee, P., Valadez, A. and Hirleman, E.D. (2007) Light scattering, fiber optic-and cell-based sensors for sensitive detection of foodborne pathogens. *J Rapid Methods Automat Microbiol* **15**, 121-145.

Bhunia, A.K., Westbrook, D.G., Story, R. and Johnson, M.G. (1995) Frozen stored murine hybridoma cells can be used to determine the virulence of *Listeria monocytogenes*. *Journal of Clinical Microbiology* **33**, 3349-3351.

Borse, V.B., Konwar, A.N., Jayant, R.D. and Patil, P.O. (2020) Perspectives of characterization and bioconjugation of gold nanoparticles and their application in lateral flow immunosensing. *Drug Delivery and Translational Research* **10**, 878-902.

Buzby, J.C., Farah-Wells, H. and Hyman, J. (2014) The estimated amount, value, and calories of postharvest food losses at the retail and consumer levels in the United States. *USDA-ERS Economic Information Bulletin Number 121*.

CDC (2018) Salmonella-reports of selected *Salmonella* outbreak investigations; https://www.cdc.gov/salmonella/outbreaks.html. Atlanta, GA: CDC.

CDC (2020) *Salmonella* https://www.cdc.gov/salmonella/index.html. Atlanta, GA: CDC.

Chen, J., Alcaine, S.D., Jiang, Z., Rotello, V.M. and Nugen, S.R. (2015a) Detection of *Escherichia coli* in drinking water using T7 bacteriophage-conjugated magnetic probe. *Anal Chem* **87**, 8977-8984.

Chen, J. and Park, B. (2018) Effect of immunomagnetic bead size on recovery of foodborne pathogenic bacteria. *International Journal of Food Microbiology* **267**, 1-8.

Chen, M., Yu, Z., Liu, D., Peng, T., Liu, K., Wang, S., Xiong, Y., Wei, H., Xu, H. and Lai, W. (2015b) Dual gold nanoparticle lateral flow immunoassay for sensitive detection of *Escherichia coli* O157:H7. *Analytica Chimica Acta* **876**, 71-76.

Chen, R., Huang, X., Li, J., Shan, S., Lai, W. and Xiong, Y. (2016) A novel fluorescence immunoassay for the sensitive detection of *Escherichia coli* O157:H7 in milk based on catalase-mediated fluorescence quenching of CdTe quantum dots. *Analytica Chimica Acta* **947**, 50-57.

Cho, I.-H., Radadia, A.D., Farrokhzad, K., Ximenes, E., Bae, E., Singh, A.K., Oliver, H., Ladisch, M., Bhunia, A., Applegate, B., Mauer, L., Bashir, R. and Irudayaraj, J. (2014) Nano/Micro and spectroscopic approaches to food pathogen detection. *Annu Rev Anal Chem* **7**, 65-88.

Cui, X., Huang, Y., Wang, J., Zhang, L., Rong, Y., Lai, W. and Chen, T. (2015) A remarkable sensitivity enhancement in a gold nanoparticle-based lateral flow immunoassay for the detection of *Escherichia coli* O157:H7. *Rsc Adv* **5**, 45092-45097.

Curtis, T.M., Widder, M.W., Brennan, L.M., Schwager, S.J., van der Schalie, W.H., Fey, J. and Salazar, N. (2009) A portable cell-based impedance sensor for toxicity testing of drinking water. *Lab on a Chip* **9**, 2176-2183.

Dibao-Dina, A., Follet, J., Ibrahim, M., Vlandas, A. and Senez, V. (2015) Electrical impedance sensor for quantitative monitoring of infection processes on HCT-8 cells by the waterborne parasite *Cryptosporidium*. *Biosensors and Bioelectronics* **66**, 69-76.

dos Reis, R.S. and Horn, F. (2010) Enteropathogenic *Escherichia coli, Samonella, Shigella* and *Yersinia:* cellular aspects of host-bacteria interactions in enteric diseases. *Gut pathogens* **2**, 8.

Drolia, R. and Bhunia, A.K. (2019) Crossing the intestinal barrier via *Listeria* adhesion protein and internalin A. *Trends Microbiol* **27**, 408-425.

Drolia, R., Tenguria, S., Durkes, A.C., Turner, J.R. and Bhunia, A.K. (2018) *Listeria* adhesion protein induces intestinal epithelial barrier dysfunction for bacterial translocation. *Cell Host & Microbe* **23**, 470-484.

Elkhishin, M.T., Gooneratne, R. and Hussain, M.A. (2017) Microbial safety of foods in the supply chain and food security. *Adv Food Technol Nutr Sci Open J* **3**, 22-32.

Eltoum, I., Fredenburgh, J. and Grizzle, W.E. (2001) Advanced Concepts in Fixation: 1. Effects of fixation on immunohistochemistry, reversibility of fixation and recovery of proteins, nucleic acids, and other molecules from fixed and processed tissues. 2. Developmental methods of fixation. *Journal of Histotechnology* **24**, 201-210.

Eriksson, E. and Aspan, A. (2007) Comparison of culture, ELISA and PCR techniques for *Salmonella* detection in faecal samples for cattle, pig and poultry. *BMC veterinary research* **3**, 21.

Farooq, U., Yang, Q., Ullah, M.W. and Wang, S. (2018) Bacterial biosensing: Recent advances in phage-based bioassays and biosensors. *Biosensors and Bioelectronics* **118**, 204-216.

FDA (2001) Bacteriological Analytical Manual Online, 8th ed AOAC International, Arlington, VA. http://www.fda.gov/Food/ScienceResearch/LaboratoryMethods/BacteriologicalAnalyticalManualBAM/default.htm.

FDA (2016) Recalls, Corrections and Removals (Devices): http://www.fda.gov/MedicalDevices/DeviceRegulationandGuidance/PostmarketRequirements/RecallsCorrectionsAndRemovals.

Fei, J., Dou, W. and Zhao, G. (2015) A sandwich electrochemical immunosensor for *Salmonella* pullorum and *Salmonella* gallinarum based on a screen-printed carbon electrode modified with an ionic liquid and electrodeposited gold nanoparticles. *Microchimica Acta* **182**, 2267-2275.

Fei, J., Dou, W. and Zhao, G. (2016) Amperometric immunoassay for the detection of *Salmonella* Pullorum using a screen - printed carbon electrode modified with gold nanoparticle-coated reduced graphene oxide and immunomagnetic beads. *Microchimica Acta* **183**, 757-764.

Finlay, B.B. and Falkow, S. (1997) Common themes in microbial pathogenicity revisited. *Microbiol Mol Biol Rev* **61**, 136-169.

Franche, N., Vinay, M. and Ansaldi, M. (2017) Substrate-independent luminescent phage-based biosensor to specifically detect enteric bacteria such as *E. coli*. *Environmental Science and Pollution Research* **24**, 42-51.

Fratamico, P.M. and Strobaugh, T.P. (1998) Simultaneous detection of *Salmonella* spp and *Escherichia coli* O157:H7 by multiplex PCR. *Journal of Industrial Microbiology & Biotechnology* **21**, 92-98.

FSIS, U. (2019) Pathogen Reduction-Salmonella and Campylobacter Performance Standards Verification Testing Objectives. pp.25-25.

FSIS, U. (2020) RTE Timeline (Changes to the Program): https://www.fsis.usda.gov/wps/portal/fsis/newsroom/meetings/!ut/p/a1/1ZNdb8IgFIZ_jZcEsFrbS2eiTpcaP6e9MQi0wxSoFJe5Xz9wMfvIjJp4s3JRDjzn5XDIC1O4hKkiryInVmhFCh-n4RqNUYjjDhqMuu0uekyC7iJKehjNAwesfgAx9sBiPBp2OihKgkv5zzCFKVW2tC9wlVWiAlQry5WtIeH-RnE3k0SoGrK6FLSqIUYscVRRcOqrBEQxYHipjXWbUlCjN0IXOj-4FF5ZoXJQGp0bIkGmDTCWA8mJPeaVel9Yc_AA21MvYDhhB2A18IgVkhdCcbfssk6RL7kkOWe8Erk6RlQwuIpJK6Mho4CFKACNGFOw4ZiBDa3HddKMsigITw0787XRVQ37jiDshkOmjf4gCdAw_A388SafwPkaVq7I1pdCb-KP6E5nuNd8wFEbw-mNt74gGNxZcIzuLVi_t-DtPRxc4UWx3e3StnOUN9Gbhcv_YqlSzmW0zZ7CSf99lkm5ThJANhEKmkX-AY73xE8!/.

Fu, Y., Zhou, X. and Xing, D. (2018) Integrated paper-based detection chip with nucleic acid extraction and amplification for automatic and sensitive pathogen detection. *Sensors and Actuators, B: Chemical* **261**, 288-296.

Fulgione, A., Cimafonte, M., Della Ventura, B., Iannaccone, M., Ambrosino, C., Capuano, F., Proroga, Y.T.R., Velotta, R. and Capparelli, R. (2018) QCM-based immunosensor for rapid detection of *Salmonella* Typhimurium in food. *Scientific Reports* **8**, 1-8.

Galikowska, E., Kunikowska, D., Tokarska-Pietrzak, E., Dziadziuszko, H., Łoś, J.M., Golec, P., Węgrzyn, G. and Łoś, M. (2011) Specific detection of Salmonella enterica and Escherichia coli strains by using ELISA with bacteriophages as recognition agents. *European journal of clinical microbiology & infectious diseases* **30**, 1067-1073.

Ge, Q., Ge, P., Jiang, D., Du, N., Chen, J., Yuan, L., Yu, H., Xu, X., Wu, M., Zhang, W. and Zhou, G. (2018) A novel and simple cell-based electrochemical biosensor for evaluating the antioxidant capacity of *Lactobacillus plantarum* strains isolated from Chinese dry-cured ham. *Biosensors and Bioelectronics* **99**, 555-563.

Gehring, A.G., Albin, D.M., Bhunia, A.K., Kim, H., Reed, S.A. and Tu, S.-I. (2012) Mixed culture enrichment of *Escherichia coli* O157:H7, *Listeria monocytogenes*, *Salmonella enterica*, and *Yersinia enterocolitica*. *Food Control* **26**, 269-273.

Goodridge, L., Fong, K., Wang, S. and Delaquis, P. (2018) Bacteriophage-based weapons for the war against foodborne pathogens. *Current Opinion in Food Science* **20**, 69-75.

Gray, K.M., Banada, P.P., O'Neal, E. and Bhunia, A.K. (2005) Rapid Ped-2E9 cell-based cytotoxicity analysis and genotyping of *Bacillus* species. *J Clin Microbiol* **43**, 5865-5872.

Hahm, B.K. and Bhunia, A.K. (2006) Effect of environmental stresses on antibody-based detection of *Escherichia coli* O157:H7, *Salmonella enterica* serotype Enteritidis and *Listeria monocytogenes*. *Journal of Applied Microbiology* **100**, 1017-1027.

Hice, S.A., Clark, K.D., Anderson, J.L. and Brehm-Stecher, B.F. (2018) Capture, concentration, and detection of *Salmonella* in foods using magnetic ionic liquids and recombinase polymerase amplification. *Anal Chem* **91**, 1113-1120.

Hicks, M., Bachmann, T.T. and Wang, B. (2020) Synthetic biology enables programmable cell-based biosensors. *ChemPhysChem* **21**, 132-144.

Horikawa, S., Chen, I.H., Du, S., Liu, Y., Wikle, H.C., Suh, S.-J., Barbaree, J.M. and Chin, B.A. (2016) Method for detection of a few pathogenic bacteria and determination of live versus dead cells. In *Sensing for Agriculture and Food Quality and Safety VIII*. pp.98640H-98640H.

Hristov, D.R., Rodriguez-Quijada, C., Gomez-Marquez, J. and Hamad-Schifferli, K. (2019) Designing paper-based immunoassays for biomedical applications. *Sensors (Basel, Switzerland)* **19**, 554.

Hu, J., Tang, F., Jiang, Y.Z. and Liu, C. (2020) Rapid screening and quantitative detection of *Salmonella* using a quantum dot nanobead-based biosensor. *Analyst* **145**, 2184-2190.

Hu, L. and Wai, T.T. (2017) Comparing invasive effects of five foodborne bacterial pathogens in human embryonic intestine 407 cells and human ileocecum HCT-8 cells. *Asian Pacific Journal of Tropical Biomedicine* **7**, 937-944.

Hu, Y., Hua, S., Li, F., Jiang, Y., Bai, X., Li, D. and Niu, L. (2011) Green-synthesized gold nanoparticles decorated graphene sheets for label-free electrochemical impedance DNA hybridization biosensing. *Biosensors and Bioelectronics* **26**, 4355-4361.

Huff, K., Aroonnual, A., Littlejohn, A.E.F., Rajwa, B., Bae, E., Banada, P.P., Patsekin, V., Hirleman, E.D., Robinson, J.P. and Richards, G.P. (2012) Light-scattering sensor for real-time identification of *Vibrio parahaemolyticus*, *Vibrio vulnificus* and *Vibrio cholerae* colonies on solid agar plate. *Microb Biotechnol* **5**, 607-620.

Jaradat, Z.W. and Bhunia, A.K. (2003) Adhesion, invasion and translocation characteristics of *Listeria monocytogenes* serotypes in Caco-2 cell and mouse models. *Appl Environ Microbiol* **69**, 3640-3645.

Jaradat, Z.W., Bzikot, J.H., Zawistowski, J. and Bhunia, A.K. (2004) Optimization of a rapid dot-blot immunoassay for detection of *Salmonella enterica* serovar Enteritidis in poultry products and environmental samples. *Food Microbiol* **21**, 761-769.

Jiang, D., Feng, D., Jiang, H., Yuan, L., Yongqi, Y., Xu, X. and Fang, W. (2017) Preliminary study on an innovative, simple mast cell-based electrochemical method for detecting foodborne pathogenic bacterial quorum signaling molecules (N-acyl-homoserine-lactones). *Biosensors and Bioelectronics* **90**, 436-442.

Jiang, D., Liu, Y., Jiang, H., Rao, S., Fang, W., Wu, M., Yuan, L. and Fang, W. (2018a) A novel screen-printed mast cell-based electrochemical sensor for detecting spoilage bacterial quorum signaling molecules (N-acyl-homoserine-lactones) in freshwater fish. *Biosensors and Bioelectronics* **102**, 396-402.

Jiang, H., Yang, J., Wan, K., Jiang, D. and Jin, C. (2020) Miniaturized paper-supported 3D cell-based electrochemical sensor for bacterial lipopolysaccharide detection. *ACS Sensors* **5**, 1325-1335.

Jiang, P., Wang, Y., Zhao, L., Ji, C., Chen, D. and Nie, L. (2018b) Applications of gold nanoparticles in non-optical biosensors. *Nanomaterials* **8**, 1-23.

Jończyk, E., Kłak, M., Międzybrodzki, R. and Górski, A. (2011) The influence of external factors on bacteriophages-review. *Folia Microbiologica* **56**, 191-200.

Kasturi, K.N. and Drgon, T. (2017) Real-time PCR Method for detection of *Salmonella* spp. in environmental samples. *Appl Environ Microbiol* **83**, e00644-00617.

Kaur, H. and Shorie, M. (2019) Nanomaterial based aptasensors for clinical and environmental diagnostic applications. *Nanoscale Advances* **1**, 2123-2138.

Kaushik, S., Pandey, A., Tiwari, U.K. and Sinha, R.K. (2018) A label-free fiber optic biosensor for Salmonella Typhimurium detection. *Optical Fiber Technology* **46**, 95-103.

Kaushik, S., Tiwari, U.K., Pal, S.S. and Sinha, R.K. (2019) Rapid detection of *Escherichia coli* using fiber optic surface plasmon resonance immunosensor based on biofunctionalized Molybdenum disulfide (MoS 2) nanosheets. *Biosensors and Bioelectronics* **126**, 501-509.

Kavita, V. (2017) DNA Biosensors-A Review. *Journal of Bioengineering & Biomedical Science* **07**.

Khang, J., Kim, D., Chung, K.W. and Lee, J.H. (2016) Chemiluminescent aptasensor capable of rapidly quantifying *Escherichia coli* O157:H7. *Talanta* **147**, 177-183.

Kim, H. and Bhunia, A.K. (2008) SEL, a selective enrichment broth for simultaneous growth of *Salmonella enterica*, *Escherichia coli* O157:H7, and *Listeria monocytogenes*. *Appllied and Environmental Microbiology* **74**, 4853-4866.

Kim, K.P., Singh, A.K., Bai, X., Leprun, L. and Bhunia, A.K. (2015) Novel PCR assays complement laser biosensor-based method and facilitate *Listeria* species detection from food. *Sensors (Switzerland)* **15**, 22672-22691.

Kirk, M.D., Pires, S.M., Black, R.E., Caipo, M., Crump, J.A., Devleesschauwer, B., Doepfer, D., Fazil, A., Fischer-Walker, C.L., Hald, T., Hall, A.J., Keddy, K.H., Lake, R.J., Lanata, C.F., Torgerson, P.R., Havelaar, A.H. and Angulo, F.J. (2015) World Health Organization estimates of the global and regional disease burden of 22 foodborne bacterial, protozoal, and viral diseases, 2010: A data synthesis. *Plos Medicine* **12**, e1001921.

Kline, K.A., Fälker, S., Dahlberg, S., Normark, S. and Henriques-Normark, B. (2009) Bacterial adhesins in host-microbe interactions. *Cell host & microbe* **5**, 580-592.

Kolenda, R., Ugorski, M. and Grzymajło, K. (2019) Everything you always wanted to know about *Salmonella* type 1 fimbriae, but were afraid to ask. *Frontiers in microbiology* **10**, 1017.

Kruspe, S. and Giangrande, P.H. (2017) Aptamer-siRNA chimeras: Discovery, progress, and future prospects. *Biomedicines* **5**, 1-20.

Kuang, H., Yang, F., Zhang, Y., Wang, T. and Chen, G. (2018) The impact of egg nutrient composition and its consumption on cholesterol homeostasis. *Cholesterol* **2018**, Article ID 6303810.

Lee, K.-M., Runyon, M., Herrman, T.J., Phillips, R. and Hsieh, J. (2015) Review of *Salmonella* detection and identification methods: Aspects of rapid emergency response and food safety. *Food Control* **47**, 264-276.

Liu, J., Jasim, I., Shen, Z., Zhao, L., Dweik, M., Zhang, S. and Almasri, M. (2019) A microfluidic based biosensor for rapid detection of *Salmonella* in food products. *PLoS One* **14**, 1-18.

Luo, K., Kim, H.-Y., Oh, M.-H. and Kim, Y.-R. (2020) Paper-based lateral flow strip assay for the detection of foodborne pathogens: principles, applications, technological challenges and opportunities. *Critical Reviews in Food Science and Nutrition* **60**, 157-170.

Majdinasab, M., Hayat, A. and Marty, J.L. (2018) Aptamer-based assays and aptasensors for detection of pathogenic bacteria in food samples. *TrAC - Trends in Analytical Chemistry* **107**, 60-77.

Mansfield, L.P. and Forsythe, S.J. (2000) The detection of *Salmonella* using a combined immunomagnetic separation and ELISA end-detection procedure. *Letters in applied microbiology* **31**, 279-283.

Martelet, A., Lhostis, G., Nevers, M.C., Volland, H., Junot, C., Becher, F. and Muller, B.H. (2015) Phage amplification and immunomagnetic separation combined with targeted mass spectrometry for sensitive detection of viable bacteria in complex food matrices. *Anal Chem* **87**, 5553-5560.

Masdor, N.A., Altintas, Z. and Tothill, I.E. (2017) Surface plasmon resonance immunosensor for the detection of *Campylobacter jejuni*. *Chemosensors* **5**, 1-15.

Masi, A. and Zawistowski, J. (1995) Detection of live and heat-treated *Salmonella* Enteritidis by a D1-serospecific anti-lipopolysaccharide O-9 monoclonal antibody. *Food and Agricultural Immunology* **7**, 351-363.

McKee, M.L. and O'Brien, A.D. (1995) Investigation of enterohemorrhagic *Escherichia coli* O157: H7 adherence characteristics and invasion potential reveals a new attachment pattern shared by intestinal *E. coli*. *Infect Immun* **63**, 2070-2074.

McWilliams, B.D. and Torres, A.G. (2014) Enterohaemorrhagic adhesins. *Microbiology spectrum* **2**, EHEC-0003.

Mendonca, M., Conrad, N., Conceicao, F., Moreira, A., da Silva, W., Aleixo, J. and Bhunia, A. (2012) Highly specific fiber optic immunosensor coupled with immunomagnetic separation for detection of low levels of *Listeria monocytogenes* and *L. ivanovii*. *BMC Microbiology* **12**, 275.

Mendonça, M., Conrad, N.L., Conceição, F.R., Moreira, Â.N., Silva, W.P.d., Aleixo, J.A. and Bhunia, A.K. (2012) Highly specific fiber optic immunosensor coupled with immunomagnetic separation for detection of low levels of Listeria monocytogenes and L. ivanovii. *BMC Microbiology*.

Mohamadi, E., Moghaddasi, M., Farahbakhsh, A. and Kazemi, A. (2017) A quantum-dot-based fluoroassay for detection of food-borne pathogens. *Journal of Photochemistry and Photobiology B: Biology* **174**, 291-297.

Morlay, A., Duquenoy, A., Piat, F., Calemczuk, R., Mercey, T., Livache, T. and Roupioz, Y. (2017a) Label-free immuno-sensors for the fast detection of *Listeria* in food. *Measurement* **98**, 305-310.

Morlay, A., Duquenoy, A., Piat, F., Calemczuk, R., Mercey, T., Livache, T. and Roupioz, Y. (2017b) Label-free immuno-sensors for the fast detection of Listeria in food. *Measurement: Journal of the International Measurement Confederation* **98**, 305-310.

Ngamwongsatit, P., Banada, P.P., Panbangred, W. and Bhunia, A.K. (2008) WST-1-based cell cytotoxicity assay as a substitute for MTT-based assay for rapid detection of toxigenic *Bacillus* species using CHO cell line. *J Microbiol Methods* **73**, 211-215.

Nordin, N., Yusof, N.A., Abdullah, J., Radu, S. and Hushiarian, R. (2016) Sensitive detection of multiple pathogens using a single DNA probe. *Biosensors and Bioelectronics* **86**, 398-405.

Ohk, S.H. and Bhunia, A.K. (2013) Multiplex fiber optic biosensor for detection of Listeria monocytogenes, Escherichia coli O157:H7 and Salmonella enterica from ready-to-eat meat samples. *Food Microbiol* **33**, 166-171.

Ohk, S.H., Koo, O.K., Sen, T., Yamamoto, C.M. and Bhunia, A.K. (2010) Antibody-aptamer functionalized fibre-optic biosensor for specific detection of *Listeria monocytogenes* from food. *Journal of Applied Microbiology* **109**, 808-817.

Paczesny, J., Richter, Ł. and Hołyst, R. (2020) Recent progress in the detection of bacteria using bacteriophages: A review. *Viruses* **12**, 845.

Paião, F.G., Arisitides, L.G.A., Murate, L.S., Vilas-Bôas, G.T., Vilas-Boas, L.A. and Shimokomaki, M. (2013) Detection of *Salmonella* spp, *Salmonella* Enteritidis and Typhimurium in naturally infected broiler chickens by a multiplex PCR-based assay. *Brazilian Journal of Microbiology* **44**, 37-42.

Pan, R., Jiang, Y., Sun, L., Wang, R., Zhuang, K., Zhao, Y., Wang, H., Ali, M.A., Xu, H. and Man, C. (2018) Gold nanoparticle-based enhanced lateral flow immunoassay for detection of *Cronobacter sakazakii* in powdered infant formula. *Journal of Dairy Science* **101**, 3835-3843.

Papadakis, G., Murasova, P., Hamiot, A., Tsougeni, K., Kaprou, G., Eck, M., Rabus, D., Bilkova, Z., Dupuy, B., Jobst, G., Tserepi, A., Gogolides, E. and Gizeli, E. (2018) Micro-nano-bio acoustic system for the detection of foodborne pathogens in real samples. *Biosensors and Bioelectronics* **111**, 52-58.

Piro, B., Shi, S., Reisberg, S., Noël, V. and Anquetin, G. (2016) Comparison of electrochemical immunosensors and aptasensors for detection of small organic molecules in environment, food safety, clinical and public security. *Biosensors* **6**.

Pissuwan, D., Gazzana, C., Mongkolsuk, S. and Cortie, M.B. (2020) Single and multiple detections of foodborne pathogens by gold nanoparticle assays. *Nanomed Nanobiotechnol* **12**, 1-19.

Quintela, I.A., De Los Reyes, B.G., Lin, C.S. and Wu, V.C.H. (2019) Simultaneous colorimetric detection of a variety of Salmonella spp. In food and environmental samples by optical biosensing using oligonucleotide-gold nanoparticles. *Frontiers in Microbiology* **10**, 1-12.

Raeisossadati, M.J., Danesh, N.M., Borna, F., Gholamzad, M., Ramezani, M., Abnous, K. and Taghdisi, S.M. (2016) Lateral flow based immunobiosensors for detection of food contaminants. *Biosensors and Bioelectronics* **86**, 235-246.

Rajapaksha, P., Elbourne, A., Gangadoo, S., Brown, R., Cozzolino, D. and Chapman, J. (2019) A review of methods for the detection of pathogenic microorganisms. *Analyst* **144**, 396-411.

Rashid, J.I.A. and Yusof, N.A. (2017) The strategies of DNA immobilization and hybridization detection mechanism in the construction of electrochemical DNA sensor: A review. *Sensing and Bio-Sensing Research* **16**, 19-31.

Ricke, S.C., Kim, S.A., Shi, Z. and Park, S.H. (2018) Molecular-based identification and detection of *Salmonella* in food production systems: current perspectives. *J Appl Microbiol* **125**, 313-327.

Ríos-Corripio, M.A., Arcila-Lozano, L.S., Garcia-Perez, B.E., Jaramillo-Flores, M.E., Hernández-Pérez, A.D., Carlos-Martínez, A., Rosales-Perez, M. and Rojas-López, M. (2016) Fluorescent gold nanoparticle-based bioconjugate for the detection of *Salmonella*. *Analytical Letters* **49**, 1862-1873.

Rodríguez-Lorenzo, L., Garrido-Maestu, A., Bhunia, A.K., Espiña, B., Prado, M., Diéguez, L. and Abalde-Cela, S. (2019) Gold Nanostars for the detection of foodborne pathogens via surface-enhanced Raman scattering combined with microfluidics. *ACS Applied Nano Materials* **2**, 6081-6086.

Roggo, C. and van der Meer, J.R. (2017) Miniaturized and integrated whole cell living bacterial sensors in field applicable autonomous devices. *Current Opinion in Biotechnology* **45**, 24-33.

Scallan, E., Hoekstra, R.M., Angulo, F.J., Tauxe, R.V., Widdowson, M.A., Roy, S.L., Jones, J.L. and Griffin, P.M. (2011) Foodborne illness acquired in the United States—major pathogens. *Emerg Infect Dis* **17**, 7-15.

Scharff, R. (2012) Economic burden from health losses due to foodborne illness in the United States. *Journal of Food Protection* **75**, 123-131.

Schlaberg, R., Chiu, C.Y., Miller, S., Procop, G.W., Weinstock, G., Professional Practice, C., Committee on Laboratory Practices of the American Society for, M. and Microbiology Resource Committee of the College of American, P. (2017) Validation of metagenomic next-generation sequencing tests for universal pathogen detection. *Archives of Pathology and Laboratory Medicine* **141**, 776-786.

Senturk, E., Aktop, S., Sanlibaba, P. and Tezel, B.U. (2018) Biosensors: A novel approach to detect food-borne pathogens. *Applied Microbiology: Open Access* **04**, 4-11.

Silk, T.M., Roth, T.M.T. and Donnelly, C.W. (2002) Comparison of growth kinetics for healthy and heat-injured *Listeria monocytogenes* in eight enrichment broths. *Journal of Food Protection* **65**, 1333-1337.

Silva, N.F.D., Almeida, C.M.R., Magalhães, J.M.C.S., Gonçalves, M.P., Freire, C. and Delerue-Matos, C. (2019) Development of a disposable paper-based potentiometric immunosensor for real-time detection of a foodborne pathogen. *Biosensors and Bioelectronics* **141**, 111317-111317.

Singh, A.K., Bettasso, A.M., Bae, E., Rajwa, B., Dundar, M.M., Forster, M.D., Liu, L., Barrett, B., Lovchik, J., Robinson, J.P., Hirleman, E.D. and Bhunia, A.K. (2014) Laser optical sensor, a label-free on-plate *Salmonella enterica* colony detection tool. *mBio* **5 (1)**, e01019-01013.

Singh, A.K. and Bhunia, A.K. (2016) Optical scatter patterns facilitate rapid differentiation of *Enterobacteriaceae* on CHROMagar(TM) Orientation medium. *Microb Biotechnol* **9**, 127-135.

Singh, A.K. and Bhunia, A.K. (2018) Optical Biosensors in Foodborne Pathogen Detection. In *Smart Biosensor Technology*. p.443: CRC Press.

Singh, A.K., Drolia, R., Bai, X. and Bhunia, A.K. (2015a) Streptomycin induced stress response in *Salmonella enterica* serovar Typhimurium shows distinct colony scatter signature. *PLoS One* **10**, e0135035.

Singh, A.K., Leprun, L., Drolia, R., Bai, X., Kim, H., Aroonnual, A., Bae, E., Mishra, K.K. and Bhunia, A.K. (2016) Virulence gene-associated mutant bacterial colonies generate differentiating two-dimensional laser scatter fingerprints. *Applied and Environmental Microbiology* **82**, 3256-3268.

Singh, A.K., Sun, X., Bai, X., Huisung Kim, H., Abdalhaseib, M., Bae, E. and Bhunia, A.K. (2015b) Label-free, non-invasive light scattering sensor for rapid screening of *Bacillus* colonies. *Journal of Microbiological Methods* **109**, 56-66.

Singh, S., Dhanjal, D.S., Thotapalli, S., Kumar, V., Datta, S., Kumar, V., Kumar, M. and Singh, J. (2020) An insight in bacteriophage based biosensors with focus on their detection methods and recent advancements. *Environmental Technology & Innovation*, 101081.

Snyder, T.R., Boktor, S.W. and M'Ikanatha, N.M. (2019) Salmonellosis outbreaks by food vehicle, serotype, season, and geographical location, United States, 1998 to 2015. *Journal of food protection* **82**, 1191-1199.

Song, C., Liu, J., Li, J. and Liu, Q. (2016) Dual FITC lateral flow immunoassay for sensitive detection of Escherichia coli O157:H7 in food samples. *Biosensors and Bioelectronics* **85**, 734-739.

Sun, J., Zhu, P., Wang, X., Ji, J., Habimana, J.D.D., Shao, J., Lei, H., Zhang, Y. and Sun, X. (2018) Cell Based-Green Fluorescent Biosensor Using Cytotoxic Pathway for Bacterial Lipopolysaccharide Recognition. *Journal of Agricultural and Food Chemistry* **66**, 6869-6876.

Tabrizi, M.A. and Shamsipur, M. (2015) A label-free electrochemical DNA biosensor based on covalent immobilization of salmonella DNA sequences on the nanoporous glassy carbon electrode. *Biosensors and Bioelectronics* **69**, 100-105.

Tang, Y., Kim, H., Singh, A.K., Aroonnual, A., Bae, E., Rajwa, B., Fratamico, P.M. and Bhunia, A.K. (2014) Light scattering sensor for direct identification of colonies of *Escherichia coli* serogroups O26, O45, O103, O111, O121, O145 and O157. *PLoS One* **9**, e105272.

To, C., Banerjee, P. and Bhunia, A.K. (2020) Cell-Based Biosensor for Rapid Screening of Pathogens and Toxins. In *Handbook of Cell Biosensors* ed. Thouand, G. pp.1-16. Cham: Springer International Publishing.

To, C.Z. and Bhunia, A.K. (2019a) Three dimensional vero cell-platform for rapid and sensitive screening of Shiga-toxin producing Escherichia coli. *Frontiers in Microbiology* **10**, 1-15.

To, C.Z. and Bhunia, A.K. (2019b) Three dimensional Vero cell-platform for rapid and sensitive screening of Shiga-toxin producing *Escherichia coli*. *Frontiers in Microbiology* **10**, 949.

USDA (2015) Recall Summaries: .

USDA (2019a) Laboratory Guidebook Title: Isolation and Identification of Salmonella from Meat, Poultry, Pasteurized Egg, and Siluriformes (Fish) Products and Carcass and Environmental Sponges. pp.18-18: https://www.fsis.usda.gov/wps/wcm/connect/700c05fe-06a2-492a-a6e1-3357f7701f52/mlg-4.pdf?MOD=AJPERES.

USDA (2019b) Recall Summaries 2019: https://www.fsis.usda.gov/wps/portal/fsis/topics/recalls-and-public-health-alerts/recall-summaries.

USDA (2020) Laboratory Guidebook Notice of Change Chapter new , revised , or archived : MLG Appendix 3 . 03 Title : FSIS Laboratory Regulatory Sample Pathogen Methods Table and Definitions Effective Date : 02 / 24 / 20 Description and purpose of change (s): Revised.

USDA-FSIS (2013) Isolation and Identification of *Salmonella* from Meat, Poultry, Pasteurized Egg and Catfish Products. Method number MLG 4.06.: http://www.fsis.usda.gov/wps/wcm/connect/700c05fe-06a2-492a-a6e1-3357f7701f52/MLG-4.pdf?MOD=AJPERES.

Vaisocherová-Lísalová, H., Víšová, I., Ermini, M.L., Špringer, T., Song, X.C., Mrázek, J., Lamačová, J., Scott Lynn, N., Šedivák, P. and Homola, J. (2016) Low-fouling surface plasmon resonance biosensor for multi-step detection of foodborne bacterial pathogens in complex food samples. *Biosensors and Bioelectronics* **80**, 84-90.

Valadez, A., Lana, C., Tu, S.-I., Morgan, M. and Bhunia, A. (2009) Evanescent wave fiber optic biosensor for *Salmonella* detection in food. *Sensors* **9**, 5810-5824.

Wagner, C. and Hensel, M. (2011) Adhesive mechanisms of *Salmonella enterica*. In *Bacterial adhesion*. pp.17-34: Springer.

Wang, B. and Park, B. (2020) Immunoassay biosensing of foodborne pathogens with surface plasmon resonance imaging: A review. *Journal of Agricultural and Food Chemistry*.

Wang, L., Shen, X., Wang, T., Chen, P., Qi, N., Yin, B.C. and Ye, B.C. (2020) A lateral flow strip combined with Cas9 nickase-triggered amplification reaction for dual food-borne pathogen detection. *Biosensors and Bioelectronics* **165**, 112364-112364.

Wang, S.J. and Yeh, D.B. (2002) Designing of polymerase chain reaction primers for the detection of *Salmonella* Enteritidis in foods and faecal samples. *Letters in applied microbiology* **34**, 422-427.

Wang, W., Liu, L., Song, S., Xu, L., Zhu, J. and Kuang, H. (2017) Gold nanoparticle-based paper sensor for multiple detection of 12 *Listeria* spp. by P60-mediated monoclonal antibody. *Food and Agricultural Immunology* **28**, 274-287.

Widder, M.W., Brennan, L.M., Hanft, E.A., Schrock, M.E., James, R.R. and van der Schalie, W.H. (2015) Evaluation and refinement of a field-portable drinking water toxicity sensor utilizing electric cell-substrate impedance sensing and a fluidic biochip. *Journal of Applied Toxicology* **35**, 701-708.

Widyastuti, E., Puspitasari Schonherr, M.F., Masruroh, A., Anggraeni, R.A., Nisak, Y.K. and Mursidah, S. (2018) A sandwich-type optical immunosensor based on the alkaline phosphatase enzyme for *Salmonella* Typhimurium detection. In *IOP Conference Series: Earth and Environmental Science*.

Wu, V.C.H. (2008) A review of microbial injury and recovery methods in food. *Food Microbiol* **25**, 735-744.

Xiang, C., Li, R., Adhikari, B., She, Z., Li, Y. and Kraatz, H.B. (2015) Sensitive electrochemical detection of *Salmonella* with chitosan-gold nanoparticles composite film. *Talanta* **140**, 122-127.

Xu, L., Bai, X., Tenguria, S., Liu, Y., Drolia, R. and Bhunia, A.K. (2020) Mammalian cell-based immunoassay for detection of viable bacterial pathogens. *Frontiers in Microbiology* **11**.

Xu, Y., Wei, Y., Cheng, N., Huang, K., Wang, W., Zhang, L., Xu, W. and Luo, Y. (2018) Nucleic acid biosensor synthesis of an all-in-one universal blocking linker recombinase polymerase amplification with a peptide nucleic acid-based lateral flow device for ultrasensitive detection of food pathogens. *Anal Chem* **90**, 708-715.

Xue, L., Huang, F., Hao, L., Cai, G., Zheng, L., Li, Y. and Lin, J. (2020) A sensitive immunoassay for simultaneous detection of foodborne pathogens using MnO_2 nanoflowers-assisted loading and release of quantum dots. *Food Chemistry* **322**, 126719-126719.

Ye, Y., Guo, H. and Sun, X. (2019) Recent progress on cell-based biosensors for analysis of food safety and quality control. *Biosensors and Bioelectronics* **126**, 389-404.

Yetisen, A.K., Akram, M.S. and Lowe, C.R. (2013) Paper-based microfluidic point-of-care diagnostic devices. *Lab on a Chip* **13**, 2210-2251.

Yu, X., Chen, F., Wang, R. and Li, Y. (2018a) Whole-bacterium SELEX of DNA aptamers for rapid detection of *E. coli* O157:H7 using a QCM sensor. *Journal of Biotechnology* **266**, 39-49.

Yu, X., Chen, F., Wang, R. and Li, Y. (2018b) Whole-bacterium SELEX of DNA aptamers for rapid detection of E.coli O157:H7 using a QCM sensor. *Journal of Biotechnology* **266**, 39-49.

Zhang, C., Wang, C., Xiao, R., Tang, L., Huang, J., Wu, D., Liu, S., Wang, Y., Zhang, D., Wang, S. and Chen, X. (2018) Sensitive and specific detection of clinical bacteria: Via vancomycin-modified Fe3O4@Au nanoparticles and aptamer-functionalized SERS tags. *Journal of Materials Chemistry B* **6**, 3751-3761.

Zhang, D., Coronel-Aguilera, C.P., Romero, P.L., Perry, L., Minocha, U., Rosenfield, C., Gehring, A.G., Paoli, G.C., Bhunia, A.K. and Applegate, B. (2016a) The use of a novel nanoLuc -based reporter phage for the detection of *Escherichia coli* O157:H7. *Scientific Reports* **6**, 33235.

Zhang, D., Coronel-Aguilera, C.P., Romero, P.L., Perry, L., Minocha, U., Rosenfield, C., Gehring, A.G., Paoli, G.C., Bhunia, A.K. and Applegate, B. (2016b) The Use of a Novel NanoLuc-Based Reporter Phage for the Detection of Escherichia coli O157:H7. *Scientific Reports* **6**, 6-13.

Zhang, L., Huang, Y., Wang, J., Rong, Y., Lai, W., Zhang, J. and Chen, T. (2015) Hierarchical flowerlike gold nanoparticles labeled immunochromatography test strip for highly sensitive detection of *Escherichia coli* O157:H7. *Langmuir* **31**, 5537-5544.

Zhang, W., Tang, S., Jin, Y., Yang, C., He, L., Wang, J. and Chen, Y. (2020) Multiplex SERS-based lateral flow immunosensor for the detection of major mycotoxins in maize utilizing dual Raman labels and triple test lines. *Journal of Hazardous Materials* **393**, 122348-122348.

Zhang, W., Zong, P., Zheng, X. and Wang, L. (2013) An enhanced sensing platform for ultrasensitive impedimetric detection of target genes based on ordered FePt nanoparticles decorated carbon nanotubes. *Biosensors and Bioelectronics* **42**, 481-485.

Zhang, Y., Zhu, L., He, P., Zi, F., Hu, X. and Wang, Q. (2019) Sensitive assay of *Escherichia coli* in food samples by microchip capillary electrophoresis based on specific aptamer binding strategy. *Talanta* **197**, 284-290.

Zhu, X., Liu, D., Singh, A.K., Drolia, R., Bai, X., Tenguria, S. and Bhunia, A.K. (2018) Tunicamycin mediated inhibition of wall teichoic acid affect *Staphylococcus aureus* and *Listeria monocytogenes* cell morphology, biofilm formation and virulence. *Frontiers in Microbiology* **9**, 1352.

APPENDIX A. ENTEROHAEMORRHAGIC *E. COLI* DETECTION USING ANTI-TIR ANTIBODY

Enterohaemorrhagic *E. coli* Detection Using Anti-TIR antibody

Introduction:

Type III secretion system (TTSS) plays an imperative role in enterohaemorrhagic *E. coli* (EHEC) pathogenesis. This system helps EHEC deliver virulence factors directly into the host cytoplasm. TTSS assembles as a needle complex, which consists of multiple Esc proteins. TTSS, along with its delivered effector proteins in the host cytoplasm, assists EHEC to better adhere and colonize the host primarily by disrupting the actin polymerization and cellular structures. Translocate Intimin Receptor (Tir) as one of the major effector proteins, mediates intimin binding. The binding of TIR and intimin triggers the formation of the pedestal by extensive actin accumulation, which leads to EHEC adhesion, A/E lesion, and further EHEC infections.

When TIR is phosphorylated by the cell enzyme protein kinase A after injection, it will be integrated into the host cell membrane for an interaction with Intimin, which makes it available as the target for Tir-based immunosensor. The objective was to develop a Tir-based immunoassay for rapid pathogenic *E. coli* detection. However, the objective was not met as the antibody we used cannot differentiate pathogenic *E. coli* from non-pathogenic *E. coli* or other common foodborne pathogens.

Methods

Mammalian Cell Culture

HeLa cells and HCT-8 cells were maintained in Dulbecco's modified Eagles medium with 10 % fetal bovine serum (FBS) (Bio-techne Sales Corp, Minneapolis, MN) at 37°C with 5% CO_2 in cell culture flasks (T25). For all experiments, HeLa cells or HCT-8 were seeded in 96-well tissue culture plates (Fisher Scientific) at a density of 2×10^5 cell/mL/well to achieve a final cell density of 8×10^7 cell/mL and the formation of the monolayer.

Bacterial culture

Bacterial strains were stored as 10% glycerol stocks at -80°C. To revive frozen cultures, each strain was streaked onto tryptic soy agar (TSA) (Thermo Fisher Scientific, Rochester, NY) plate and

incubated at 37°C for 18 h to obtain pure colonies. A single colony of each strain was inoculated and propagated in tryptic soy broth containing 0.5% yeast extract (TSBYE) (Thermo Fisher Scientific) at 37°C for 18 h with shaking at 120 rpm.

Tir-based biosensor

HeLa cell monolayers were prepared and maintained as described above in 24-well plates. Two hundred microliter of overnight grown bacterial cultures was added into each well containing HeLa cells and incubated for 6 h at 37°C. Cell monolayers were washed 2-3 times with PBS gently and were fixed with 3% formalin. For experiment including permeabilization, the cell monolayer was incubated with Triton-X for another 10 min followed by PBS wash. Sequential antibody probing was then performed with pAB-anti-Tir or pAB-anti-GroEl as primary antibodies and pABanti-rabbit Alexa 488 conjugated IgG or pAB-anti-rabbit HRP-conjugated IgG as secondary antibodies for 2 h each at room temperature. Both antibodies were suspended in PBS containing 3% bovine serum albumin (BSA) (Sigma-Aldrich). Cell monolayers were washed 3 times with PBS and the color was developed by adding 500 µl/well substrate solution (o-phenyl diamine, OPD) containing hydrogen-peroxide) (Sigma-Aldrich). The oxidative coupling of OPD to 2,3-diaminophenazine, an orange-brown substance, was catalyzed by HRP at room temperature in the dark for 10 min. The intensity of the colored product was measured using a microplate reader (BioTek, Winooski, VT) at a wavelength of 450 nm.

Western Blot

Overnight grown *E. coli* K12 and EDL933 culture, and the heat-killed *E. coli* EDL933 were used to infect the HCT-8 cell monolayers. After 2 h and 6 h infection, the whole-cell lysate of HCT-8 cells was prepared by cell lysis buffer kit (Cell Signaling). The protein concentration was determined by the BCA method (Thermo Fisher Scientific). Equal amounts of proteins were separated on SDS-PAGE gel (10% polyacrylamide) and electro-transferred to polyvinylidene difluoride (PVDF) membrane (Fisher Scientific). Primary and secondary antibodies were diluted as above. Membranes were first probed with rabbit pAb-anti-Tir (developed in our laboratory by Titikhsa Dixit) at 4°C overnight, and then with anti-rabbit HRP-conjugated antibody at room temperature for 1.5 h. LumiGLO reagent (Cell-Signaling Technology) was used to visualize the bands using the Chemi-Doc XRS system (Bio-Rad).

Immunofluorescence staining

After exposure of HCT-8 cell monolayers to *E. coli* EDL 933 for 6 h, the wells of the chamber slides were washed with PBS to remove unattached bacterial cells (as above). After immunoprobing with pAB-anti-Tir, the monolayers were washed and probed with Alexa Fluro 488 conjugated anti-rabbit antibody for 1.5 h at room temperature in the dark, followed by three PBS wash. Images were acquired using the Leica DAS Microscope at the magnification of 100 × and 400 ×.

Results and Discussion

i) Validation of the principle

Overnight grown *E. coli* EDL933 was incubated with HCT-8 cell and HeLa cell monolayer (permeabilized and non-permeabilized) for 6 h and was then probed with anti-Tir antibody and Alexa 488 conjugated anti-rabbit sequentially. Microscopic images show that permeabilized cells have a stronger signal in both HCT-8 cells and HeLa cell monolayers (**Figure A.1**). The activity of the anti-Tir antibody was also confirmed with Western blot (**Figure A.2**). However, when the test is performed in the 96-well plate using HRP-conjugated anti-rabbit antibody as a secondary antibody, only the non-permeabilized cells showed significant differences comparing to the negative control. A similar trend was shown when using the anti-GroEL antibody as the primary antibody (**Figure A.3**). The result suggests that permeabilization is not necessary to perform the assay. From **Figure A.3**, HCT-8 cells also show a slightly higher absorbance value comparing to the HeLa cells, suggesting that HCT-8 cell monolayer is a better platform for Tir-based immunosensor.

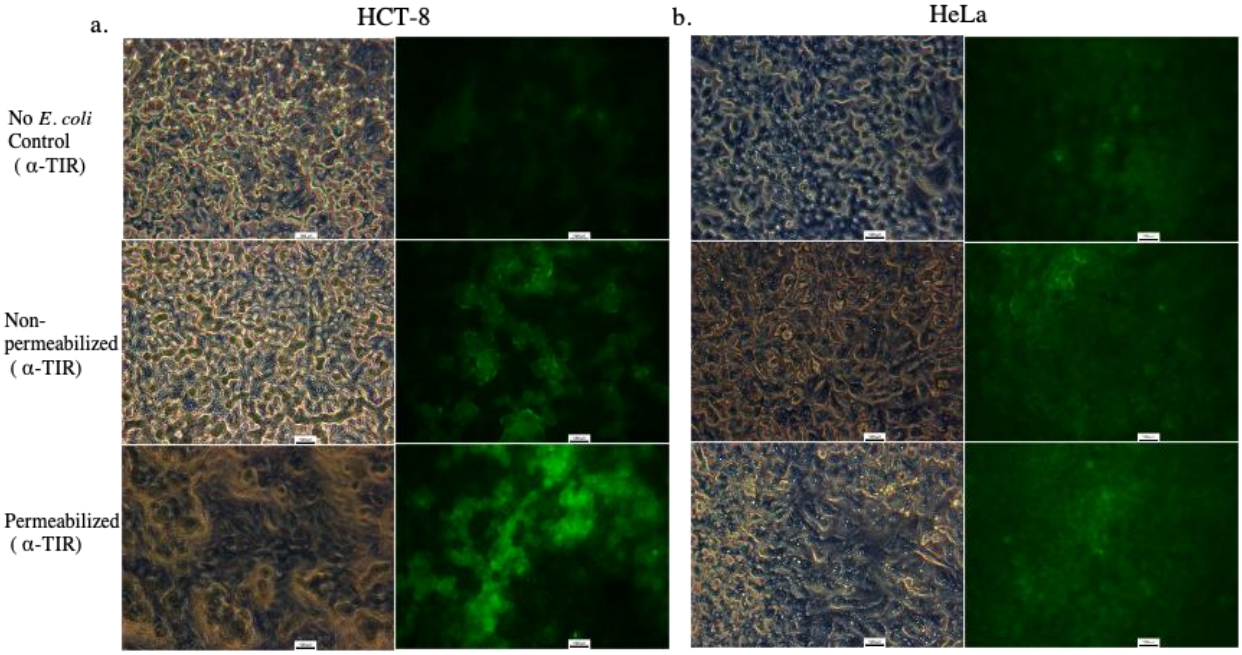

Figure A.1. Microscopic images of Tir expression on (a) HCT- 8 cells and (b) HeLa cells after 6-h exposure of *E. coli* EDL 933. Scale bar:100 μM.

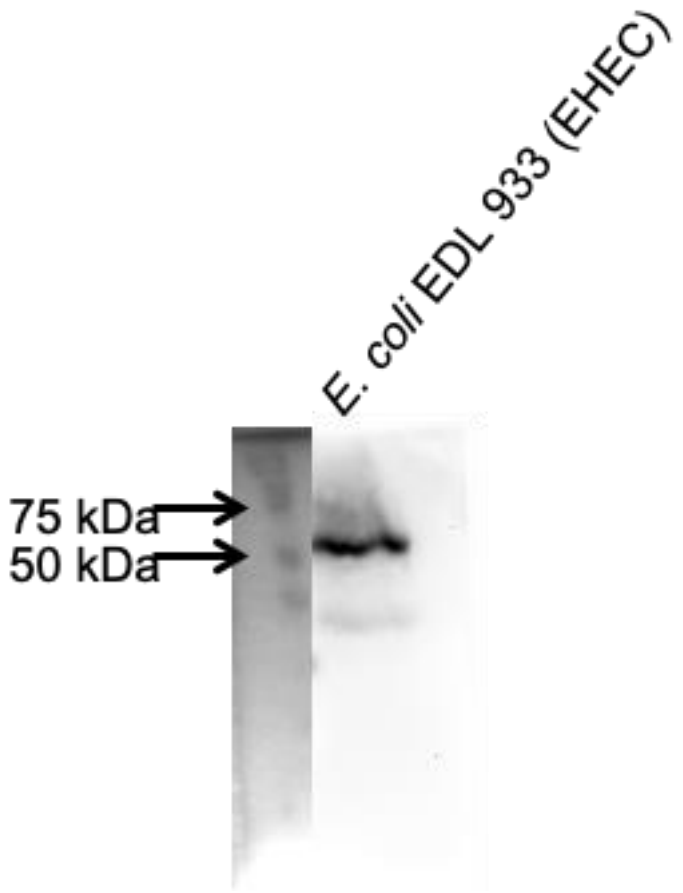

Figure A.2. Western blot of Tir expression on HCT- 8 after 6-h of exposure of *E. coli* EDL 933.

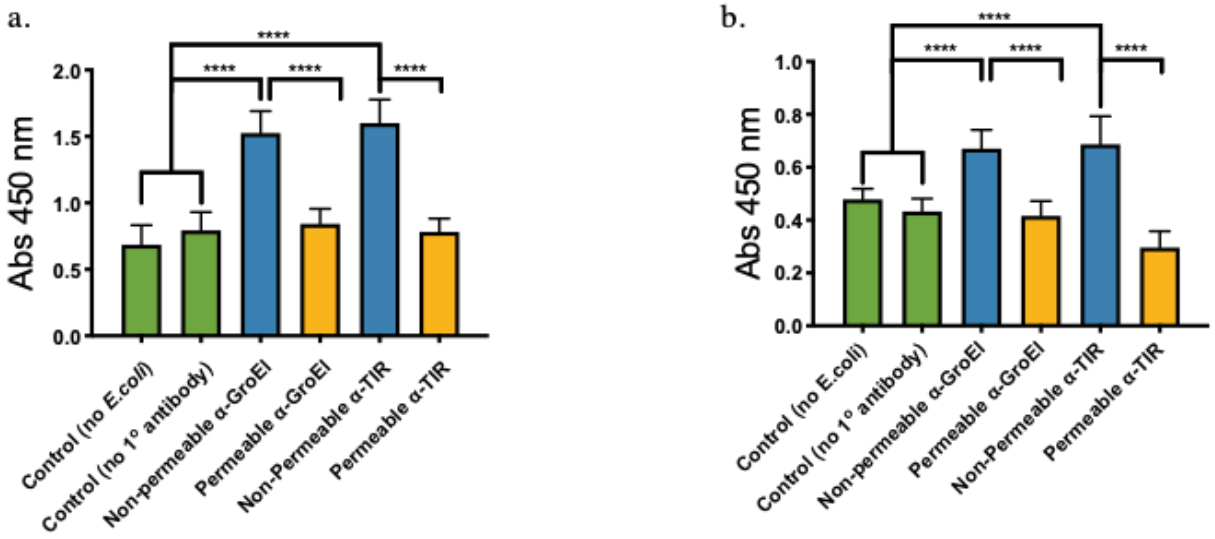

Figure A.3. Tir-based immunosensor using (a) HCT-8 cells and (b) HeLa cells.

ii) Specificity of Tir-based immunosensor

To test if Tir-based immunosensor can differentiate pathogenic *E. coli* and non-pathogenic *E. coli*, Overnight culture of pathogenic *E. coli* (and its dead equivalent), and non-pathogenic *E. coli* were incubated with the HCT-8 cell monolayers for 6 h. Though the pathogenic *E. coli* shows significant differences to both dead E. coli and negative control, it does not show a significant difference to *E. coli* BL21 (**Figure A.4)**, indicating its inability of differentiating pathogenic and non-pathogenic *E. coli*. The primary antibody concentration was optimized to improve sensitivity. However, it does not show any improvement as shown in **Figure A.5**. When the primary antibody concentration decreases, the absorbance value decreases as well in both bacteria containing and negative control samples. The non-specificity was further confirmed with Western blot (**Figure A.6**). Non-specific bands were shown for *E. coli* K12, which is a non-pathogenic strain, incubated with HCT-8 cells for 2 h, and the band with the correct size was shown for 6-h of incubation with that strain. Similar pattern was found in the lanes of pathogenic strain *E. coli* EDL 933. All of the results suggested that Tir-based immunosensor is not the perfect tool for *E. coli* detection, given its inability of differentiating between pathogenic *E. coli* and non-pathogenic *E. coli.*

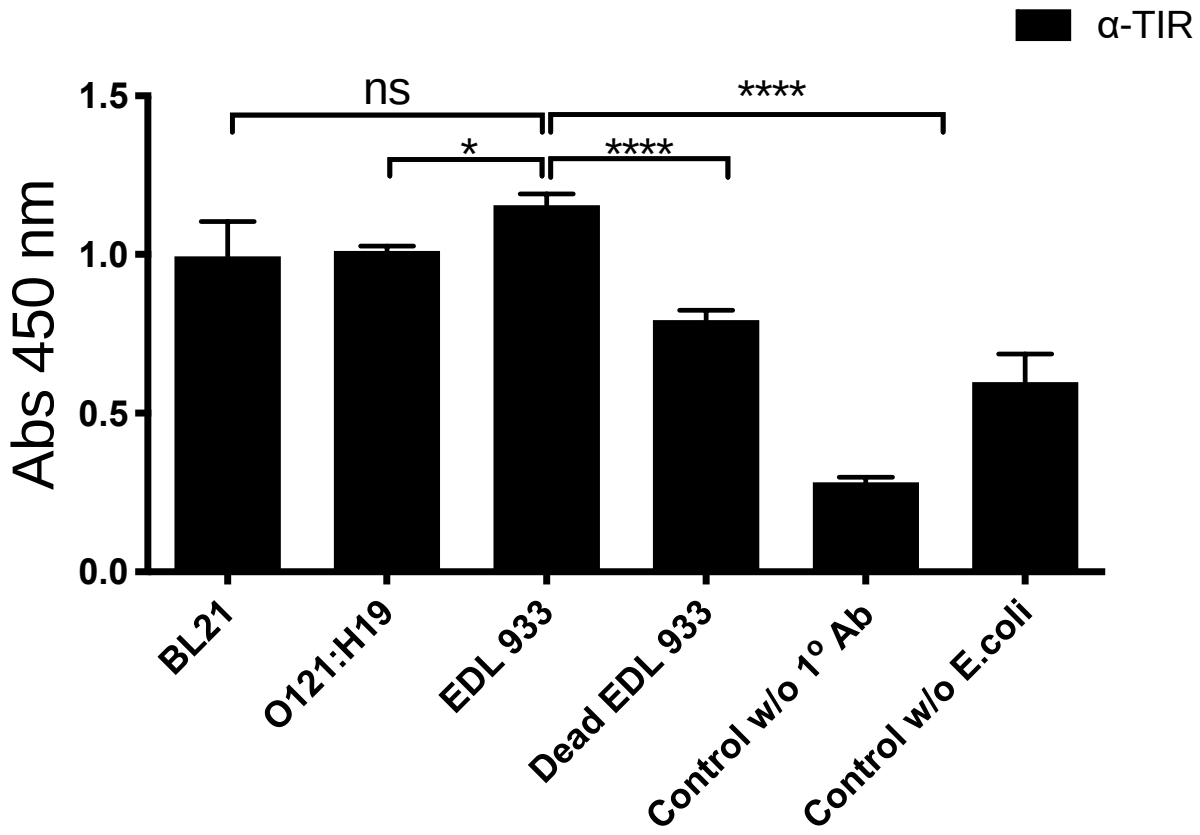

Figure A. 4. Tir-based immunosensor using HCT-8 cells and various *E. coli* strains.

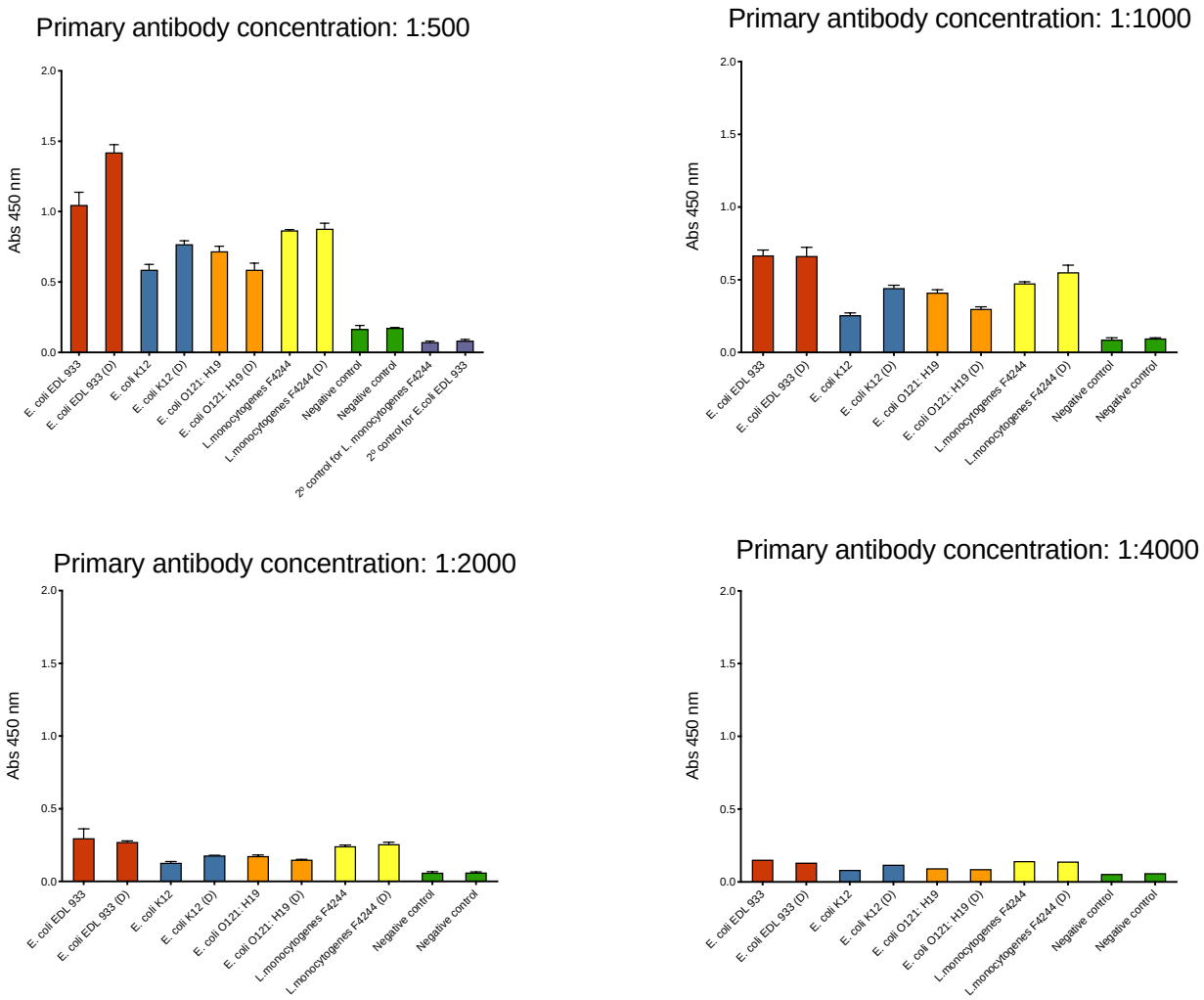

Figure A.5. Primary antibody concentration optimization. The original primary antibody concentration is 1 µg/mL.

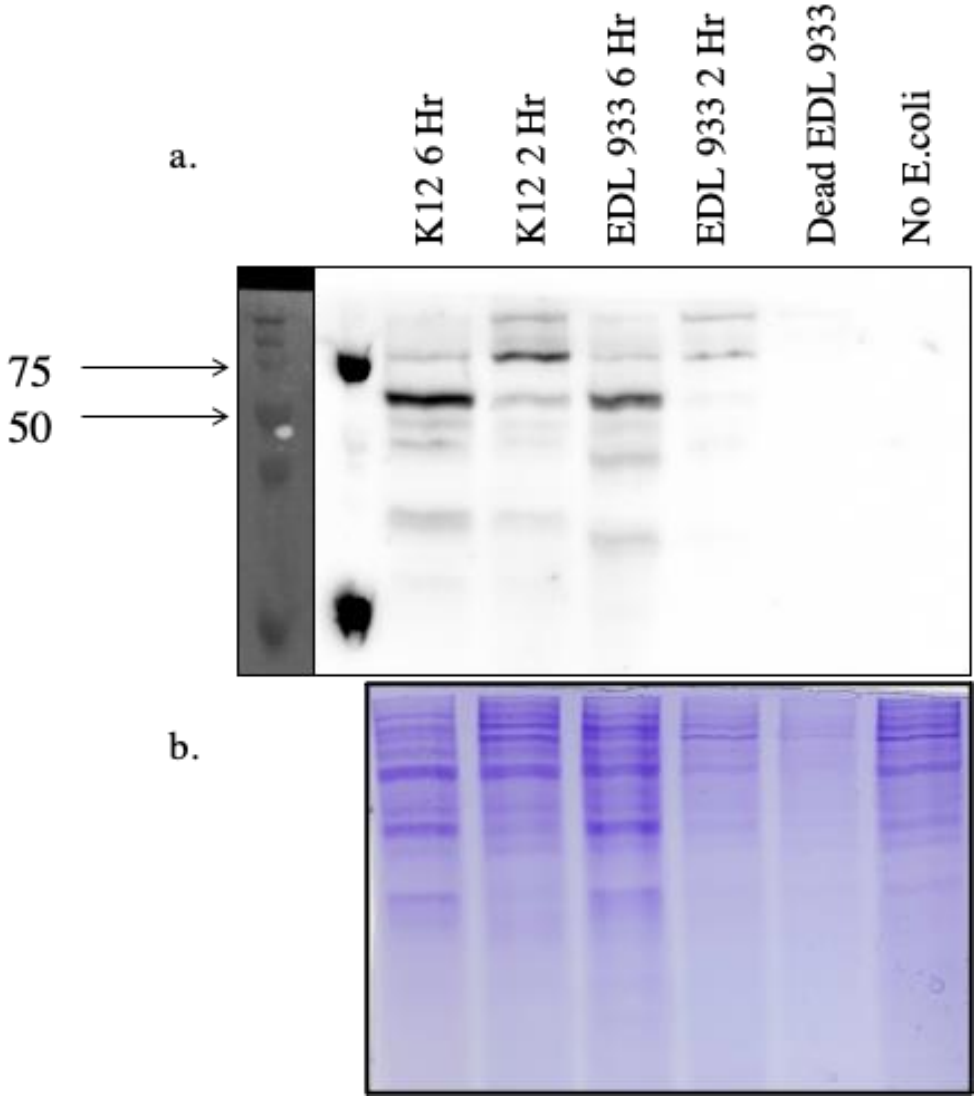

Figure A.6. (a) Western blot of the whole HCT-8 cell lysate after incubating with the bacteria followed by reaction with pAb anti-Tir. (b) Coomassie stained SDS-PAGE.

APPENDIX B. MACIA FOR DETECTION OF *LISTERIA MONOCYTOGENES*

MaCIA for detection of *Listeria monocytogenes*

*All experiments below are performed with non-fixed HCT-8 cell platform and monolayer peeling was observed at some degree with this platform. Other procedures of MaCIA were same as decribed in the previous Chapter.

Results

i) MaCIA can detect viable *Lm* in the presence of other bacteria

Overnight grown *L. monocytogenes* F4244, *E. coli* EDL 933, *P.* aeruginosa PRI99 and *S.* Enteritids PT21 cultures were added on to the HCT-8 cell monolayer and incubated at 37^{o}C for 30 min. Anti-*Lm* pAb (our lab) was used as the primary antibody and HRP conjugated anti-rabbit antibody was used as the secondary antibody. Sequential antibody probing was performed. Upon the addition of OPD substrate, absorbance value at the wavelength of 450 nm was measured. The result shows that the MaCIA could successfully detect *Lm* even with the presence of other pathogens (**Figure B.1**).

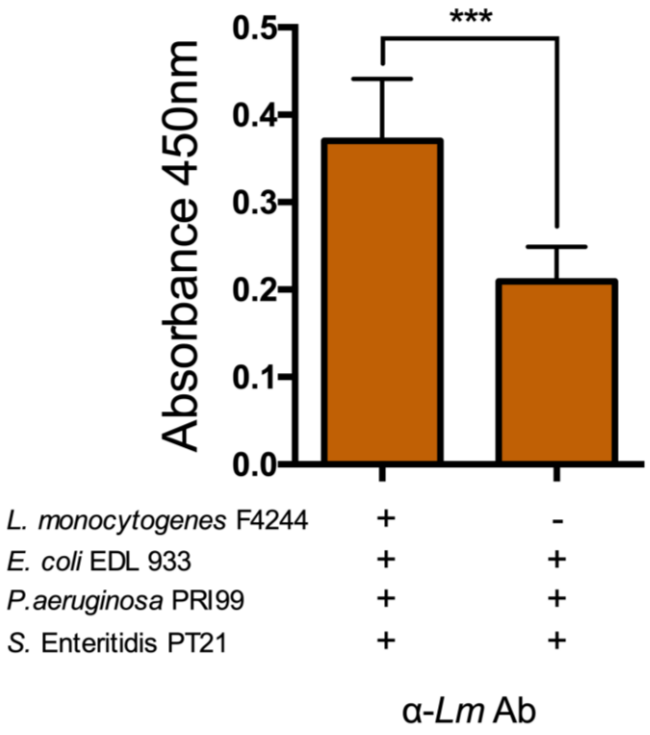

Figure B.1. MaCIA reaction to viable *Lm* in the presence of othe bactieria.

ii) On cell enrichment is feasible for the detection of *Lm*

Overnight grown *Lm* culture was diluted to 10^7 – 10 CFU/mL with D10F. One mililiter of each diluted culture was enriched on the live HCT-8 cell monolayer for 9 h. D10F instead of other enrichment broth was chosen because the live HCT-8 cell monolayer is susceptible to monolayer peeling and detaching. D10F could maintain the morphology and physiological activity of live HCT-8 cell monolayer. By the end of the enrichment process, sequential antibody probing was performed, followed by the substrate addition and absorbance measurement. The result shows that 9-h of on cell enrichment could detect viable *Lm* with LOD of 10^4 CFU/mL (**Figure B.2**). However, significant HCT-8 monolayer peeling was observed, which makes the results less convincing. Besides, the growth curve of *Lm* in D10F appears atypical, as it reaches the end of the exponential phase within 5 hours and entered the death phase immediately (**Figure B.3**).

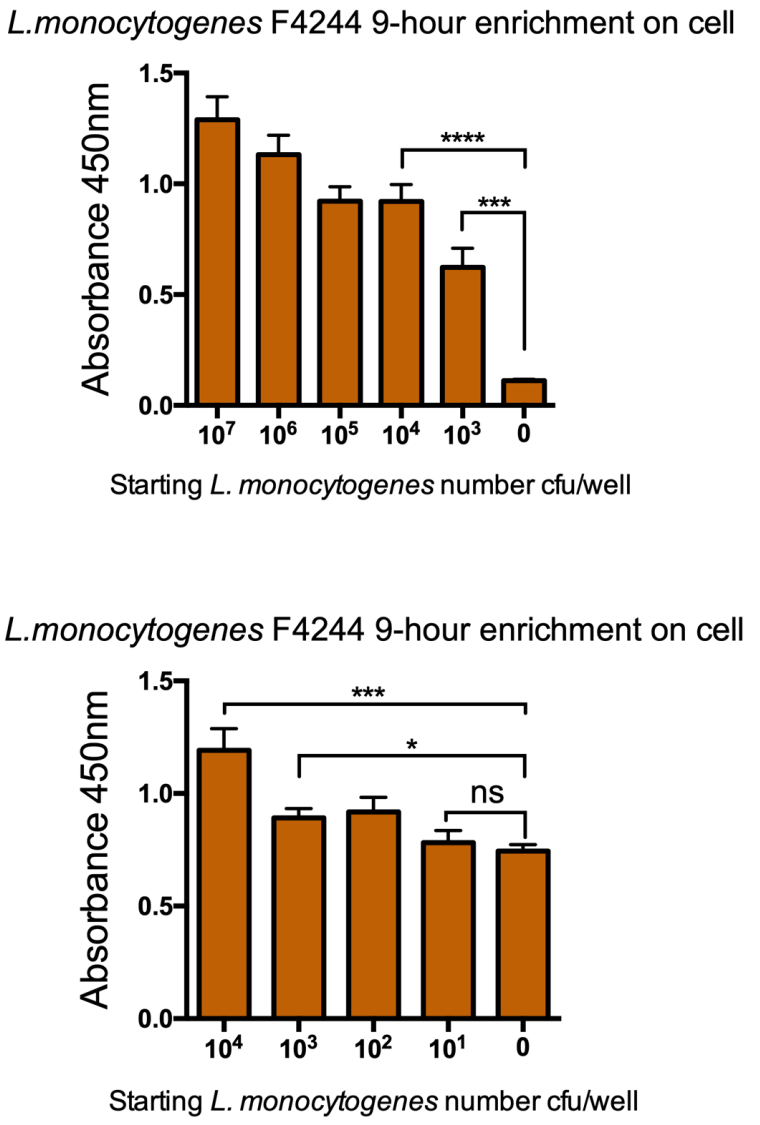

Figure B.2. On cell enrichment of *Lm* on live HCT-8 cell monolayers.

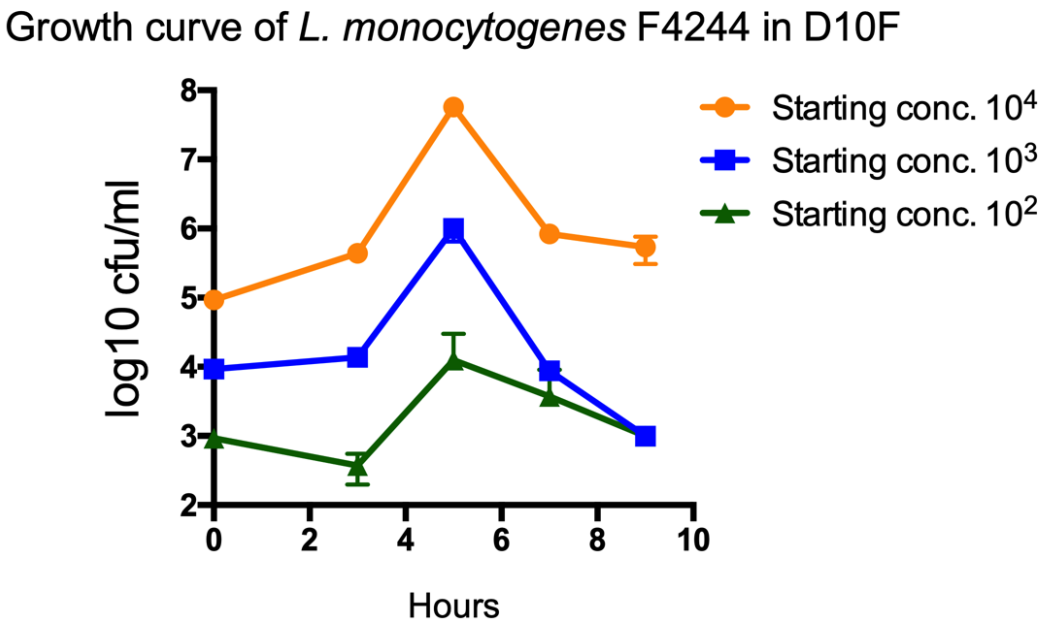

Figure B.3. Growth curve of *Lm* in D10F.

Future suggetions

Live HCT-8 cell monolayer is not suitable for the detection of *Lm*, especially when on-cell enrichment method is considered. Monolayer peeling will significantly affect the reliability of the result. For future development, fixed cell platform of MaCIA should be implemented for the detection of *Lm*. A careful selection of primary and secondary antibodies will be important to improve MaCIA's specificity.

PUBLICATIONS

Xu, L., Bai, X., Tenguria, S., Liu, Y., Drolia, R., and Bhunia, A.K. (2020). Mammalian Cell-based Immunoassay for Detection of viable bacterial pathogens. Front. Microbiol. 11:575615; doi: 10.3389/fmicb.2020.575615.

Xu, L., Bai, X., Bhunia, A.K. (2021). Practical Utility and Application of Biosensors for Foodborne Pathogen Detection. (Submitted to Journal of Food Protection, under review).

Bai, X., Liu, D., **Xu, L**., Tenguria S., Drolia R., Cox A. D., Koo, O., & Bhunia, A. K. (2021). Biofilm-isolated *Listeria monocytogenes* exhibits reduced systemic dissemination at the early (12-24 h) stage of infection in a mouse model. npj Biofilms Microbiomes. 7, 18; https://doi.org/10.1038/s41522-021-00189-5.

Drolia, R., Amalaradjou, M., Ryan, V., Tenguria S., Liu, D., Bai, X., **Xu, L**., Singh, A., Cox A. D., Bernal-Crespo, V., Schaber, J., Applegate, B., Vemulapalli, R., & Bhunia, A. K. (2020). Receptor-targeted engineered probiotics mitigate lethal *Listeria* infection. *Nature Commun*. 11, 6344; https://doi.org/10.1038/s41467-020-20200-5.